

UNIVERSITI SAINS MALAYSIA

Laporan Akhir Projek Penyelidikan Jangka Pendek

Photocatalytic Degradation of Phenol in a Fluidized Bed Reactor Using Nano Photocatalysts

by

Prof. Dr. Abdul Rahman Mohamed

Dr. Lee Keat Teong

2008

APPENDIX

Appendix A

PENURUNAN FENOL BERFOTOMANGKIN DI DALAM REAKTOR LAPISAN TERBENDALIR MENGGUNAKAN TiO_2 TERSEKAT GERAK

ABSTRAK

Penurunan fenol berfotomangkin di dalam larutan akues dikaji di dalam reaktor lapisan terbendalir. Kaedah sol gel terubahsuai digunakan untuk menghasilkan nano-TiO_2 dan disekat gerakan pada pasir kuarza, gel silica dan manik kaca. Nano-TiO_2 itu telah dicirikan dengan menggunakan analisis XRD, TEM, SEM, EDX dan BET. Prestasi perbandingan di antara reaktor lapisan terbendalir dan reaktor kelompok dinilai pada keadaan-keadaan eksperimen yang sama. Reaktor lapisan terbendalir didapati lebih efektif berbanding reaktor kelompok. Prestasi reaktor lapisan terbendalir dikaji dengan mengubah parameter-parameter proses yang berbeza dengan kepekatan awal fenol 25 – 200 ppm, bebanan mangkin 0.16 – 0.55 g/L, nilai pH awal 3 – 9 dan kadar aliran udara 1 – 2.5 L/min. Peningkatan kepekatan awal dari 50 ppm kepada 200 ppm menunjukkan pengurangan dalam kadar penurunan. Bebanan TiO_2 dan pH yang optimum adalah 0.33 g/L dan pH 3 masing-masing. Peratus penurunan fenol dioptimumkan dengan menentukan keadaan-keadaan optimum menggunakan metodologi permukaan sambutan. Penurunan fenol maksimum sebanyak 99% diperolehi pada kepekatan awal fenol 45 mg/L, bebanan mangkin 0.35 g/L dan nilai pH awal 4.2.

PHOTOCATALYTIC DEGRADATION OF PHENOL IN A FLUIDIZED BED REACTOR USING NANO PHOTOCATALYST

ABSTRACT

Photocatalytic degradation of phenol in aqueous solution was studied in a fluidized bed reactor. A modified sol gel method was employed to synthesize nano-TiO_2 and immobilized on quartz sand, silica gel and glass beads. The nano-TiO_2 was subjected to XRD, TEM, SEM, EDX and BET analysis. A comparative performance between the fluidized bed reactor and the batch reactor was evaluated under the same experimental conditions. The fluidized bed reactor was found to be more effective compared to that of the batch reactor. The performance of the fluidized bed reactor was studied by varying different process parameters with initial phenol concentration of 25 – 200 ppm, catalyst loading of 0.16 – 0.55 g/L, initial pH value of 3 – 9 and air flow rate of 1 – 2.5 L/min. The increase of the initial concentration from 50 ppm to 200 ppm resulted in the decrease in degradation rate. Optimum TiO_2 loading and pH were found to be 0.33 g/L dan pH of 3, respectively. The percentage of phenol degradation was optimized by determining the optimum conditions using response surface methodology. A maximum phenol degradation of 99% was obtained at initial phenol concentration of 45 ppm, catalyst loading of 0.35 g/L and initial pH value of 4.2.

APPENDIX B

Comprehensive Technical Report

Introduction:

Phenol and substituted phenols are widely distributed at low concentration in natural waters. However, at the high concentrations, it can be in some industrial wastewater discharge and agricultural activities. Phenol and its derivatives are widely used as raw materials in many chemical, petrochemical, pharmaceutical, textile industries. They generate large quantities of the wastewater including highly concentrated phenol and its derivatives [1]. Recently, considerable attention has been focused on complete oxidation of organic compounds to harmless products such as CO_2 and H_2O by the advanced oxidation processes (AOP) [2]. The photocatalytic degradation of organic compounds using semiconductor catalyst has attracted much attention [1]. Among the various advanced oxidation processes, TiO_2-mediated photocatalysis was shown to be potentially advantageous as it may lead to complete mineralization of pollutants to CO_2, water and mineral acids [3]. Indeed among different semiconductors, titania (TiO_2) seems to be the most widely used catalyst because of its high oxidative power, low cost, nontoxicity, corrosion resistively [4] and photostability under operation conditions [5]. Recent studies showed that the photocatalytic activity of TiO_2 is greatly influenced by its grain size. The decrease of grain size implies the increase of surface area and high redox potential, which leads to high photocatalytic activity [6]. The overall photocatalytic activity of nano TiO_2 is greatly influenced by its phase composition [7], crystal structure, particle size, size distribution, the ratio between anatase and rutile crystal phases, surface area, morphology, and the material to be degraded [8,9,10].

The nano TiO_2 photocatalysts were synthesized using sol-gel method and $TiCl_4$ as a precursor. The photocatalytic activity of catalysts was measured as a function of their calcination temperature in the range of 100 to 1000 ˚C in the batch reactor. The relation between photoactivity and physico-chemical properties is discussed in relation with the anatase and rutile particles synthesized.

Methodology:

The important sections involved in this research are:

1. Preparation of nano-TiO_2
2. Characterization of nano-TiO_2
3. Studying the performance of the nano-TiO_2 in the batch reactor

1. Preparation of nano-TiO_2:

1.1. Chemicals

All chemicals used in this study are of high purity and supplied by Merck. The chemicals used are: titanium tetrachloride ($TiCl_4$), ammonia solution (NH_4OH), nitric acid (HNO_3), phenol (99.99 %, Fisher chemicals) (C_6H_5OH). The water used in all preparation was doubly-distilled and deionized.

1.2. Preparation of nano-TiO_2:

The nanocrystalline titania catalysts were prepared by the sol-gel method using $TiCl_4$. The appropriate amount of $TiCl_4$ was titrated with 10 % NH_4OH until the white precipitates were obtained at pH value of 7. The precipitates formed washed by decantation using doubly-distilled and deionized water. The precipitated titanium dioxide was then treated with HNO_3 until the pH value become 1.5. Subsequently, a certain amount of water was added to this mixture to form an aqueous suspension. The mixture was stirred at high speed at the hydrolysis temperature of 60 °C for 24 h. Then the stable titanium oxide sol was formed. The hydrous oxides were dried in air at 50 °C to form white powder. The TiO_2 powders were calcined at various calcination temperatures for 3 h to obtain nanocrystalline TiO_2 powders.

2. Characterization of nano-TiO_2:

The crystallization phases of the TiO_2 photocatalysts were studied by X-ray diffraction using the Siemens D5000 powder diffractometer operating in the reflection mode with Cu Kα radiation (40 KV, 30 mA) diffracted beam monochromator, using a step scan mode with the step size of 0.1˚ in the range of 20-80°. The weight fractions of the anatase and

rutile phases in the catalysts were estimated from the relative intensities of the strongest peaks corresponding to anatase and rutile respective integrated XRD peak intensities using the equation (1) [11]:

$$X_A = \left(1 + 1.26\frac{I_R}{I_A}\right)^{-1} \qquad (1)$$

where X_A is a weight fraction of anatase in powder, and I_A and I_R are the X-ray integrated intensities of the (1 0 1) reflection of anatase and (1 1 0) reflection of rutile, respectively.

The crystallite size can be determined from the broadening of corresponding X-ray spectral peaks by Scherrer formula (equation (2)) [2]:

$$L = \frac{K\lambda}{(\beta \cos\theta)} \qquad (2)$$

where L is the crystallite size, λ is the wavelength of the X-ray radiation (Cu Kα= 1.5406 ˚A), shape factor K is usually taken as 0.89, and β is the line width at half-maximum height.

Transmission electron micrographs (TEM) were taken on a Philips CM12 equipped with an analysis Docu Version 3.2 image analysis system. The SEM micrographs were obtained using Philips XL 30 CP equipped with EDAX. The Brunauer–Emmett–Teller (BET) surface area, pore volume and mean pore diameter of the nano TiO_2 catalysts were determined by using a Micromeritics ASAP 2000 V2.05 nitrogen adsorption apparatus. All the samples were degassed at 180 °C prior to BET measurements.

3. Studying the performance of the nano-TiO_2 in the batch reactor:

The laboratory experiments were performed in a self-constructed batch reactor which is shown in Fig.1. It consist of a Pyrex glass jacketed reactor with an inside diameter of 8 cm, an outside diameter of 10 cm and the length of 23 cm. The reactor was surrounded with a cooling water jacket and a fan. The used source of UV irradiation was a 15 W low pressure mercury lamp ((The Pen-Ray® lamp from UVP, Inc.), with a lighted length of 22.86 cm and a total length is 29.52 cm was used. The tube diameter was 0.95 cm and the handle diameter was 1.27 cm. It emitted ultraviolet light at a wavelength of 254 nm (UV-

C) with the maximum intensity of 5400 W/cm^2. The lamp was installed at the center of the reactor through the inside of the quartz tube of 1.3 cm diameter and 27 cm long. A lamp and reactor were placed inside a wooden box painted. At the top of the reactor there are a thermocouple to monitor the reaction temperature and a sample port to withdraw samples. Samples were taken out at a regular time intervals, and they were immediately stored in 5 ml screw cap amber glass before subjected to analysis. A high performance liquid chromatography (HPLC) was used to measure the concentration of phenol in the solution. All experiment runs were performed at room temperature and atmospheric pressure. The HPLC system used in the experiment comprised of Perkin-Elmer UV/VIS 200 HPLC Detector, a Luna 5 μm C18 (2) 100A column and a Perkin-Elmer 200 HPLC pump with an injector port. The mobile phase in this HPLC system consisted of 40 % acetonitrile and 60 % deionized water. The flow rate was adjusted to 1 ml/min. Full loop injection at 20 μL was conducted and the retention time of phenol was 3.66 min. The syringe was cleaned by acetonitrile after each injection and washed by the next sample solution before injection. Before HPLC analysis, all samples were filtered using BOECO filter (SFCA-membrane, 0.45 μm). Photocatalytic experiments were carried out by 500 ml of 50 mg/l phenol solution and the required quantity of nano TiO_2 catalyst into the Pyrex glass. The concentration of the catalyst was 1.2 g/l. The mixtures of phenol solution and catalysts powder were sonicated for 20 min with a sonicator (140 W, 50-60 Hz) before use. The prepared suspension was then magnetically stirred for about 30 min in dark to achieve the adsorption / desorption equilibrium. After then, 2 ml was taken as a blank probe before irradiation and, later than filtration of the catalyst injected for HPLC analysis. Following that, the suspension was irradiated with the UV lamp. The TiO_2 and phenol solution were mixed by means of an overhead stirrer at 250 rpm to unsure an efficient mixing of photocatalyst. At the appreciate irradiation times, 2 ml probes of the irradiated suspensions were taken and analyzed by HPLC in the same way as a blank probe.

4. Studying the performance of the nano-TiO_2 in the fluidized bed reactor:

The fluidized bed reactor is used as the main reactor to study the effect of different operating parameters. The experimental rig consisted of a quartz glass column with inner diameter = 55 mm, outer diameter = 60 mm, height = 600 mm as the main chamber for

the photocatalytic reaction. Air distributor with mesh size of 200 μm was used to provide uniform fluidization of the photocatalyst. Thermocouple was placed in the centre of quartz glass column of the fluidized bed reactor to monitor temperature changes during the degradation process. A UV lamp enclosure with four UV lamps fitted inside provides illumination for the photocatalytic degradation. The UV lamps are 20 W germicidal lamps (Sankyo Denki Co. Ltd.) with wavelength of 254 nm and tube length of 588 mm and tube diameter of 32 mm. UV lamp intensity is controlled by applying voltage from 0 – 250V. UV intensity was measured with Series 9811 Radiometer (Cole-Parmer, USA). Air compressor was used to provide air for fluidization throughout the experiment. A flow meter (Cole-Parmer, model 32464-12) is used to control the air flow rate entering through the distributor. The pressure drop across the column of the reactor is monitor by using differential pressure transmitter (Foxboro, model IDP10-T22B11F-L1T). The reactor was operated in batch mode for all experiments conducted. Photocatalytic degradation of phenol was performed at atmospheric pressure and at reaction temperature of 30 °C in fluidized bed reactor as shown in Fig. 2. A calculated amount of photocatalyst with pre-determined TiO_2 content were charged into the top loading of the reactor column. Photocatalyst in the range of 20 – 80 g were added. A fixed amount of 1400 ml phenol solution was subsequently added into the reactor column from the top loading. The air control valve was slowly opened to allow air to enter into the reaction column through the distributor. The air control valve was adjusted to the appropriate air flow rate so that fluidization of the photocatalyst particles was achieved. The air flow rate was adjusted so that at least 70% of the bed expansion was ensured throughout the experiment. Next, the UV lamp enclosure was put in place surrounding the reaction column. The UV lamps were then switched on. Photocatalytic reaction started at the point when the UV lamps were switched on. Samples were taken out at a regular time intervals such as in the batch mode, and they were immediately stored in 5 ml screw cap amber glass before subjected to analysis by using HPLC.

Results and discussion

1. Characterization

Fig. 3 shows XRD patterns for synthesized catalysts calcined at various temperatures range from 100 to 1000 ˚C for the residence time of 3 h. The patterns evidenced that anatase was the only titania crystalline phase in the temperature range of 100-400 ˚C, of which diffraction lines were sharpened with increasing calcination temperature. The gradual transformation of anatase phase to rutile phase occurred at 500 ˚C, whereas in the catalyst calcined at 900 ˚C anatase phase disappeared and rutile as a major phase is observed e. i. Sample calcined at 500 ˚C contains 89 % of anatase and 11 % of rutile at 500 ˚C. However with increasing temperature up to 800 ˚C, the amount of anatase decreased and powders produced up to 1000 ˚C are predominantly in rutile phase (refer Table 1). In Table 1, phase composition and crystallite sizes of anatase and rutile phases of the catalysts is summarized as a function of calcination temperature. As it was mentioned in Table 1, catalyst undergoes the phase transition from anatase to rutile over a wide range of temperature region from 500 to 800 ˚C indicating the high thermal stability of anatase herein although rutile coexists with anatase at 500 ˚C. As the calcination temperature increases from 800 to 1000 ˚C, the crystallite sizes of rutile grow progressively and the anatase phase was disappeared completely up to this temperature, as it is published before [2]. Typical SEM micrographs of catalysts calcined at 400, 600, 1000 ˚C and Degussa P-25 are shown in Fig. 4. Figures indicate that the particles are spherical in nature in these samples. Fig. 4 (a) shows that TIC 40/400 has more uniform size and more agglomeration of particles as compared to others. However, in the catalyst calcined at 600 ˚C and 1000 ˚C, larger particles are seen, which are likely to be aggregates of the smaller particles. The SEM micrograph for the Degussa P-25 is also shows that the particles are spherical and they are agglomerated together. As it was shown in the TEM micrographs of catalysts calcined at 400 ˚C, 600 ˚C, 1000 ˚C and Degussa P-25 (Fig 5 (a)-(d)), respectively. The TEM images clearly show that the average particle size increases significantly as the calcination temperature increases from 400 to 1000 ˚C and the particles are randomly oriented and exhibit irregular shapes which the size and the shape of crystallites in each sample are also quite different. The particle size of the catalysts determined from the TEM micrographs are listed in Table 1. It is obvious from these

images that catalyst TIC calcined at 400 ˚C consists of the fine particles with the average size of about 7.02 nm, being rather homogenous in size. However, after calcination at 600 ˚C, the particles grow up to about 33.37 nm, of which crystallinity looks to become better and being consistent with sharpening of diffraction lines of X-rays. However, TEM observation reveals that catalyst TIC 40/1000 has polyhedral shaped morphologies and average particle size of 114.15 nm. Furthermore, Degussa P-25, consist of the particle in spherical and polyhedral shaped which the average particle size is 21.33 nm. The specific surface area, pore volumes, average pore sizes of the catalysts calcined at 400 ˚C, 600 ˚C, 1000 ˚C and Degussa P-25 are listed in Table 2. It can be seen that catalyst calcined at 400 °C shows very large BET value of 134.43 m^2g^{-1}. It is almost three times higher than that of Degussa P-25. However, the BET surface area and the pore volumes all become smaller with increasing calcination temperature. These results indicate that the diameter of the TiO_2 particles increase corresponding to transforming of the TiO_2 structural , leading to decreasing in pore volume and BET surface area. Whereas the average pore diameters of these catalysts increase which maybe due to that the nano particles trend to agglomerate intensively in the high temperature and higher calcination temperature could make the pore collapsed [11, 12]. For Degussa P-25 containing 77 % anatase and 23 % rutile, the surface area is 47.07 m^2g^{-1}.

2. Studying the photocatalytic activity of the nano-TiO_2 in the batch reactor:

The purpose of this research is to investigate the photocatalytic degradation of phenol, a toxic and harmful pollutant, using nano TiO_2. The course of phenol photocatalyzed decomposition using prepared nano TiO_2 catalysts calcined at various temperatures is shown in Fig. 6. As it is evidence in Fig. 6, the photocatalytic activity of catalysts increases significantly until calcination temperature of 600 ˚C. However, at further increase of calcination temperature, the photocatalytic activity of these catalysts decrease significantly, which catalyst calcined at 600 ˚C exhibits the highest photocatalytic efficiency on the photocatalytic degradation of phenol of the all these catalysts. The photoactivity of these catalysts is comparable to the Degussa P-25. The photocatalytic activity of Degussa P-25 is almost similar to the catalyst calcined at 400 ˚C.

Catalyst calcined at 400 ˚C consists of pure anatase and its crystalline size as fine as 6.86 nm with the surface area of 134.43 m^2g^{-1}. We expected that it shows the highest photocatalytic activity than others. However, catalyst calcined at 600 ˚C consists of the mixture of both phases (χ = 0.21) with the anatase crystalline size of 24.12 nm, rutile crystalline size of 29.72 nm, which have lower surface area shows highest activity than those in the pure anatase or rutile phases do. The lower activity of catalyst calcined at 400 ˚C may due to its poor crystallinity, more agglomeration of particles and exciting nitrate in the surface during the preparation which is responsible for its relative low photocatalytic activity. The high photocatalytic activity of catalyst calcined at 600 ˚C is partially due to the fact that nano TiO_2 crystallized perfectly at the elevated temperature, for example, compared to catalyst calcined at 400 ˚C, the catalyst calcined at 600 ˚C and 1000 ˚C are in good crystallinity and has little amorphous part on its crystal planes. However in details, catalyst calcined at 1000 ˚C contains pure rutile with crystalline size of 61.03 nm and polyhedral shaped morphologies indicates very low activity, although its surface area is as low as 0.778 m^2g^{-1} with an average pore diameter of 19.359 nm.

3. Performance Comparison Studies between Batch Reactor and Fluidized Bed Reactor:

A fluidized bed reactor with supported catalysts is essential to provide an opportunity to escape mass transfer limitations. A fluidized bed with quartz support particles impregnated with titanium dioxide is a reasonable reactor alternative compared to the batch reactor. At proper flow regimes, good mixing conditions are ensured throughout the bed, thus producing high renewal rates for the fluid in the region closer to the UV source, where radiation field is stronger. A comparison study on the reactor performance between the batch reactor and the fluidized bed reactor was investigated. The reactor performance was evaluated through photocatalytic degradation of phenol under the same experimental conditions. In this study, TiO_2 immobilized on quartz sand was used. The comparison results are presented in Fig. 7. Photocatalytic degradation of phenol in batch reactor and fluidized bed reactor gave 82% and 98% of degradation within 6 hours of UV illumination, respectively. It showed that the performance in the fluidized bed reactor was better than in the batch reactor in terms of photocatalytic degradation of phenol.

References:

[1] K.B. Dhanalakshmi, S. Anandan, J. Madhavan, P. Maruthamuthu, Solar Energy Materials & Solar Cells (2008) 92: 457–463.

[2] Z. Wang, W. Cai, X. Hong, X. Zhao, F. Xu & C. Cai, Applied Catalysis B: Environmental, (2005) 57: 223-231.

[3] M. Kaneko, I. Okura (Eds.), Photocatalysis: science and technology. Springer (2002).

[4] M. Moonsiri, P. Rangsunvigit, S.Chavadej & E.Gulari, J. Chemical Engineering, (2004) 97: 241-248.

[5] Y. Su, S. Han, X. Zhang, X. Chen, L. Lei, Materials Chemistry and Physics (2008) 110: 239–246.

[6] Mao, L., Q. Li, H. Dang & Z. Zhang, Materials Research Bulletin, (2005) 40: 201-208.

[7] Y. V. Kolen'ko, A. V. Garshev, B. R. Churagulov, S. Boujday, P. Portes, C. Colbeau-Justin, J. Photochemistry and Photobiology A: Chemistry (2005) 172: 19-26.

[8] L. Mao, Q. Li, H. Dang, Z. Zhang, Mater Research Bulletin (2005) 40: 201–208.

[9] C. S. Kim, B. K. Moon, J. H. Park, S. T. Chung, S. Sond, J. Crystal Growth (2003) 254: 405–410.

[10] Q. Zhang, L. Gao, J. Guo, Applied Catalysis B: Environmental (2000) 26: 207–215.

[11] J. Yang, J. Zhang, L. Zhu, S. Chen, Y. Zhang, Y. Tang , Y. Zhu, Y. Li, J. Hazardous Material (2006) 137: 952–958.

[14] Z. Wang, W. Cai, X. Hong, X. Zhao, F. Xu, C. Cai, Applied Catalysis B: Environmental (2005) 57: 223–231.

List of Figures

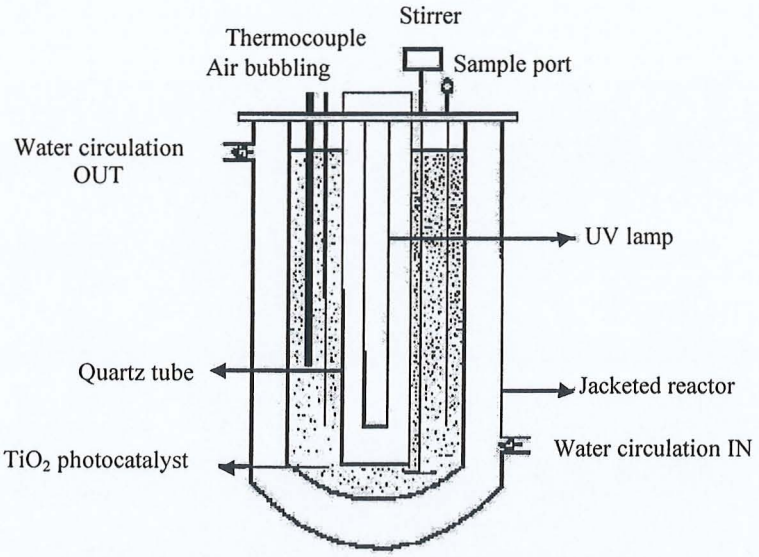


Fig. 1. The schematic diagram of the experimental set-up

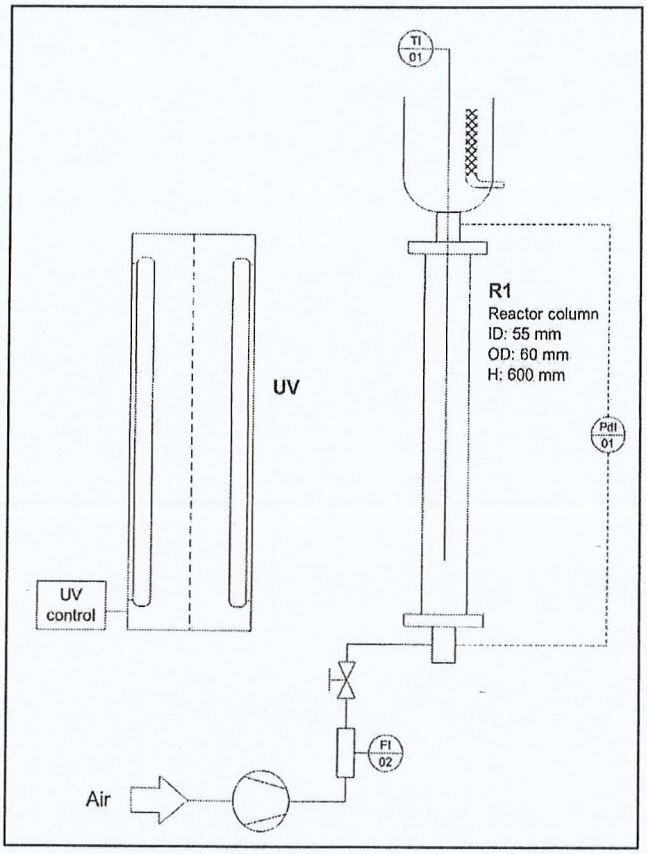


Fig. 2. Schematic diagram of fluidized bed reactor

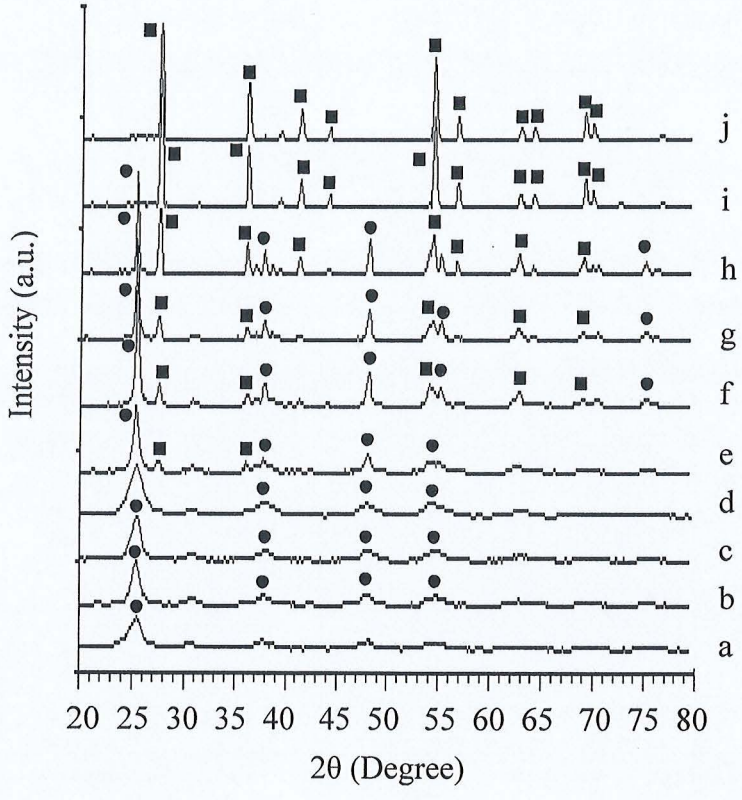
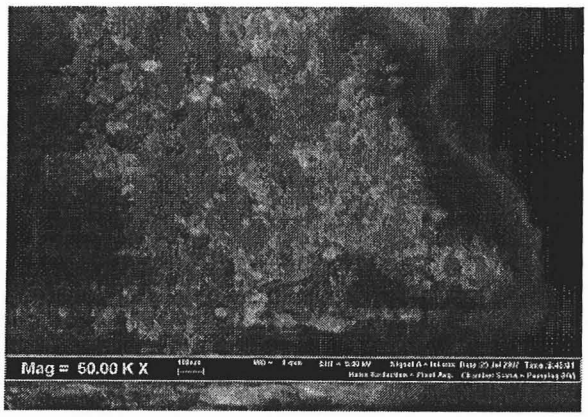
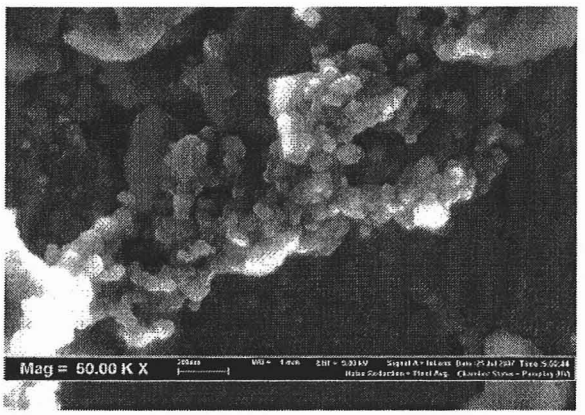


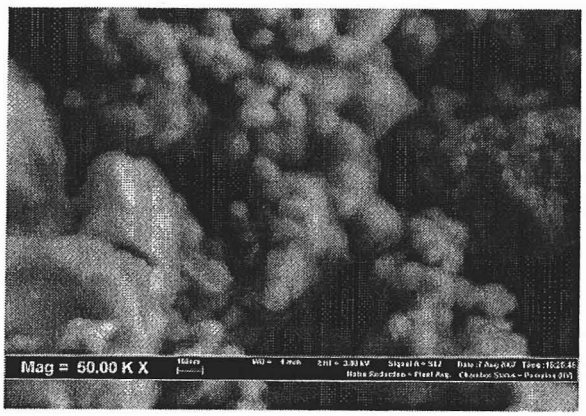
Fig.3. XRD diffraction pattern of calcined at (a) 100 ˚C; (b) 200 ˚C; (c) 300˚C; (d) 400 ˚C; (e) 500 ˚C; (f) 600 ˚C; (g) 700 ˚C; (h) 800 ˚C; (i) 900 ˚C; (j) 1000 ◦C (● Anatase, ■ Rutile)



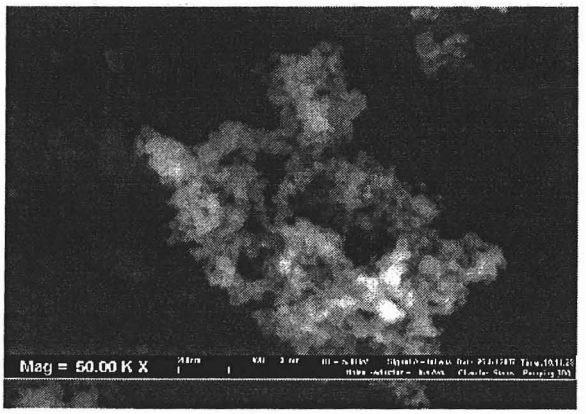
(a)



(b)



(c)



(d)

Fig. 4. Scanning electron micrograph of catalysts calcined at (a) 400, (b) 600 (c) 1000 (d) Degussa P-25

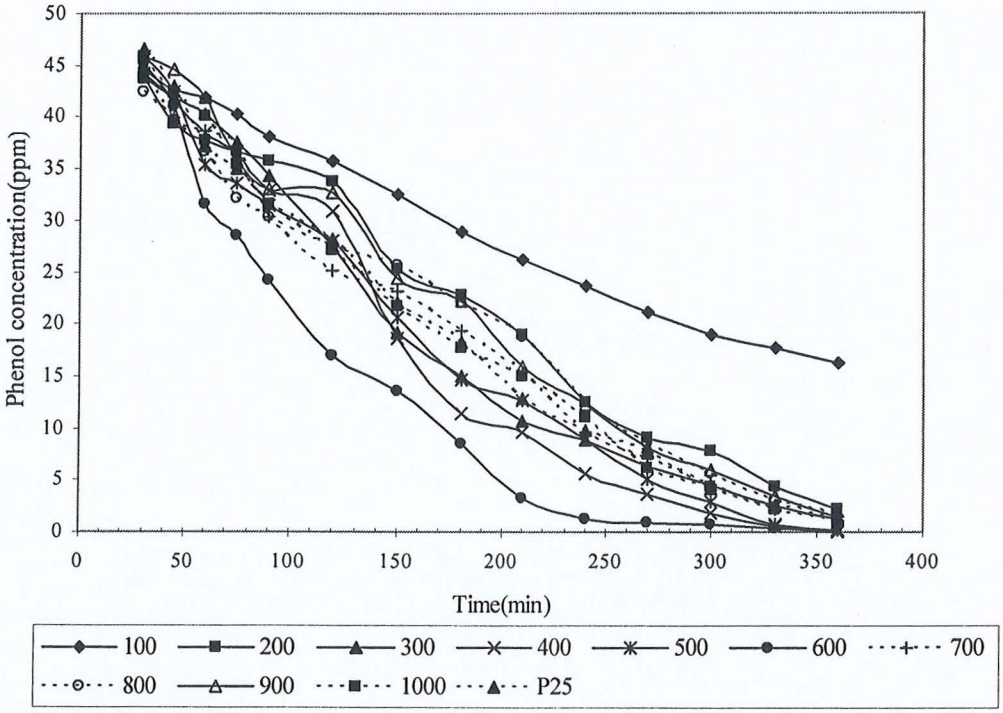


Fig. 6. The photocatalytic activity of the nano TiO_2 samples calcined at different temperatures

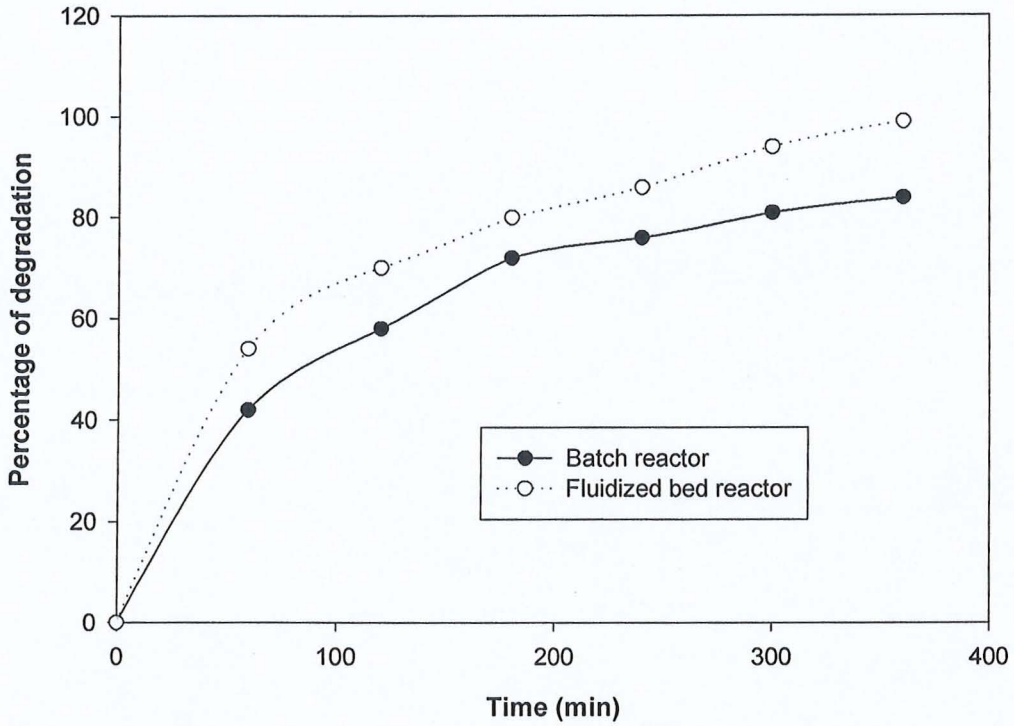


Fig. 7. Photocatalytic degradation of phenol in fluidized bed reactor and batch reactor using synthesized TiO_2/quartz sand. Conditions; C_{po}= 50 mg/L, Catalyst loading= 0.33 g/L

Table1. Summary of the properties and calcination temperature of nano TiO_2 photocatalysts

Sample	Calcination temperature (°C)	Anatase by XRD (%)	Rutile by XRD (%)	Anatase crystallite size (nm)	Rutile crystallite size (nm)	Particle size from TEM (nm)
TIC 40	0	100	0	6.03	-	-
TIC 40/100	100	100	0	7.03	-	-
TIC 40/200	200	100	0	9.86	-	-
TIC 40/300	300	100	0	7.97	-	-
TIC 40/400	400	100	0	6.86	-	7.02
TIC 40/500	500	89	11	13.91	27.95	-
TIC 40/600	600	79	21	24.12	29.72	33.37
TIC 40/700	700	74	26	28.43	47.87	-
TIC 40/800	800	50	50	45.48	54.01	-
TIC 40/900	900	0	100	-	56.30	-
TIC 40/1000	1000	0	100	-	61.03	114.15
Degussa P-25	-	77	23	23.6	38.6	21.33

Table 2.Textural properties of the nano TiO_2 photocatalysts

Sample	BET surface area [a] (m^2/g)	Pore volume [b] (cm^3/g)	Average pore diameter [c] (nm)
TIC 40/400	134.43	0.095	2.838
TIC 40/600	29.46	0.096	12.989
TIC 40/1000	0.778	0.0038	19.359
Degussa P-25	47.07	0.155	13.175

APPENDIX C

List of Publications

International journals

1. Minoo Tasbihi, Che Rohaida Ngah, Norashid Aziz, Anis Mansor, Ahmad Zuhairi Abdullah, Lee Keat Teong and Abdul Rahman Mohamed, Lifetime and regeneration studies of various supported TiO_2 photocatalysts for the degradation of phenol under UV-C light in a batch reactor, *Ind. Eng. Chem Res. 46 (2007) 9006-9014.*
2. Abdul Rahman Mohamed, Shwu-Miin Tan, Minoo Tasbihi, Siang-Piao Chai, The effects of catalytic nanoparticles on the growth of singlwalled carbon nanotubes and photodegradation of phenol, *Indonesian nano letter, Vol 2, No.1, Jun 2007.*
3. Abdul Rahman Mohamed, Minoo Tasbihi, Siang-Piao Chai, Advances in Nanocatalysis Research for Carbon Nanotubes Formation and Photocatalytic Degradation of Phenol, *Bulletin of Chemical Reaction Engineering & Catalysis*, 2(1), 2007, 17-19.
4. Minoo Tasbihi, Lee Keat Teong and Abdul Rahman Mohamed, Effect of the ratio of anatase and rutile phases on the photocatalytic properties for phenol degradation has been submitted to the journal 'Catalysis Today'.

Conferences

5. Nor Fauziah Zainudin, Ahmad Zuhairi Abdullah and Abdul Rahman Mohamed, Development of Supported TiO_2 Photocatalyst Based Adsorbent for Photocatalytic Degradation of Phenol, *International Conference on Environment 2008, 15 - 17 December 2008, Penang, Malaysia.*
6. Abdul Rahman Mohamed, Minoo Tasbihi, Siang-Piao Chai, Advances in nanocatalysis research for carbon nano tubes formation and photocatalytic degradation of phenol, *The Second Symposium and National Congress Indonesian Catalyst Society 2007, 18-19 April, Semarang, Indonesia.*
7. M. Tasbihi, K. T. Lee, A. R. Mohamed, Synthesis and Characterization of TiO_2 Nanocrystalline Powder by Sol-gel Process and Hydrazine Method, *International Conference on Environment 2006, 13 - 15 November 2006, Penang, Malaysia.*
8. Zulfakar Mokhtar, Mohamed, A.R. and M.Z Abu Bakar, Studies of Photocatalytic Degradation of Phenols in a Fluidized Bed Reactor Utilizing TiO_2 Photocatalyst Immobilized onto Inert Supports, *International Conference on Environment 2006, 13 - 15 November 2006, Penang, Malaysia.*
9. Zulfakar Mokhtar, Mohamad Zailani Abu Bakar and Abdul Rahman Mohamed, Photocatalytic Degradation of Phenols and Chlorophenols: a Review, *National Postgraduate Colloquium (NAPCOL), 8-9 December, 2004, Penang, Malaysia.*

Lifetime and Regeneration Studies of Various Supported TiO_2 Photocatalysts for the Degradation of Phenol under UV-C Light in a Batch Reactor

Minoo Tasbihi, Che Rohaida Ngah, Norashid Aziz, Anis Mansor, Ahmad Zuhairi Abdullah, Lee Keat Teong, and Abdul Rahman Mohamed*

School of Chemical Engineering, Engineering Campus, Universiti Sains Malaysia, 14300 Nibong Tebal, Seberang Perai Selatan, Penang, Malaysia

Combined photolysis and predominantly photocatalytic degradation of phenol under UV-C light (λ = 254 nm) with the maximum intensity of 5400 μW/cm^2 was carried out in a batch reactor. The TiO_2 photocatalysts were supported on glass beads, silica gel, and quartz sand using a sol−gel method. The supported TiO_2 catalysts were characterized by XRD, SEM, and EDX analyses. Factors affecting the photocatalytic degradation of phenol such as pH, oxygen supply rate, initial phenol concentration, and H_2O_2 concentration were investigated. TiO_2 supported on quartz sand gave the highest efficiency with 90% degradation of 50 mg/L phenol solution in 6 h, followed by TiO_2 supported on silica gel and glass beads with 86% and 74%, respectively. The higher photoactivity of supported TiO_2 on quartz sand was ascribed to the high crystallinity and high quantity of Ti, and the absence of ions which could inhibit the crystallization on the catalyst surface. The supported TiO_2 was found to be stable for repeated use. The results suggested that TiO_2/quartz sand and TiO_2/glass beads gave very good performances in the phenol degradation reaction. However, with TiO_2/silica gel, the percentage of degradation decreased to about 11% when used for the second time and then the percentage of degradation decreased slightly when reused again in the third and fourth runs.

1. Introduction

Wastewater derived from different chemical industries such as resin manufacturing, petrochemical, oil refineries, papermaking, textile dyeing, and iron smelting usually has high concentrations of phenol and its derivatives.[1] Heterogeneous photocatalysis using low-energy UV-irradiated TiO_2 has been shown to be an effective means of removing organic contaminants, especially priority pollutants, by converting them to carbon dioxide, water, and the oxidized forms of inorganic anions of any heteroatoms present.[2] It should also be highlighted that, at a certain wavelength, a significant contribution of photolysis to the overall degradation could result. Among the metal oxide semiconductors studied so far, TiO_2 seems to be the most widely used photocatalyst because of its high efficiency,[3] low cost, low toxicity, corrosion resistance, and high stability to light illumination.[4]

TiO_2 is a polymorphic compound that has three polymorphous phases: anatase, rutile, and brookite. Anatase and rutile phases have been used in photocatalytic investigations dealing with photodegradation of organic pollutants in water and air. Both phases are semiconductors with a band gap of 3.23 eV for anatase and 3.10 eV for rutile.[5] For photocatalytic degradation process, two methods of TiO_2 application are favored: (1) TiO_2 suspended in aqueous media and (2) TiO_2 immobilized on suitable support material. Although suspended photocatalyst systems always give higher degradation rates, there is one obvious problem arising from it. Basically, the particle sizes of catalyst powders synthesized by the industry are in the range of 30−200 nm.[6] Therefore, the reactor must be installed with a liquid−solid separator, which increases the costs of the whole process.[7] The second problem arising from a suspension system is that the fine solid particles from the effluent may cause turbidity in the downstream. Taking into account the above problems and also from the economics point of view, immobilization of photocatalyst seems to offer a plausible solution.

Many techniques were proposed for the immobilization of TiO_2 on solid supports to eliminate this problem. Various supports were investigated, in particular, different classes of glass, quartz sand, silica, activated carbon, zeolite, and glass fibers. For example, Matthews[8] reported his work on the immobilization of TiO_2-coated sand in a flat bed configuration for photooxidative degradation of colored organic back in 1991. Thereafter, most of the work generally focused on ways to improve the supported photocatalyst performance. This includes the search for better supports and the best method for immobilization. A good photocatalyst support must have the following characteristics: (i) is transparent to UV radiation; (ii) favors strong surface chemical and physical bonding with the TiO_2 particles without negatively affecting their activity; (iii) offers a high specific surface area; (iv) has good adsorption capability for the organic compounds to be degraded; (v) is in a physical configuration which favors the ultimate liquid−solid phase separation; (vi) allows reactor design that facilitates the mass transfer processes; and (vii) is chemically inert. Furthermore, the supported photocatalyst should be recyclable and reusable. The ability of the photocatalyst to be reused is an essential practical aspect of the cost effectiveness in every related process.[9]

In this study, the TiO_2 photocatalyst was prepared using sol−gel method and it was then supported on three different types of support materials, i.e., quartz sand, silica gel, and glass beads. The supported TiO_2 catalysts were characterized using X-ray diffraction (XRD), scanning electron microscopy (SEM), and energy-dispersive X-ray (EDX) methods. In this study, factors affecting the photocatalytic degradation of phenol in a batch reactor such as pH, air flow rate (or oxygen supply rate), initial concentration of phenol, and effect of H_2O_2 concentration were investigated and elucidated. As most of the literature reports focus on the photocatalytic behavior under UV-B,[1,2] this study aimed to further elucidate the specific behavior of the process

* To whom correspondence should be addressed. Tel.: +604-5996410. Fax: +604-5941013. E-mail address: chrahman@eng.usm.my.

10.1021/ie070284x CCC: $37.00 © 2007 American Chemical Society
Published on Web 11/22/2007

under higher energy UV-C irradiation, under which photolysis of organic pollutants could be significant.

The combined photolysis–photocatalytic degradation of phenol under UV-C (where the protocatalytic route predominated) was studied in a batch reactor using supported TiO_2 photocatalyst. Initial phenol concentration, pH, H_2O_2 concentration, and oxygen supply rate (achieved by varying the purified air flow rate) were studied. The reusability aspect of supported TiO_2 was also studied. The supported TiO_2 photocatalysts were calcined again after each run at different temperatures to evaluate the performance after repeated use.

2. Materials and Methods

2.1. Chemicals. All chemicals were of the highest purity available, used as received without any further purification. Titanium tetraisopropoxide (TTIP), isopropyl alchohol, diethanolamine (DEA), acetone, and silica gel (particle size between 0.2 and 0.5 mm) were purchased from Acros Organics, while phenol was purchased from Merck. All solvents used were of analytical grade and obtained from Fisher Scientific. Quartz sand (particle size about 0.25 mm) was purchased from Sigma-Aldrich. Glass beads (particle size about 0.4 mm) were purchased from BDH.

2.2. Synthesis of TiO_2 Photocatalyst. TiO_2 photocatalyst was synthesized using a sol–gel method as proposed by Balasubramanian et al.[11] to be subsequently supported on glass beads, silica gel, and quartz sand. A 0.5 M solution of titanium tetraisopropoxide in isopropyl alcohol was initially prepared, and 0.2 mol of diethanolamine was subsequently added to the solution. The solution was then continuously stirred for 2 h at room temperature to undergo a hydrolysis process for the formation of homogeneous solution. Water was then added drop by drop under vigorous stirring for 30 min. The molar ratio of the mixture was 1 TTIP:22 *i*-PrOH:4 DEA:2 H_2O, and a clear sol was obtained. It was then sealed and left for aging for at least 1 day before use. This sol was stable at room temperature, and no visible changes were observed even after storage for several months.

Before the quartz sand was used as the support, it was first washed with acetone to remove any organic impurity, followed by thorough rinsing with distilled water. Then, it was dried in an oven at 80 °C for 1 h. Conversely, glass beads and silica gel were used as received. The impregnation process was carried out in a rotary evaporator for 1 h. After that, the catalyst samples were dried for 2 h at 120 °C. Then they were calcined in a multisegment programmable furnace (Carbolite, U.K.). The furnace temperature was increased at a ramp rate of 3 °C/min until it reached 100 °C, where it was held for 1 h. Subsequently, the temperature was increased at a ramp rate of 3 °C/min to the final temperature and held for another 1 h. The final temperature was 600 °C for quartz sand and silica gel and 700 °C for glass beads. Then, the catalyst was cooled to 32 °C at a rate of 5 °C/min.

2.3. Characterization. The crystallization phases of the TiO_2 photocatalysts were studied by means of X-ray diffraction (XRD) using a Philips PW 1820 diffractometer. The diffraction patterns were obtained using Cu Kα radiation and taken in a 2θ range of 5–70° with a step size of 0.01°. The surface texture and morphology of the catalyst samples were analyzed using a scanning electron microscope (SEM) (Leo Supra 50 VP system). The SEM equipment was equipped with an Oxford INCA 400 energy-dispersive X-ray (EDX) system. EDX was used to determine the elemental composition at selected spots of the sample surface. The EDX analysis used Mn Kα as the energy source and operated at 15 kV accelerating voltage, 155 eV resolution, and 22.4° takeoff angle.

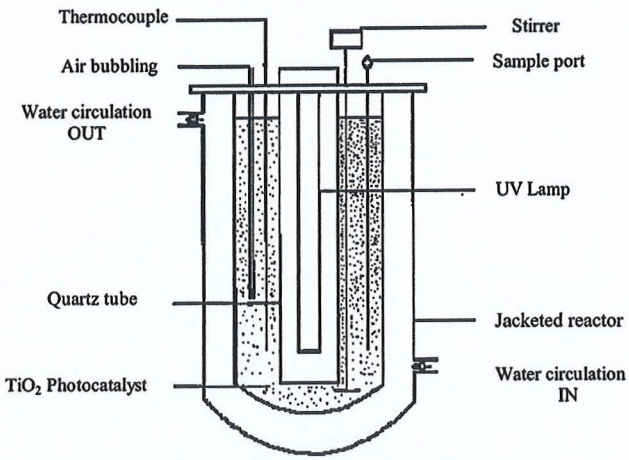


Figure 1. Schematic diagram of the experimental setup.

2.4. Photocatalytic Experiments. The schematic diagram of the experimental test setup is shown in Figure 1. In order to evaluate the activity of the prepared photocatalysts, the degradation of phenol in this batch reactor was studied. The weight of the TiO_2 photocatalyst used was 0.25 g, and this amount was supported on 30 g of different supports. The concentration of the supported catalyst in the reactor was 50.4 g/L (or 0.42 g/L based on TiO_2 alone). The concentration of phenol was varied from 25 to 115 ppm. The batch reactor was a cylindrical Pyrex glass jacketed reactor with a length of 23 cm, an inside diameter of 8 cm, and an outside diameter of 10 cm. A 15 W low-pressure mercury lamp (Pen-Ray lamp from UVP, Inc.) with a lighted length of 22.86 cm and a total length is 29.52 cm was used. The tube diameter was 0.95 cm, and the handle diameter was 1.27 cm. It emitted ultraviolet light at a wavelength of 254 nm (UV-C) with a maximum intensity of 5400 W/cm^2. The lamp was installed at the center of the reactor and placed inside a quartz tube 1.3 cm in diameter and 27 cm long. The lamp and reactor were placed inside a wooden box painted black so that no stray light from the surrounding could enter the reactor. In order to conduct experiments at a controlled temperature and to protect the lamp from overheating, the reactor was surrounded with a cooling water jacket and a fan. The TiO_2 and phenol solution were mixed by means of an overhead stirrer at 250 rpm to ensure the efficient mixing of photocatalyst. At the top of the reactor, there were a thermocouple to monitor the reaction temperature and a sample port to withdraw liquid samples.

The set of experimental conditions used in this study were carefully selected so that they were in a range that eliminated the external and internal mass transfers of phenol, or in other words, the system was reaction controlling. The experimental procedure was as follows. The prepared phenol solution and the immobilized TiO_2 photocatalysts were charged to the reactor, and the content was continuously stirred. After 30 min of dark run, the UV lamp was turned on to initiate the photocatalytic reaction. The dark run was carried out to ensure that the adsorption equilibrium was reached. When the lamp was turned on, the counting of reaction time started after 10 min. In this respect, it was assumed that the lamp already reached its maximum intensity. As all experimental runs were carried out in the same manner, the results were comparable. Furthermore, errors due to maximum light intensity were ignorable as the first sample was only collected after 20 min, i.e., 30 min after the lamp was turned on. The sampling of the solution was carried out using a 1 mL pipet at a 15 min interval for 1 h, and

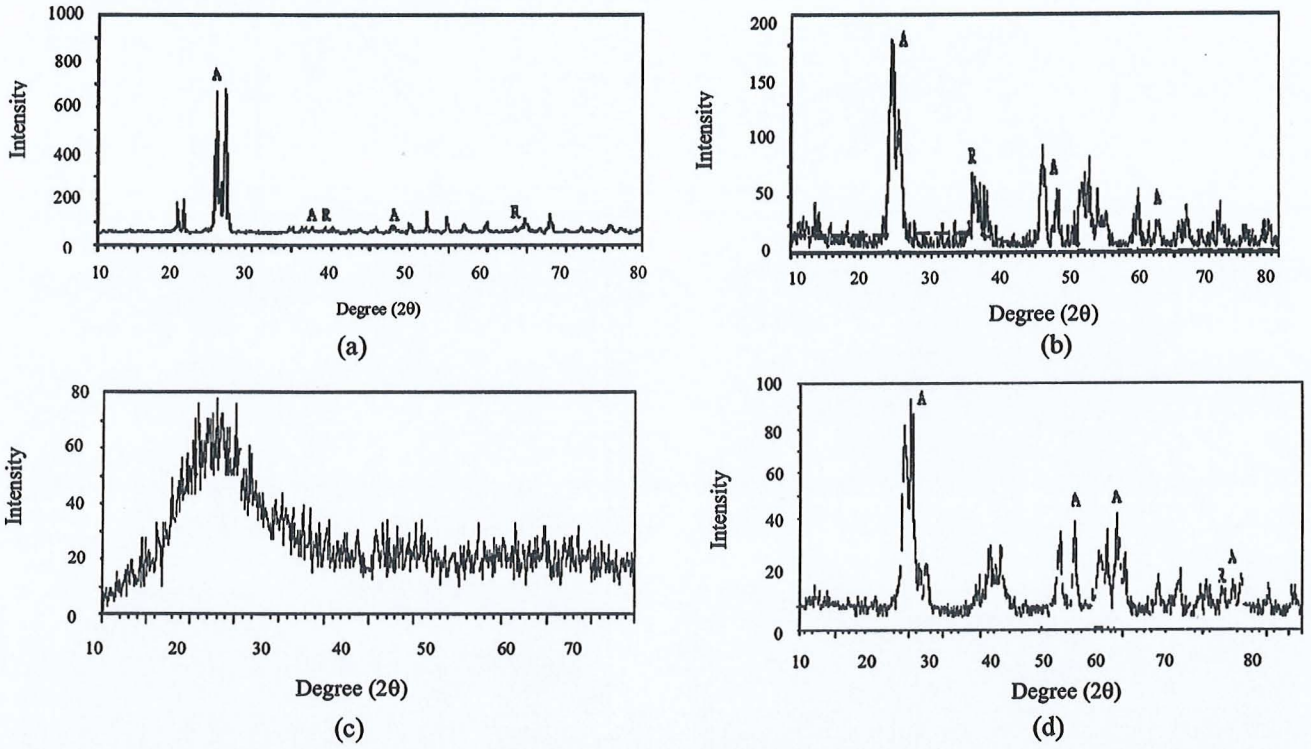


Figure 2. XRD patterns of supported TiO_2 on (a) quartz sand calcined at 600 °C, (b) silica gel calcined at 600 °C, (c) glass beads calcined at 600 °C, and (d) glass beads calcined at 700 °C. A, anatase; R, rutile.

then at a 1 h interval for the next 5 h. These samples were immediately stored in 5 mL screw cap amber glasses before being subjected to analysis. In order to avoid possible errors in the results, all the samples were tested immediately after collection. Before HPLC analysis, all samples were filtered with a Millex-HA filter (Millipore, 0.45 μm). In this study, the reaction of phenol with H_2O_2 at room temperature was negligible and was not likely to significantly affect the result. All experiment runs were performed at room temperature and atmospheric pressure.

A high-performance liquid chromatography (HPLC) method was used to measure the concentration of phenol in the solution. This measurement was performed by means of a Shimadzu device with an LC-10 AT pump, SPD-10A vp UV−vis detector, and Inertsil 5μ ODS-2 column. A mixture of 10 mM KH_2PO_4 in 60% acetonitrile at a rate of 1 mL/min was used as the mobile phase, and a detection wavelength of 230 nm was used.

3. Results and Discussion

3.1. Catalyst Characterization. Figure 2 shows XRD patterns of the TiO_2 supported on quartz sand, silica gel, and glass beads. It can be seen that crystallization behavior was greatly influenced by the type of support and the calcination temperature. When the calcination was carried out at 600 °C, the photocatalyst samples showed crystallinity structure (Figure 2a,b) except for TiO_2 supported on glass beads, which had a relatively amorphous structure (Figure 2c). Interestingly, when TiO_2/glass beads were calcined at 700 °C, polycrystalline anatase TiO_2 could be obtained (Figure 2d). Anatase or rutile peaks were not detected when the TiO_2/glass beads were calcined at 600 °C. The structure was in amorphous form. However, when TiO_2/glass beads photocatalyst was calcined at 700 °C, a peak appeared. Hence, it can be concluded that the heat treatment needed for glass beads to obtain crystallinity was 700 °C. From the figure, it can be observed that the anatase and rutile peaks appeared on all catalyst samples. However, the major phase present was anatase. The results also suggest that the anatase peak intensity for TiO_2/quartz sand was the highest followed by those for TiO_2/silica gel and TiO_2/glass beads. This polycrystalline phase was formed through the arrangement of a Ti−O−Ti network in a tetrahedrally coordinated lattice structure. In this case, 600 °C was found to be too low to promote the formation of polycrystalline TiO_2.

Amorphous TiO_2 seldom displays photocatalytic activity due to some nonbridging oxygen (NBO) in bulk TiO_2 as defects.[11] Amorphous form of the glass beads supported TiO_2 resulted when an alkoxy group remained in the particles and acted as structural impurities that inhibit crystallization. Thus it is very important to ensure that the TiO_2 thin film must have crystalline structure. To achieve crystallization, hydrolysis should go to completion before the polycondensation reaction proceeds significantly.[12] In this study, the phase transformation from anatase to rutile occurred at 600 °C for thin films coated on quartz sand and silica gel. However, Chao et al.[13] reported the presence of rutile phase when the heat treatment was performed at a temperature higher than 750 °C. It was reported in earlier studies that the phase transformation of rutile was influenced by various factors such as the chemicals used in the preparation of sol, pH of sol, time, and rate of heating as well as the temperature used in the heat treatment process.[14,15]

The structure and morphology of TiO_2/quartz sand, TiO_2/silica gel, and TiO_2/glass beads are shown in Figure 3. From the figure it is noted that the surface of each support was completely covered with TiO_2 films. The TiO_2 supported on quartz sand and silica gel had similar irregular shapes. However, their surface was nonuniform and rough, with the visible existence of macrocracks. The cracks were created at different steps in the catalyst preparation process. When the support was mixed with the sol in the rotary evaporator, it was very difficult to control the quantity of sol attached to the support so that the

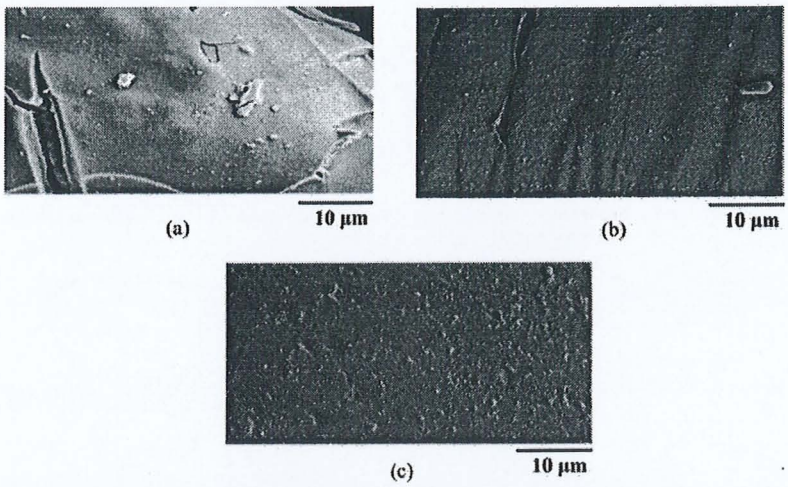


Figure 3. Scanning electron micrographs of supported TiO_2 on (a) quartz sand, (b) silica gel, and (c) glass beads.

Table 1. Results of EDX Analysis for TiO_2 with Different Supports

	composition (wt %)		
element	TiO_2/quartz sand	TiO_2/silica gel	TiO_2/glass beads
Ti	57.67	45.06	45.55
C	2.23	2.78	2.61
O	39.51	33.69	44.79
Si	0.59	18.47	4.36
K			1.96
Mg			0.64
Na			0.09

same thickness could not be obtained. It is important to note that the thickness of the film played a crucial role in the formation of cracks. Thick films tended to fracture, and the possibility of macrocracking occurring was high.[16] This was due to the intrinsic film stresses that occurred during the drying, crystallization, and densification processes. These stresses were experienced during drying due to differences in thermal expansion coefficients between the supports and TiO_2 film, grain interaction, and grain size of the TiO_2 film.[17] In the case of glass beads, the shape was fairly uniform with smooth surfaces. Thus, the supported TiO_2 exhibited continuous films except for some minor cracks (Figure 3c). In their study, Qui et al.[18] also reported similar observations where glass beads gave rise to the smoothest surface compared to silica gel and quartz sand. They also reported that the hydroxylation treatment etched the surface of glass beads and silica gel.

We continued our characterization work by applying energy-dispersive X-ray (EDX) analysis. This technique was used in conjunction with the SEM analysis. This analysis was used to characterize the elemental composition of selected spots on the thin films immobilized on the support. The elemental compositions of TiO_2/quartz sand, TiO_2/silica gel, and TiO_2/glass beads are given in Table 1. It was noted that, besides Ti, Si, and O, there was a small amount of residual carbon from the starting organic components. The results also indicated the presence of small quantities of K, Mg, and Na in TiO_2/glass beads. As for TiO_2/quartz sand and TiO_2/silica gel, these elements were not detected. The EDX peaks for K, Mg, and Na spectrum impled that some chemical reactions occurred in the interface between the films and the glass substrate and these ions migrated from the glass substrates into the thin films. Guilard et al.[19] reported the presence of the same cations in their photocatalysts. These cations perturbed the crystallinity of TiO_2 and affected the formation of anatase structure. This was the reason for TiO_2/glass beads that showed the poorest crystallinity, as suggested by its XRD patterns (Figure 2c), where it showed the least

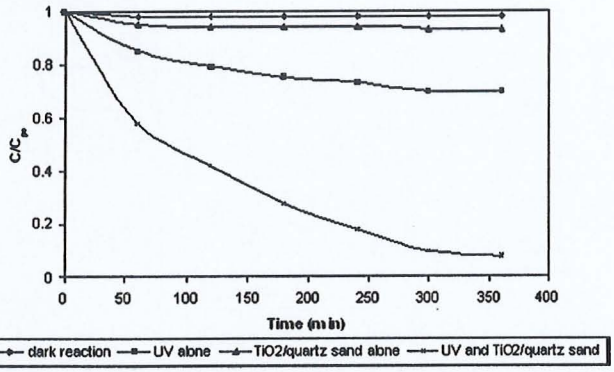


Figure 4. Photocatalytic degradation of phenol under different conditions. (C_{po} = 50 mg/L, pH 7, and maximum UV intensity of lamp = 5400 μW/cm^2.)

intensity of anatase peaks. There were two factors that contributed to this result: (1) the diffusion of ions[16] and (2) the nonporous characteristics of glass beads.[19] The presence of these ions might be due to the calcination process at 700 °C, which was very close to the melting point of glass. The heating process resulted in the diffusion of these ions to the surface of TiO_2 films and affected the electron−hole recombination center.

The XRD results show that TiO_2/quartz sand had the highest anatase peak, i.e., the desired crystallinity phase of TiO_2. Despite the occurrence of macrocracks as shown by SEM, a thick film of TiO_2 was successfully immobilized onto the support. It was confirmed by EDX analysis that Ti, Si, and O elements were present in the film's matrix. In fact, the percentage of Ti element on quartz sand was the highest at 57.67% compared to 45.06% on silica gel and 45.55% on glass beads.

3.2. Effect of Process Parameters. The preliminary experiments for the determination of photocatalytic degradation of phenol in UV light alone, in TiO_2/quartz sand alone, in the presence of UV light and TiO_2/quartz sand, and in the absence of UV light and TiO_2/quartz sand were conducted. As shown in Figure 4, the degradation of phenol in 360 min was 30%, 5%, and 90% for the experiments carried out in UV alone, TiO_2/quartz sand alone, and in the presence of both UV and TiO_2/quartz sand, respectively. There was no significant reduction in the phenol concentration for the experiment carried out without the UV light and TiO_2 catalyst. The minimum of 2% was attributed to physical processes such as adsorption.

The results in Figure 4 suggest that the removal of phenol was mainly caused by the photolysis and photocatalytic reaction

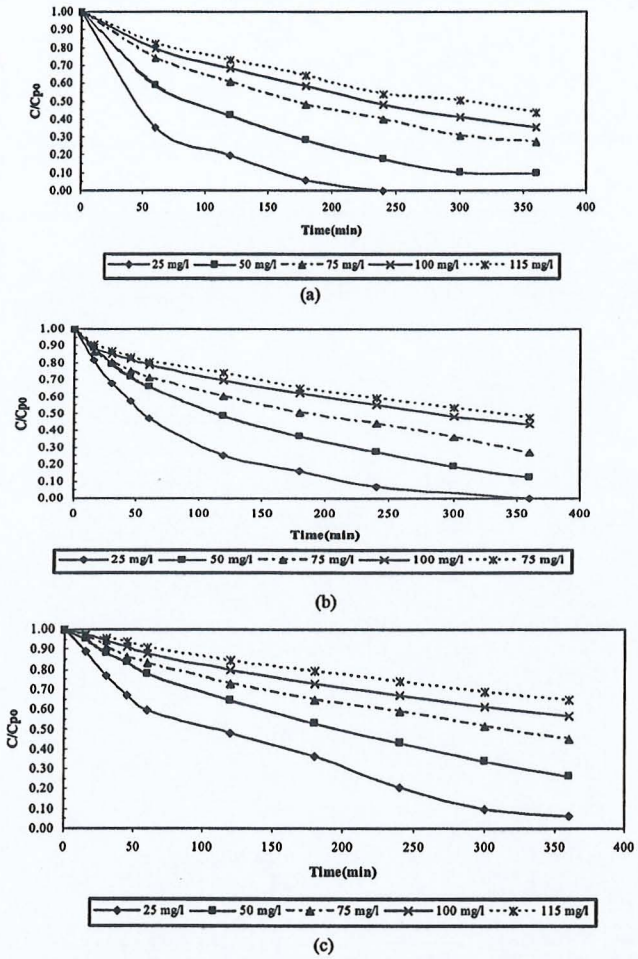


Figure 5. Degradation of phenol at various initial phenol concentrations by supported TiO_2 on (a) quartz sand, (b) silica gel, and (c) glass beads (T = 30 °C, pH 7).

while another mechanism such as adsorption was negligible. From this result it was concluded that phenol degradation was achieved through direct photolysis in a homogeneous phase and photocatalysis in a heterogeneous phase. However, the photocatalytic degradation reaction of phenol was the more dominant mechanism compared to the photolysis reaction. This result was slightly different compared to a report by Alapi and Dombi[20] that reported the higher significance of photolysis under UV-C irradiation to phenol degradation. However, the difference was attributed to the significantly lower initial phenol concentration, smaller reaction vessel, and higher intensity of UV-C light used in their study.

3.2.1. Effect of Initial Concentration. (a) Degradation of Phenol at Different Initial Concentrations. The degradation of phenol with illumination time at various initial phenol concentrations is shown in Figure 5. In this study, differences were expected in terms of the absorption of the radiation with different supports, but that was among the contributors to the differences in the performances of the photocatalysts, which was the main aspect investigated in the present study. The figure clearly suggests that the magnitude of phenol degradation at any reaction time was, in fact, higher at higher phenol concentration. This observation held true for all three types of photocatalysts used. Hence, the result clearly suggests the absence of internal diffusion limitations, or in other words, the system was confirmed to be operated under a kinetic-controlling regime.

Table 2. Half-Life Time, $t_{1/2}$, of Phenol Degradation for TiO_2 Supported on Quartz Sand, Silica Gel, and Glass Beads

	half-life time, $t_{1/2}$ (min)		
concn (mg/L)	TiO_2/quartz sand	TiO_2/silica gel	TiO_2/glass beads
25	46	56	133
50	91	116	180
75	171	187	314
100	228	286	448
115	305	342	575

It is also noted in Figure 5 that when the initial concentration of phenol was increased, the degradation of phenol decreased. This observation could be explained by several factors such as saturation of active sites and the formation of intermediates such as hydroquinone, catechol, resorcinol, and *p*-benzoquinone on the surface of catalyst.[21] Also, it should be noted that the increase in concentration affected light penetration into the phenol solution. Therefore, at higher initial concentration, the light penetration was reduced and fewer photons managed to reach the catalyst surface. The degradation followed the trend of TiO_2/quartz sand > TiO_2/silica gel > TiO_2/glass beads.

Regarding the different radiation absorptions by these catalysts, the higher activity in the degradation of phenol was obtained when TiO_2 was immobilized on the quartz sand. This means that there was no diffusion of ions to the TiO_2 films during the calcination process and the catalyst showed a higher degree of crystallinity. Pozzo et al.[10] reported that quartz sand was chosen as the supporting material because it was fairly transparent to near-UV radiation, had an acceptable surface bonding capacity with TiO_2, and provided a physical configuration that favored an easy liquid−solid separation. TiO_2 was a highly absorbing material, while quartz particles acted as an attractive alternative to immobilize small TiO_2 particles so as to permit their catalytic activity.

Chen et al.[22] reported that there were two steps that could act as the degradation determination step: the generation and migration of the photogenerated electron−hole pair and the reaction between hydroxyl radical and phenol molecules. Both steps occurred in series. At low concentration, the second step predominated and resulted in the increasing degradation rate with increased initial concentration. However, when the concentration of phenol increased further, the first step would become the governing step and degradation increased slowly with concentration until finally a virtually constant degradation was obtained. From Figure 5, it is clearly observed that the performance of TiO_2 supported on glass beads was relatively poor compared to the other two supported photocatalysts.

(b) Half-Life Time, $t_{1/2}$. Table 2 presents the value of half-life time, $t_{1/2}$, of phenol degradation for TiO_2 supported on quartz sand, silica gel, and glass beads. From the table, it is observed that the half-life time increased in this order: TiO_2/quartz sand < TiO_2/silica gel < TiO_2/glass beads. The half-life time for TiO_2/quartz sand and TiO_2/silica gel were quite close. However, the value of the half-life time for TiO_2/glass beads was significantly higher.

(c) Effect of Phenol Concentration on Reaction Rate. Figure 6 shows the relationship between the initial degradation rate against initial phenol concentration for TiO_2 supported on quartz sand, silica gel, and glass beads. The figure suggests that when the value of initial phenol concentration exceeded 50 mg/L, the initial degradation rate increment was very small and almost constant for TiO_2/quartz sand and TiO_2/silica gel. However, with TiO_2/glass beads, a slight decrease in initial rate of reaction was observed after 50 mg/L. This behavior clearly suggested the dependence of initial degradation rate on initial concentration of phenol at lower concentration.

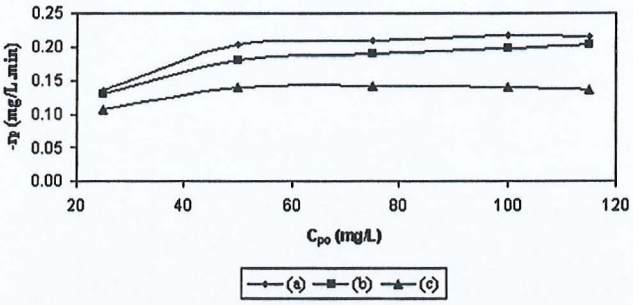


Figure 6. Plots of initial degradation rate against initial phenol concentration by supported TiO_2 on (a) quartz sand, (b) silica gel, and (c) glass beads. (Reaction time = 60 min.)

The lower rate of reaction at low phenol concentration (25 mg/L) was attributed to external mass transfer effects, and higher concentration led to higher reaction rate.[6] At phenol concentration higher than 50 mg/L, the increase in the rate of the photocatalytic reaction was generally impaired. This was due to high concentration of phenol beyond what that amount of photocatalyst was capable of degrading. Thus, an almost constant reaction rate was achieved.

Dobosz et al.[23] also reported that there were at least two reasons for the observed rate reduction. First, higher substrate concentration could favor the zero-order photocatalytic reaction kinetics (e.g., when phenol adsorption was not concentration dependent), and second, fast formation of some reaction intermediates at the very beginning of the process could result in formation of compounds such as polyphenols which would adsorb strongly onto the titania surface and block a significant part of photoreactive sites. In this study, both phenomena influenced the photoreaction rate when the concentration of phenol was higher. Therefore, under the experimental conditions, the highest removal was achieved with an initial phenol concentration of 50 mg/L.

3.2.2. Effect of pH. The effect of pH on phenol degradation using various supported TiO_2 photocatalysts was investigated in the range of pH 5.0−9.0. The results show that the phenol degradation depends significantly on the surface characteristics of the TiO_2 particles. As shown in Figure 7, TiO_2/glass beads gave the lowest removal and the phenol degradation order for the photocatalyst is as follows: TiO_2/quartz sand > TiO_2/silica gel > TiO_2/glass beads. The significant effect of pH on phenol degradation was observed, and the higher degradation was obtained at pH 5. Bouzaide et al.[24] and Parra et al.[25] reported that the point of zero charge for TiO_2 is around pH 6.8. TiO_2 particles were positively charged at lower than pH 6.8, while they carried negative charge above that pH.

It has been reported that the degradation is greatly influenced by the reaction pH. TiO_2 has amphoteric behavior that can change its surface charge properties when the pH of the solution changes. When the phenol solution is acidic, an attraction between TiO_2 photocatalyst and phenol molecules occurs and leads to an increase in the amount of phenol adsorbed on the positively charged surface of TiO_2 photocatalyst. For solution pH greater than 6.8, the groups with negative charge on the TiO_2 photocatalyst surface are assumed to increase gradually. Thus, it can be concluded that low pH values can facilitate the adsorption of the phenol molecule on the surface of supported TiO_2 photocatalyst, resulting in the enhancement of phenol degradation.

3.2.3. Effect of Hydrogen Peroxide (H_2O_2). One strategy to inhibit electron−hole pair recombination is by adding an external oxidant as an electron acceptor to the reaction. A

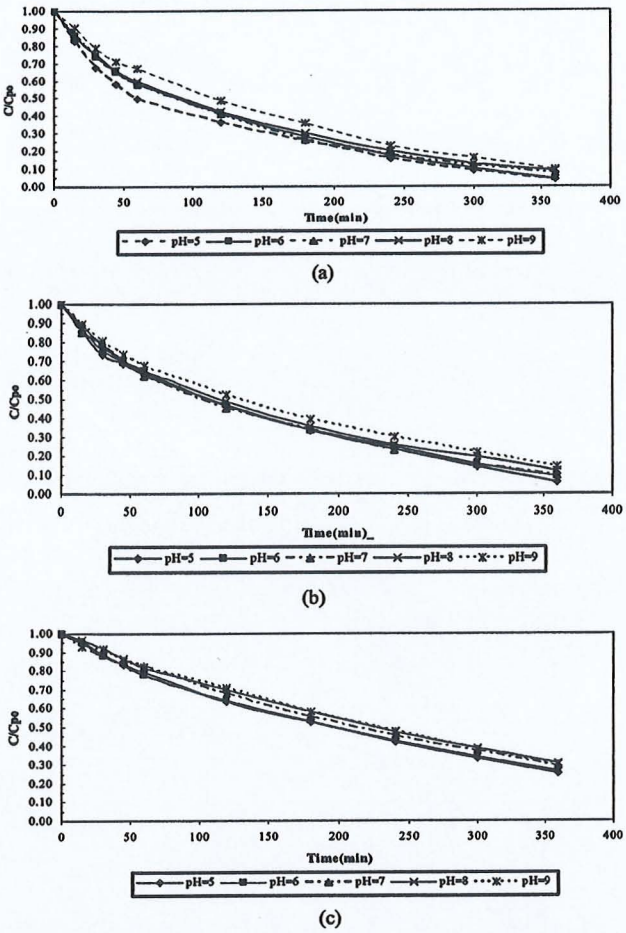


Figure 7. Effect of pH on phenol degradation by supported TiO_2 on (a) quartz sand, (b) silica gel, and (c) glass beads. (C_{po} = 50 mg/L and T = 30 °C.)

common oxidant that has been previously used to enhance the photocatalytic degradation is hydrogen peroxide (H_2O_2).[15,26] In the present study, the reaction behavior of the photocatalysts developed in the presence of H_2O_2 was studied for this role. However, as the holes were not created without the photocatalyst, the H_2O_2 had no role to play in this respect. For confirmation, this aspect was actually investigated earlier and, as expected, no significant difference was detected in the result when compared with the blank photocatalytic run (i.e., UV-C with TiO_2). Thus, the result was omitted for clarity of the data presentation in Figure 8, which shows the phenol degradation at various H_2O_2 concentrations using TiO_2/quartz sand, TiO_2/silica gel, and TiO_2/glass beads photocatalysts.

It can be seen in Figure 8 that phenol degradation increased in the presence of H_2O_2 concentration up to 200 mg/L. At this concentration, complete degradation of phenol was achieved at 3 h for TiO_2/quartz sand and TiO_2/silica gel while it was 5 h for TiO_2/glass beads. Compared to the phenol degradation in the absence of H_2O_2, this value was about 50% for TiO_2/quartz sand and TiO_2/silica gel and 38% for TiO_2/glass beads. Further increase in the concentration of H_2O_2 after this point did not increase the phenol degradation; instead, it caused the significant inhibition of phenol degradation.

H_2O_2 is suitable for trapping electrons by preventing the recombination of electron (e^-) and photogenerated hole (h^+) pairs. At the same time, the chances of formation of hydroxyl radical (°OH) on the surface of photocatalyst are also increased. However, in the presence of excess H_2O_2, the phenol degradation

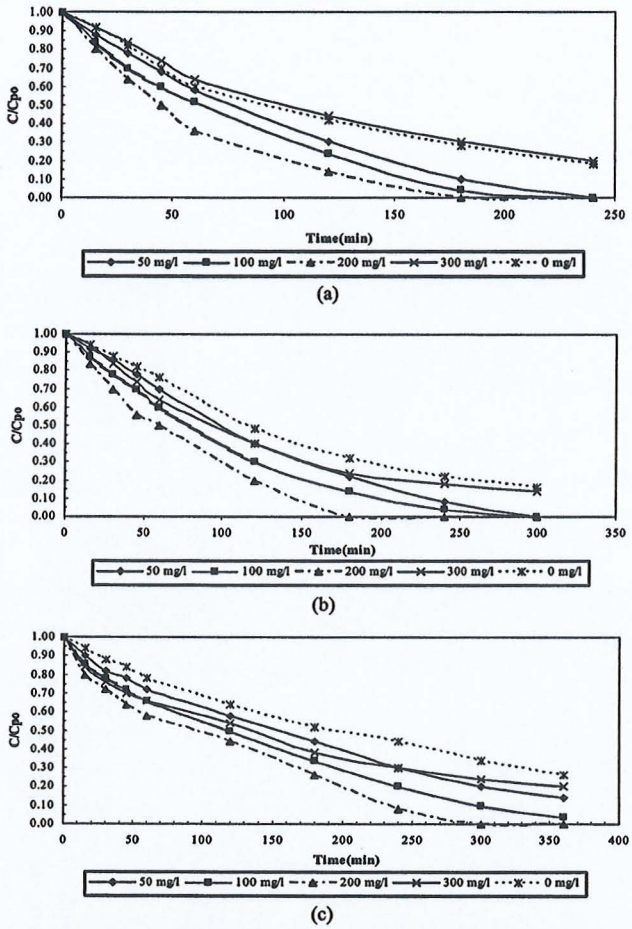


Figure 8. Phenol degradation at various H_2O_2 concentrations by supported TiO_2 on (a) quartz sand, (b) silica gel, and (c) glass beads. (C_{po} = 50 mg/L, pH 7, and T = 30 °C.)

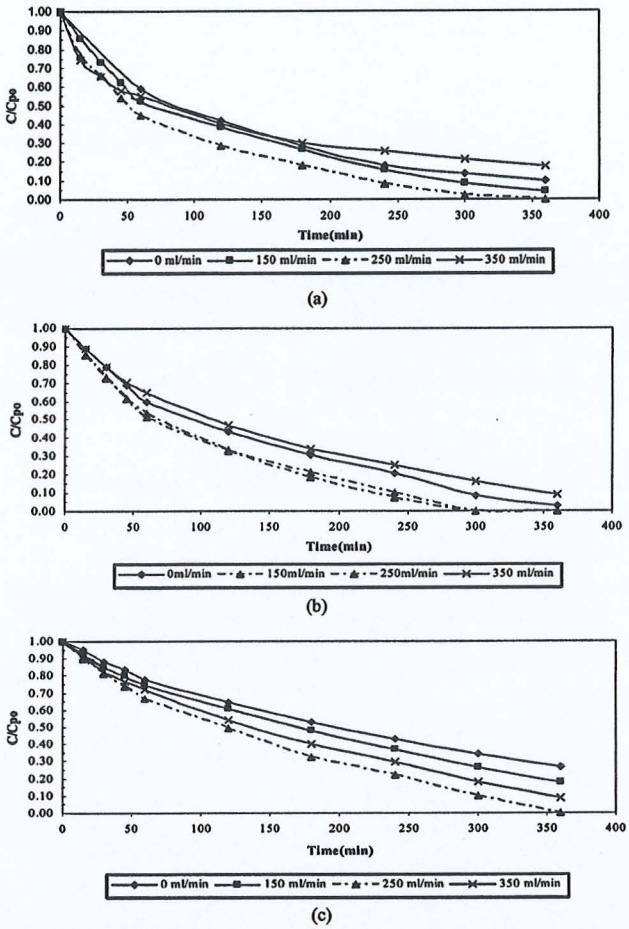


Figure 9. Phenol degradation at different air flow rates by supported TiO_2 on (a) quartz sand, (b) silica gel, and (c) glass beads. (C_{po} = 50 mg/L, pH 7, and T = 30 °C.)

decreased due to the consumption of •OH radicals and the formation of proxyl radicals (HO_2•). Therefore, it can be observed that the degradation decreased due to the consumption of •OH radicals and formation of HO_2• radicals, which were significantly less reactive than •OH radicals. Thus, the addition of H_2O_2 with a suitable concentration could assist the photocatalytic reaction in enhancing the degradation by preventing the recombination of e^- and h^+.[27]

3.2.4. Effect of Air Flow Rate. The cheapest and simplest way to supply a sufficient amount of oxygen (O_2) is by introducing air into the photocatalytic reactor. In this study, the air flow rate was varied to vary the rate at which oxygen was introduced into the reaction system. Basically, the corresponding oxygen supply rate was the actual reaction parameter. Based on 20.8% content of oxygen in purified air, the corresponding oxygen flow rates under the experimental conditions were 0, 31.2, 52.0, and 72.8 mL/min. The balance gas, i.e., nitrogen, did not participate in any reaction. Despite creating additional turbulence in the reaction vessel, no additional advantage was expected in the rate of external mass transfer as the system was already operating under the reaction-controlling regime even without air (oxygen) supplementation.

The effect of air flow rate on the photocatalytic degradation of phenol with supported TiO_2 photocatalysts is illustrated in Figure 9. From the figure, it is noted that initially, when the air flow rate was increased, the phenol degradation increased. However, when the air flow rate was further increased from 250 to 350 mL/min, the phenol degradation decreased. At the higher air flow rate, the bed expanded as the volume fraction of bubbles increased with air flow rate. Also, the larger number of bubbles might hinder absorbance of UV light to the photocatalyst.[28] Therefore, it can be concluded that the optimum value of air flow rate was 250 mL/min. The actual dissolved oxygen was measured to be 5−6 mg/L at this air flow rate. The dissolved oxygen improved the efficiency of the degradation by enhancing the separation of photogenerated electron−hole pairs, thereby increasing •OH radical concentration. The molecular oxygen adsorbed on the TiO_2 surface would trap the conduction band electrons to form the superoxide ions ($O_2^{\bullet-}$), so more •OH radicals were formed to result in the increase in the phenol degradation. The mechanistic pathway is as follows:

$$O_2(\text{ads}) + e^- \rightarrow O_2^{\bullet-} \xrightarrow{H^+} HO_2^{\bullet} \xrightarrow{HO_2^{\bullet}} O_2 + H_2O_2 \xrightarrow{e^-} O_2 + {}^{\bullet}OH + OH^-$$

The mechanism indicates that O_2 allows the increase of hole lifetime through its reaction with an electron to consequently result in the formation of oxidizing species •OH radicals.[29]

It is also shown in Figure 9 that phenol degradation was completed after 300 min at 250 mL/min air flow rate on TiO_2/quartz sand and TiO_2/silica gel. However, it was achieved only after 350 min with TiO_2/glass beads. Additionally, phenol degradation was the highest with TiO_2/quartz sand compared to the TiO_2/silica gel and TiO_2/glass beads. Besides, the concentration of phenol was the highest at 350 mL/min air flow

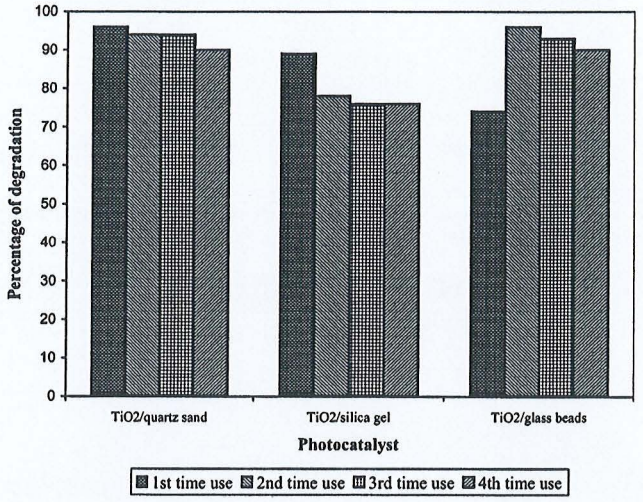


Figure 10. Comparison of photocatalytic activity of TiO_2 supported on quartz sand, silica gel, and glass beads for four times used. (C_{po} = 45 mg/L.)

Table 3. Effect of H_2O_2 Addition and Air Flow on the Half-Life Time, $t_{1/2}$, for Various Photocatalysts

	half-life time, $t_{1/2}$ (min)	
photocatalyst	H_2O_2 (200 mg/L)	O_2 (250 mL/min)
TiO_2/quartz sand	44	55
TiO_2/silica gel	60	74
TiO_2/glass beads	104	118

rate with TiO_2/quartz sand and TiO_2/silica gel. Thus, the phenol degradation from 0 to 150 mL/min was comparable with TiO_2/quartz sand and TiO_2/silica gel. However, it was significantly different with TiO_2/glass beads.

3.2.5. Effect of H_2O_2 and Air Flow. For a comparison between the effect of H_2O_2 concentration and air flow rate (dissolved oxygen supply rate), both were studied at their optimum values, i.e., 200 mg/L and 250 mL/min for H_2O_2 concentration and air flow rate, respectively. The results for these three supported TiO_2 photocatalyst are presented in Table 3. The data show the value of half-life time for the photocatalytic degradation of phenol using different supported TiO_2 photocatalysts. It is noted that the addition of H_2O_2 on the system was more effective than that of air. The addition of H_2O_2 in the phenol solution resulted in a shorter time for a complete degradation of phenol. Therefore, H_2O_2 was a better electron accepter than molecular oxygen. This was due to the minimum energy requirement to produce $^{\bullet}OH$, i.e., 3.0 eV for air flow rate while it was 2.2 eV for H_2O_2. H_2O_2 might produce $^{\bullet}OH$ radicals by photolytic splitting depending on the wavelength of the incident radiation. H_2O_2 is photosensitive, and the wavelength, $\lambda \sim 252$ nm, is needed to produce $^{\bullet}OH$ radicals.[7]

3.3. Performance of Recycled Supported TiO_2. In this study, spent supported TiO_2 photocatalyst was recycled to investigate its performance after repeated usage. After each run, the photocatalysts were calcined again at 600 °C for TiO_2/quartz sand and TiO_2/silica gel, while it was 700 °C for TiO_2/glass beads. Figure 10 shows the reusability of TiO_2 supported on quartz sand, silica gel, and glass beads obtained after four experimental runs. A reaction time of 6 h, an initial phenol concentration of 45 mg/L, and 0.25 g of each photocatalyst were chosen for each run. From the figure, it can be observed that the trend for percentage degradation of phenol was almost the same for TiO_2 supported on quartz sand and silica gel. It clearly shows that, for the TiO_2/quartz sand, the percentage of degradation for the second and third runs were only slightly lower than that in the first run and for the fourth time it was also slightly lower than for the earlier runs. For the TiO_2/silica gel, the percentage of degradation significantly decreased after the first time recycling. As for TiO_2/glass beads, the result was noticeably different. After the first run, the percentage of degradation increased significantly from 74% to 96% and then decreased slightly. This behavior was very much like the performance of TiO_2/quartz sand and TiO_2/silica gel after being recycled three and two times, respectively. TiO_2/glass beads were reactivated when it was calcined again. The possibility of a higher yield of anatase might be obtained, and this was the reason for such a good performance by TiO_2/glass beads when used for the second time.

After each run, it was observed that the color of the supported TiO_2, especially silica gel, gradually turned dark brown. The accumulation of intermediates with a poisoning effect on the surface of TiO_2/silica gel seemed higher, and this contributed to the low performance of photocatalytic activity when it was reused. The percentage degradation decreased to 78% in the second use compared to the first time use, which was 89%. The decrease in percentage of degradation was the highest for TiO_2/silica gel compared to the other two supports. However, after being regenerated at 600 °C for TiO_2/quartz sand and TiO_2/silica gel while at 700 °C for TiO_2/glass beads, all photocatalysts returned to their original color. Therefore, the deactivated photocatalyst can be regenerated by burning out all the carbon species.

This result was very encouraging that the photocatalyst activity could be recovered by a certain regeneration process. TiO_2/quartz sand and TiO_2/glass beads gave very good performances in the degradation of phenol in terms of their reusability. The result clearly suggests that supported TiO_2 photocatalysts used in this study were quite stable for repeated use. In the case of TiO_2/silica gel, the percentage of degradation decreased to about 11% when used for the second time. However, the percentage of degradation decreased slightly when reused again in the third and fourth runs.

4. Conclusion

TiO_2 photocatalysts supported on quartz sand, silica gel, and glass beads were successfully synthesized using the sol−gel method. XRD analyses confirmed the existence of crystallized anatase TiO_2 phase with some minor rutile phase as well. Different calcination temperatures were needed to obtain the anatase phase: 600 °C for TiO_2/quartz sand and TiO_2/silica gel, while TiO_2/glass beads need 700 °C. SEM pictures of the catalysts showed signs of cracks on silica gel and quartz sand, whereas only minor cracks appeared on the glass beads. The performance study of the synthesized supported TiO_2 photocatalysts under UV-C irradiation was performed in a batch reactor for the degradation of phenol. A series of experiments were conducted to investigate the effects of initial phenol concentration, solution pH, H_2O_2 concentration, and air flow rate (oxygen supply rate). The most suitable initial concentration of phenol was found to be 50 mg/L. Acidic conditions favored phenol degradation reaction. The addition of H_2O_2 and air flow increased the phenol degradation. The optimum values of H_2O_2 concentration and air flow rate were found to be 200 mg/L and 250 mL/min, respectively. After four times of repeated use, the system showed only a slight decrease in activity for TiO_2/quartz sand and TiO_2/silica gel. As for the TiO_2/glass beads, there was an increase in activity after it was regenerated. Therefore, the supported photocatalysts synthesized in this study have been proven to be stable for repeated usage.

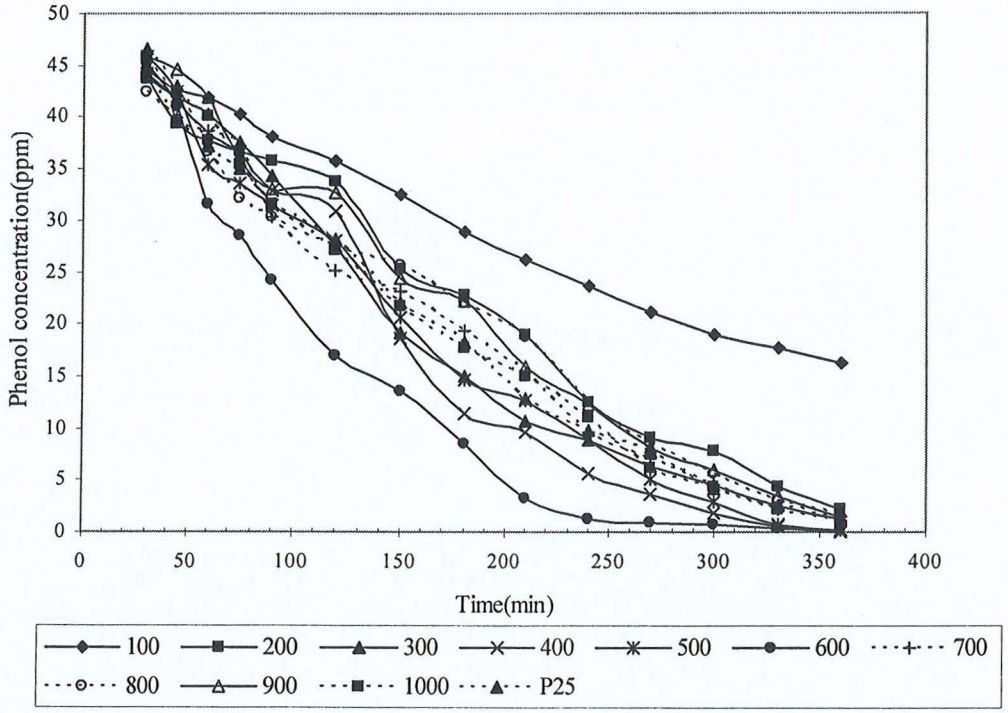


Fig. 6. The photocatalytic activity of the nano TiO_2 samples calcined at different temperatures

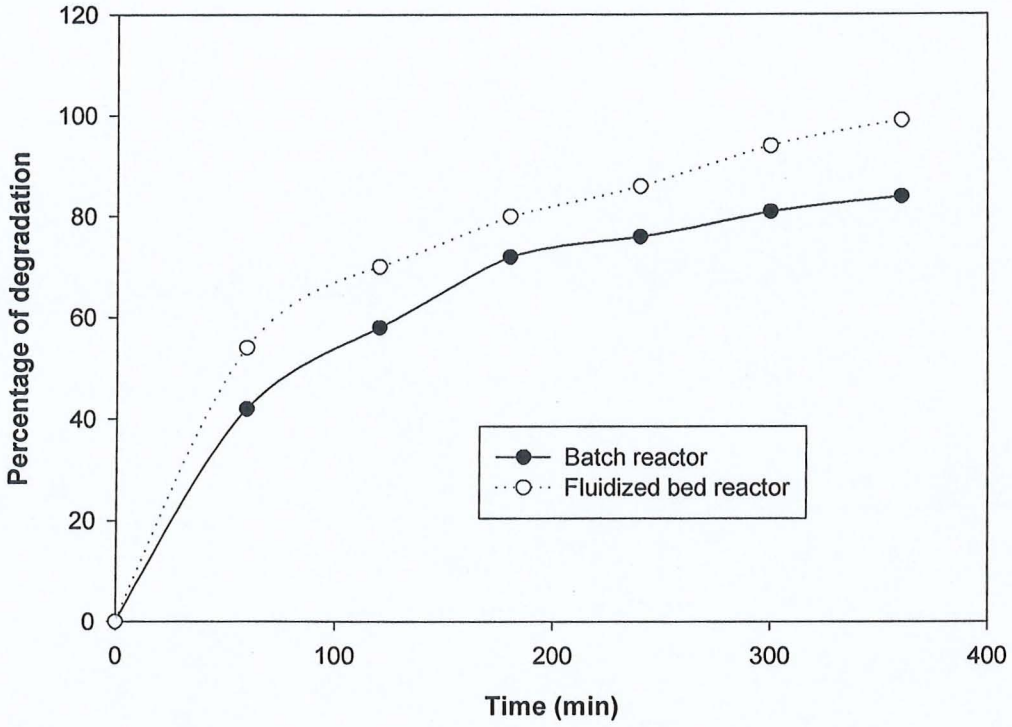


Fig. 7. Photocatalytic degradation of phenol in fluidized bed reactor and batch reactor using synthesized TiO_2/quartz sand. Conditions; C_{po}= 50 mg/L, Catalyst loading= 0.33 g/L

Table1. Summary of the properties and calcination temperature of nano TiO_2 photocatalysts

Sample	Calcination temperature (°C)	Anatase by XRD (%)	Rutile by XRD (%)	Anatase crystallite size (nm)	Rutile crystallite size (nm)	Particle size from TEM (nm)
TIC 40	0	100	0	6.03	-	-
TIC 40/100	100	100	0	7.03	-	-
TIC 40/200	200	100	0	9.86	-	-
TIC 40/300	300	100	0	7.97	-	-
TIC 40/400	400	100	0	6.86	-	7.02
TIC 40/500	500	89	11	13.91	27.95	-
TIC 40/600	600	79	21	24.12	29.72	33.37
TIC 40/700	700	74	26	28.43	47.87	-
TIC 40/800	800	50	50	45.48	54.01	-
TIC 40/900	900	0	100	-	56.30	-
TIC 40/1000	1000	0	100	-	61.03	114.15
Degussa P-25	-	77	23	23.6	38.6	21.33

Table 2.Textural properties of the nano TiO_2 photocatalysts

Sample	BET surface area [a] (m^2/g)	Pore volume [b] (cm^3/g)	Average pore diameter [c] (nm)
TIC 40/400	134.43	0.095	2.838
TIC 40/600	29.46	0.096	12.989
TIC 40/1000	0.778	0.0038	19.359
Degussa P-25	47.07	0.155	13.175

APPENDIX C

List of Publications

International journals

1. Minoo Tasbihi, Che Rohaida Ngah, Norashid Aziz, Anis Mansor, Ahmad Zuhairi Abdullah, Lee Keat Teong and Abdul Rahman Mohamed, Lifetime and regeneration studies of various supported TiO_2 photocatalysts for the degradation of phenol under UV-C light in a batch reactor, *Ind. Eng. Chem Res. 46 (2007) 9006-9014.*
2. Abdul Rahman Mohamed, Shwu-Miin Tan, Minoo Tasbihi, Siang-Piao Chai, The effects of catalytic nanoparticles on the growth of singlwalled carbon nanotubes and photodegradation of phenol, *Indonesian nano letter, Vol 2, No.1, Jun 2007.*
3. Abdul Rahman Mohamed, Minoo Tasbihi, Siang-Piao Chai, Advances in Nanocatalysis Research for Carbon Nanotubes Formation and Photocatalytic Degradation of Phenol, *Bulletin of Chemical Reaction Engineering & Catalysis*, 2(1), 2007, 17-19.
4. Minoo Tasbihi, Lee Keat Teong and Abdul Rahman Mohamed, Effect of the ratio of anatase and rutile phases on the photocatalytic properties for phenol degradation has been submitted to the journal 'Catalysis Today'.

Conferences

5. Nor Fauziah Zainudin, Ahmad Zuhairi Abdullah and Abdul Rahman Mohamed, Development of Supported TiO_2 Photocatalyst Based Adsorbent for Photocatalytic Degradation of Phenol, *International Conference on Environment 2008, 15 - 17 December 2008, Penang, Malaysia.*
6. Abdul Rahman Mohamed, Minoo Tasbihi, Siang-Piao Chai, Advances in nanocatalysis research for carbon nano tubes formation and photocatalytic degradation of phenol, *The Second Symposium and National Congress Indonesian Catalyst Society 2007, 18-19 April, Semarang, Indonesia.*
7. M. Tasbihi, K. T. Lee, A. R. Mohamed, Synthesis and Characterization of TiO_2 Nanocrystalline Powder by Sol-gel Process and Hydrazine Method, *International Conference on Environment 2006, 13 - 15 November 2006, Penang, Malaysia.*
8. Zulfakar Mokhtar, Mohamed, A.R. and M.Z Abu Bakar, Studies of Photocatalytic Degradation of Phenols in a Fluidized Bed Reactor Utilizing TiO_2 Photocatalyst Immobilized onto Inert Supports, *International Conference on Environment 2006, 13 - 15 November 2006, Penang, Malaysia.*
9. Zulfakar Mokhtar, Mohamad Zailani Abu Bakar and Abdul Rahman Mohamed, Photocatalytic Degradation of Phenols and Chlorophenols: a Review, *National Postgraduate Colloquium (NAPCOL), 8-9 December, 2004, Penang, Malaysia.*

Lifetime and Regeneration Studies of Various Supported TiO_2 Photocatalysts for the Degradation of Phenol under UV-C Light in a Batch Reactor

Minoo Tasbihi, Che Rohaida Ngah, Norashid Aziz, Anis Mansor, Ahmad Zuhairi Abdullah, Lee Keat Teong, and Abdul Rahman Mohamed*

School of Chemical Engineering, Engineering Campus, Universiti Sains Malaysia, 14300 Nibong Tebal, Seberang Perai Selatan, Penang, Malaysia

Combined photolysis and predominantly photocatalytic degradation of phenol under UV-C light (λ = 254 nm) with the maximum intensity of 5400 $\mu W/cm^2$ was carried out in a batch reactor. The TiO_2 photocatalysts were supported on glass beads, silica gel, and quartz sand using a sol−gel method. The supported TiO_2 catalysts were characterized by XRD, SEM, and EDX analyses. Factors affecting the photocatalytic degradation of phenol such as pH, oxygen supply rate, initial phenol concentration, and H_2O_2 concentration were investigated. TiO_2 supported on quartz sand gave the highest efficiency with 90% degradation of 50 mg/L phenol solution in 6 h, followed by TiO_2 supported on silica gel and glass beads with 86% and 74%, respectively. The higher photoactivity of supported TiO_2 on quartz sand was ascribed to the high crystallinity and high quantity of Ti, and the absence of ions which could inhibit the crystallization on the catalyst surface. The supported TiO_2 was found to be stable for repeated use. The results suggested that TiO_2/quartz sand and TiO_2/glass beads gave very good performances in the phenol degradation reaction. However, with TiO_2/silica gel, the percentage of degradation decreased to about 11% when used for the second time and then the percentage of degradation decreased slightly when reused again in the third and fourth runs.

1. Introduction

Wastewater derived from different chemical industries such as resin manufacturing, petrochemical, oil refineries, papermaking, textile dyeing, and iron smelting usually has high concentrations of phenol and its derivatives.[1] Heterogeneous photocatalysis using low-energy UV-irradiated TiO_2 has been shown to be an effective means of removing organic contaminants, especially priority pollutants, by converting them to carbon dioxide, water, and the oxidized forms of inorganic anions of any heteroatoms present.[2] It should also be highlighted that, at a certain wavelength, a significant contribution of photolysis to the overall degradation could result. Among the metal oxide semiconductors studied so far, TiO_2 seems to be the most widely used photocatalyst because of its high efficiency,[3] low cost, low toxicity, corrosion resistance, and high stability to light illumination.[4]

TiO_2 is a polymorphic compound that has three polymorphous phases: anatase, rutile, and brookite. Anatase and rutile phases have been used in photocatalytic investigations dealing with photodegradation of organic pollutants in water and air. Both phases are semiconductors with a band gap of 3.23 eV for anatase and 3.10 eV for rutile.[5] For photocatalytic degradation process, two methods of TiO_2 application are favored: (1) TiO_2 suspended in aqueous media and (2) TiO_2 immobilized on suitable support material. Although suspended photocatalyst systems always give higher degradation rates, there is one obvious problem arising from it. Basically, the particle sizes of catalyst powders synthesized by the industry are in the range of 30−200 nm.[6] Therefore, the reactor must be installed with a liquid−solid separator, which increases the costs of the whole process.[7] The second problem arising from a suspension system is that the fine solid particles from the effluent may cause turbidity in the downstream. Taking into account the above problems and also from the economics point of view, immobilization of photocatalyst seems to offer a plausible solution.

Many techniques were proposed for the immobilization of TiO_2 on solid supports to eliminate this problem. Various supports were investigated, in particular, different classes of glass, quartz sand, silica, activated carbon, zeolite, and glass fibers. For example, Matthews[8] reported his work on the immobilization of TiO_2-coated sand in a flat bed configuration for photooxidative degradation of colored organic back in 1991. Thereafter, most of the work generally focused on ways to improve the supported photocatalyst performance. This includes the search for better supports and the best method for immobilization. A good photocatalyst support must have the following characteristics: (i) is transparent to UV radiation; (ii) favors strong surface chemical and physical bonding with the TiO_2 particles without negatively affecting their activity; (iii) offers a high specific surface area; (iv) has good adsorption capability for the organic compounds to be degraded; (v) is in a physical configuration which favors the ultimate liquid−solid phase separation; (vi) allows reactor design that facilitates the mass transfer processes; and (vii) is chemically inert. Furthermore, the supported photocatalyst should be recyclable and reusable. The ability of the photocatalyst to be reused is an essential practical aspect of the cost effectiveness in every related process.[9]

In this study, the TiO_2 photocatalyst was prepared using sol−gel method and it was then supported on three different types of support materials, i.e., quartz sand, silica gel, and glass beads. The supported TiO_2 catalysts were characterized using X-ray diffraction (XRD), scanning electron microscopy (SEM), and energy-dispersive X-ray (EDX) methods. In this study, factors affecting the photocatalytic degradation of phenol in a batch reactor such as pH, air flow rate (or oxygen supply rate), initial concentration of phenol, and effect of H_2O_2 concentration were investigated and elucidated. As most of the literature reports focus on the photocatalytic behavior under UV-B,[1,2] this study aimed to further elucidate the specific behavior of the process

* To whom correspondence should be addressed. Tel.: +604-5996410. Fax: +604-5941013. E-mail address: chrahman@eng.usm.my.

10.1021/ie070284x CCC: $37.00 © 2007 American Chemical Society
Published on Web 11/22/2007

under higher energy UV-C irradiation, under which photolysis of organic pollutants could be significant.

The combined photolysis–photocatalytic degradation of phenol under UV-C (where the protocatalytic route predominated) was studied in a batch reactor using supported TiO_2 photocatalyst. Initial phenol concentration, pH, H_2O_2 concentration, and oxygen supply rate (achieved by varying the purified air flow rate) were studied. The reusability aspect of supported TiO_2 was also studied. The supported TiO_2 photocatalysts were calcined again after each run at different temperatures to evaluate the performance after repeated use.

2. Materials and Methods

2.1. Chemicals. All chemicals were of the highest purity available, used as received without any further purification. Titanium tetraisopropoxide (TTIP), isopropyl alchohol, diethanolamine (DEA), acetone, and silica gel (particle size between 0.2 and 0.5 mm) were purchased from Acros Organics, while phenol was purchased from Merck. All solvents used were of analytical grade and obtained from Fisher Scientific. Quartz sand (particle size about 0.25 mm) was purchased from Sigma-Aldrich. Glass beads (particle size about 0.4 mm) were purchased from BDH.

2.2. Synthesis of TiO_2 Photocatalyst. TiO_2 photocatalyst was synthesized using a sol–gel method as proposed by Balasubramanian et al.[11] to be subsequently supported on glass beads, silica gel, and quartz sand. A 0.5 M solution of titanium tetraisopropoxide in isopropyl alcohol was initially prepared, and 0.2 mol of diethanolamine was subsequently added to the solution. The solution was then continuously stirred for 2 h at room temperature to undergo a hydrolysis process for the formation of homogeneous solution. Water was then added drop by drop under vigorous stirring for 30 min. The molar ratio of the mixture was 1 TTIP:22 *i*-PrOH:4 DEA:2 H_2O, and a clear sol was obtained. It was then sealed and left for aging for at least 1 day before use. This sol was stable at room temperature, and no visible changes were observed even after storage for several months.

Before the quartz sand was used as the support, it was first washed with acetone to remove any organic impurity, followed by thorough rinsing with distilled water. Then, it was dried in an oven at 80 °C for 1 h. Conversely, glass beads and silica gel were used as received. The impregnation process was carried out in a rotary evaporator for 1 h. After that, the catalyst samples were dried for 2 h at 120 °C. Then they were calcined in a multisegment programmable furnace (Carbolite, U.K.). The furnace temperature was increased at a ramp rate of 3 °C/min until it reached 100 °C, where it was held for 1 h. Subsequently, the temperature was increased at a ramp rate of 3 °C/min to the final temperature and held for another 1 h. The final temperature was 600 °C for quartz sand and silica gel and 700 °C for glass beads. Then, the catalyst was cooled to 32 °C at a rate of 5 °C/min.

2.3. Characterization. The crystallization phases of the TiO_2 photocatalysts were studied by means of X-ray diffraction (XRD) using a Philips PW 1820 diffractometer. The diffraction patterns were obtained using Cu Kα radiation and taken in a 2θ range of 5–70° with a step size of 0.01°. The surface texture and morphology of the catalyst samples were analyzed using a scanning electron microscope (SEM) (Leo Supra 50 VP system). The SEM equipment was equipped with an Oxford INCA 400 energy-dispersive X-ray (EDX) system. EDX was used to determine the elemental composition at selected spots of the sample surface. The EDX analysis used Mn Kα as the energy source and operated at 15 kV accelerating voltage, 155 eV resolution, and 22.4° takeoff angle.

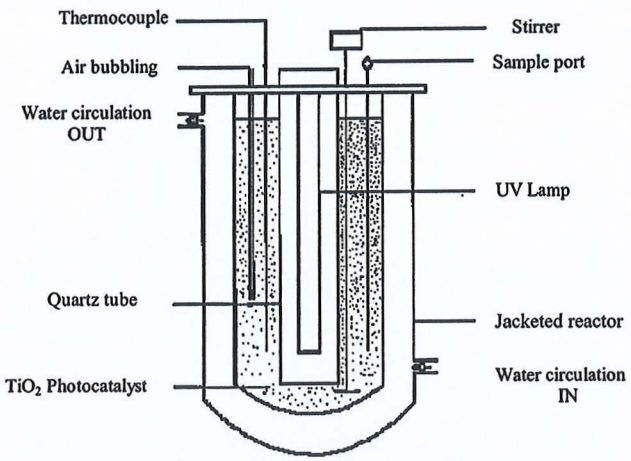


Figure 1. Schematic diagram of the experimental setup.

2.4. Photocatalytic Experiments. The schematic diagram of the experimental test setup is shown in Figure 1. In order to evaluate the activity of the prepared photocatalysts, the degradation of phenol in this batch reactor was studied. The weight of the TiO_2 photocatalyst used was 0.25 g, and this amount was supported on 30 g of different supports. The concentration of the supported catalyst in the reactor was 50.4 g/L (or 0.42 g/L based on TiO_2 alone). The concentration of phenol was varied from 25 to 115 ppm. The batch reactor was a cylindrical Pyrex glass jacketed reactor with a length of 23 cm, an inside diameter of 8 cm, and an outside diameter of 10 cm. A 15 W low-pressure mercury lamp (Pen-Ray lamp from UVP, Inc.) with a lighted length of 22.86 cm and a total length is 29.52 cm was used. The tube diameter was 0.95 cm, and the handle diameter was 1.27 cm. It emitted ultraviolet light at a wavelength of 254 nm (UV-C) with a maximum intensity of 5400 W/cm^2. The lamp was installed at the center of the reactor and placed inside a quartz tube 1.3 cm in diameter and 27 cm long. The lamp and reactor were placed inside a wooden box painted black so that no stray light from the surrounding could enter the reactor. In order to conduct experiments at a controlled temperature and to protect the lamp from overheating, the reactor was surrounded with a cooling water jacket and a fan. The TiO_2 and phenol solution were mixed by means of an overhead stirrer at 250 rpm to ensure the efficient mixing of photocatalyst. At the top of the reactor, there were a thermocouple to monitor the reaction temperature and a sample port to withdraw liquid samples.

The set of experimental conditions used in this study were carefully selected so that they were in a range that eliminated the external and internal mass transfers of phenol, or in other words, the system was reaction controlling. The experimental procedure was as follows. The prepared phenol solution and the immobilized TiO_2 photocatalysts were charged to the reactor, and the content was continuously stirred. After 30 min of dark run, the UV lamp was turned on to initiate the photocatalytic reaction. The dark run was carried out to ensure that the adsorption equilibrium was reached. When the lamp was turned on, the counting of reaction time started after 10 min. In this respect, it was assumed that the lamp already reached its maximum intensity. As all experimental runs were carried out in the same manner, the results were comparable. Furthermore, errors due to maximum light intensity were ignorable as the first sample was only collected after 20 min, i.e., 30 min after the lamp was turned on. The sampling of the solution was carried out using a 1 mL pipet at a 15 min interval for 1 h, and

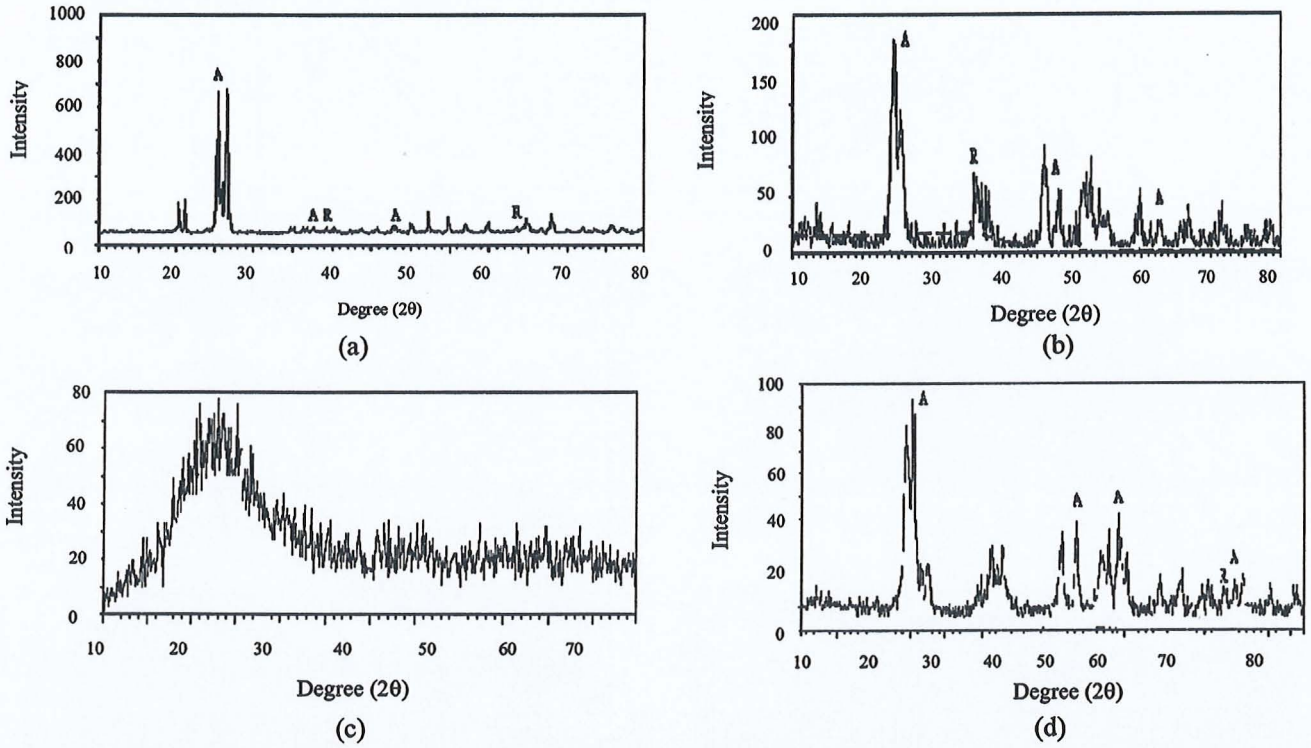


Figure 2. XRD patterns of supported TiO_2 on (a) quartz sand calcined at 600 °C, (b) silica gel calcined at 600 °C, (c) glass beads calcined at 600 °C, and (d) glass beads calcined at 700 °C. A, anatase; R, rutile.

then at a 1 h interval for the next 5 h. These samples were immediately stored in 5 mL screw cap amber glasses before being subjected to analysis. In order to avoid possible errors in the results, all the samples were tested immediately after collection. Before HPLC analysis, all samples were filtered with a Millex-HA filter (Millipore, 0.45 μm). In this study, the reaction of phenol with H_2O_2 at room temperature was negligible and was not likely to significantly affect the result. All experiment runs were performed at room temperature and atmospheric pressure.

A high-performance liquid chromatography (HPLC) method was used to measure the concentration of phenol in the solution. This measurement was performed by means of a Shimadzu device with an LC-10 AT pump, SPD-10A vp UV−vis detector, and Inertsil 5μ ODS-2 column. A mixture of 10 mM KH_2PO_4 in 60% acetonitrile at a rate of 1 mL/min was used as the mobile phase, and a detection wavelength of 230 nm was used.

3. Results and Discussion

3.1. Catalyst Characterization. Figure 2 shows XRD patterns of the TiO_2 supported on quartz sand, silica gel, and glass beads. It can be seen that crystallization behavior was greatly influenced by the type of support and the calcination temperature. When the calcination was carried out at 600 °C, the photocatalyst samples showed crystallinity structure (Figure 2a,b) except for TiO_2 supported on glass beads, which had a relatively amorphous structure (Figure 2c). Interestingly, when TiO_2/glass beads were calcined at 700 °C, polycrystalline anatase TiO_2 could be obtained (Figure 2d). Anatase or rutile peaks were not detected when the TiO_2/glass beads were calcined at 600 °C. The structure was in amorphous form. However, when TiO_2/glass beads photocatalyst was calcined at 700 °C, a peak appeared. Hence, it can be concluded that the heat treatment needed for glass beads to obtain crystallinity was 700 °C. From the figure, it can be observed that the anatase and rutile peaks appeared on all catalyst samples. However, the major phase present was anatase. The results also suggest that the anatase peak intensity for TiO_2/quartz sand was the highest followed by those for TiO_2/silica gel and TiO_2/glass beads. This polycrystalline phase was formed through the arrangement of a Ti−O−Ti network in a tetrahedrally coordinated lattice structure. In this case, 600 °C was found to be too low to promote the formation of polycrystalline TiO_2.

Amorphous TiO_2 seldom displays photocatalytic activity due to some nonbridging oxygen (NBO) in bulk TiO_2 as defects.[11] Amorphous form of the glass beads supported TiO_2 resulted when an alkoxy group remained in the particles and acted as structural impurities that inhibit crystallization. Thus it is very important to ensure that the TiO_2 thin film must have crystalline structure. To achieve crystallization, hydrolysis should go to completion before the polycondensation reaction proceeds significantly.[12] In this study, the phase transformation from anatase to rutile occurred at 600 °C for thin films coated on quartz sand and silica gel. However, Chao et al.[13] reported the presence of rutile phase when the heat treatment was performed at a temperature higher than 750 °C. It was reported in earlier studies that the phase transformation of rutile was influenced by various factors such as the chemicals used in the preparation of sol, pH of sol, time, and rate of heating as well as the temperature used in the heat treatment process.[14,15]

The structure and morphology of TiO_2/quartz sand, TiO_2/silica gel, and TiO_2/glass beads are shown in Figure 3. From the figure it is noted that the surface of each support was completely covered with TiO_2 films. The TiO_2 supported on quartz sand and silica gel had similar irregular shapes. However, their surface was nonuniform and rough, with the visible existence of macrocracks. The cracks were created at different steps in the catalyst preparation process. When the support was mixed with the sol in the rotary evaporator, it was very difficult to control the quantity of sol attached to the support so that the

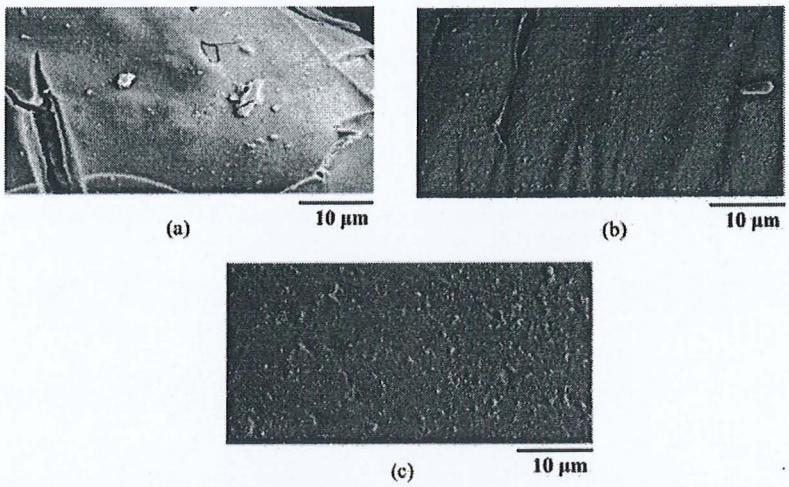


Figure 3. Scanning electron micrographs of supported TiO_2 on (a) quartz sand, (b) silica gel, and (c) glass beads.

Table 1. Results of EDX Analysis for TiO_2 with Different Supports

	composition (wt %)		
element	TiO_2/quartz sand	TiO_2/silica gel	TiO_2/glass beads
Ti	57.67	45.06	45.55
C	2.23	2.78	2.61
O	39.51	33.69	44.79
Si	0.59	18.47	4.36
K			1.96
Mg			0.64
Na			0.09

same thickness could not be obtained. It is important to note that the thickness of the film played a crucial role in the formation of cracks. Thick films tended to fracture, and the possibility of macrocracking occurring was high.[16] This was due to the intrinsic film stresses that occurred during the drying, crystallization, and densification processes. These stresses were experienced during drying due to differences in thermal expansion coefficients between the supports and TiO_2 film, grain interaction, and grain size of the TiO_2 film.[17] In the case of glass beads, the shape was fairly uniform with smooth surfaces. Thus, the supported TiO_2 exhibited continuous films except for some minor cracks (Figure 3c). In their study, Qui et al.[18] also reported similar observations where glass beads gave rise to the smoothest surface compared to silica gel and quartz sand. They also reported that the hydroxylation treatment etched the surface of glass beads and silica gel.

We continued our characterization work by applying energy-dispersive X-ray (EDX) analysis. This technique was used in conjunction with the SEM analysis. This analysis was used to characterize the elemental composition of selected spots on the thin films immobilized on the support. The elemental compositions of TiO_2/quartz sand, TiO_2/silica gel, and TiO_2/glass beads are given in Table 1. It was noted that, besides Ti, Si, and O, there was a small amount of residual carbon from the starting organic components. The results also indicated the presence of small quantities of K, Mg, and Na in TiO_2/glass beads. As for TiO_2/quartz sand and TiO_2/silica gel, these elements were not detected. The EDX peaks for K, Mg, and Na spectrum impled that some chemical reactions occurred in the interface between the films and the glass substrate and these ions migrated from the glass substrates into the thin films. Guilard et al.[19] reported the presence of the same cations in their photocatalysts. These cations perturbed the crystallinity of TiO_2 and affected the formation of anatase structure. This was the reason for TiO_2/glass beads that showed the poorest crystallinity, as suggested by its XRD patterns (Figure 2c), where it showed the least

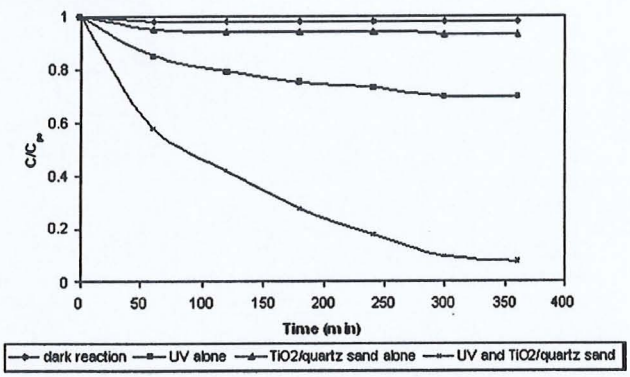


Figure 4. Photocatalytic degradation of phenol under different conditions. (C_{po} = 50 mg/L, pH 7, and maximum UV intensity of lamp = 5400 μW/cm^2.)

intensity of anatase peaks. There were two factors that contributed to this result: (1) the diffusion of ions[16] and (2) the nonporous characteristics of glass beads.[19] The presence of these ions might be due to the calcination process at 700 °C, which was very close to the melting point of glass. The heating process resulted in the diffusion of these ions to the surface of TiO_2 films and affected the electron−hole recombination center.

The XRD results show that TiO_2/quartz sand had the highest anatase peak, i.e., the desired crystallinity phase of TiO_2. Despite the occurrence of macrocracks as shown by SEM, a thick film of TiO_2 was successfully immobilized onto the support. It was confirmed by EDX analysis that Ti, Si, and O elements were present in the film's matrix. In fact, the percentage of Ti element on quartz sand was the highest at 57.67% compared to 45.06% on silica gel and 45.55% on glass beads.

3.2. Effect of Process Parameters. The preliminary experiments for the determination of photocatalytic degradation of phenol in UV light alone, in TiO_2/quartz sand alone, in the presence of UV light and TiO_2/quartz sand, and in the absence of UV light and TiO_2/quartz sand were conducted. As shown in Figure 4, the degradation of phenol in 360 min was 30%, 5%, and 90% for the experiments carried out in UV alone, TiO_2/quartz sand alone, and in the presence of both UV and TiO_2/quartz sand, respectively. There was no significant reduction in the phenol concentration for the experiment carried out without the UV light and TiO_2 catalyst. The minimum of 2% was attributed to physical processes such as adsorption.

The results in Figure 4 suggest that the removal of phenol was mainly caused by the photolysis and photocatalytic reaction

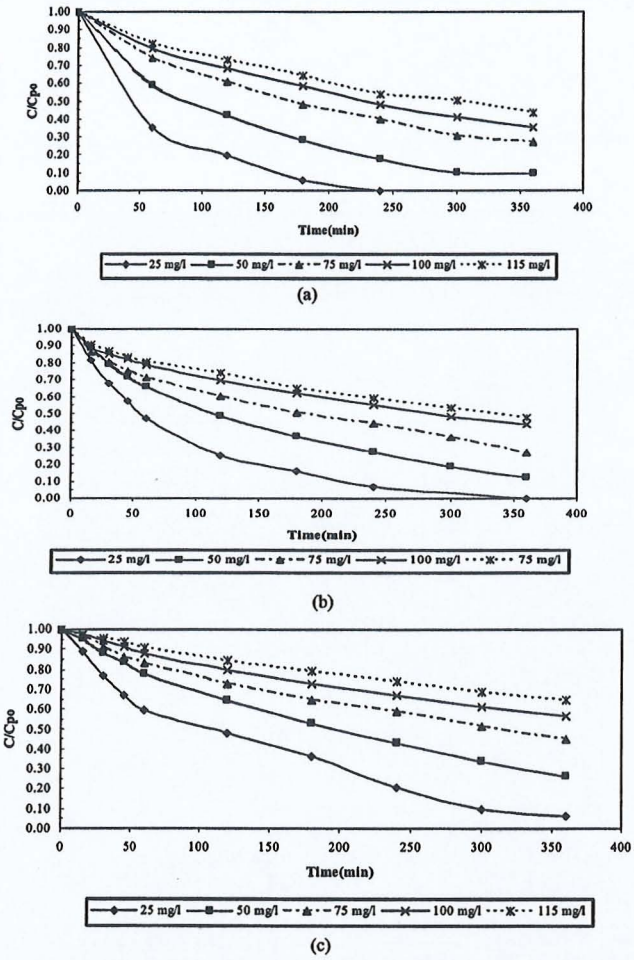


Figure 5. Degradation of phenol at various initial phenol concentrations by supported TiO_2 on (a) quartz sand, (b) silica gel, and (c) glass beads (T = 30 °C, pH 7).

while another mechanism such as adsorption was negligible. From this result it was concluded that phenol degradation was achieved through direct photolysis in a homogeneous phase and photocatalysis in a heterogeneous phase. However, the photocatalytic degradation reaction of phenol was the more dominant mechanism compared to the photolysis reaction. This result was slightly different compared to a report by Alapi and Dombi[20] that reported the higher significance of photolysis under UV-C irradiation to phenol degradation. However, the difference was attributed to the significantly lower initial phenol concentration, smaller reaction vessel, and higher intensity of UV-C light used in their study.

3.2.1. Effect of Initial Concentration. (a) Degradation of Phenol at Different Initial Concentrations. The degradation of phenol with illumination time at various initial phenol concentrations is shown in Figure 5. In this study, differences were expected in terms of the absorption of the radiation with different supports, but that was among the contributors to the differences in the performances of the photocatalysts, which was the main aspect investigated in the present study. The figure clearly suggests that the magnitude of phenol degradation at any reaction time was, in fact, higher at higher phenol concentration. This observation held true for all three types of photocatalysts used. Hence, the result clearly suggests the absence of internal diffusion limitations, or in other words, the system was confirmed to be operated under a kinetic-controlling regime.

Table 2. Half-Life Time, $t_{1/2}$, of Phenol Degradation for TiO_2 Supported on Quartz Sand, Silica Gel, and Glass Beads

	half-life time, $t_{1/2}$ (min)		
concn (mg/L)	TiO_2/quartz sand	TiO_2/silica gel	TiO_2/glass beads
25	46	56	133
50	91	116	180
75	171	187	314
100	228	286	448
115	305	342	575

It is also noted in Figure 5 that when the initial concentration of phenol was increased, the degradation of phenol decreased. This observation could be explained by several factors such as saturation of active sites and the formation of intermediates such as hydroquinone, catechol, resorcinol, and *p*-benzoquinone on the surface of catalyst.[21] Also, it should be noted that the increase in concentration affected light penetration into the phenol solution. Therefore, at higher initial concentration, the light penetration was reduced and fewer photons managed to reach the catalyst surface. The degradation followed the trend of TiO_2/quartz sand > TiO_2/silica gel > TiO_2/glass beads.

Regarding the different radiation absorptions by these catalysts, the higher activity in the degradation of phenol was obtained when TiO_2 was immobilized on the quartz sand. This means that there was no diffusion of ions to the TiO_2 films during the calcination process and the catalyst showed a higher degree of crystallinity. Pozzo et al.[10] reported that quartz sand was chosen as the supporting material because it was fairly transparent to near-UV radiation, had an acceptable surface bonding capacity with TiO_2, and provided a physical configuration that favored an easy liquid−solid separation. TiO_2 was a highly absorbing material, while quartz particles acted as an attractive alternative to immobilize small TiO_2 particles so as to permit their catalytic activity.

Chen et al.[22] reported that there were two steps that could act as the degradation determination step: the generation and migration of the photogenerated electron−hole pair and the reaction between hydroxyl radical and phenol molecules. Both steps occurred in series. At low concentration, the second step predominated and resulted in the increasing degradation rate with increased initial concentration. However, when the concentration of phenol increased further, the first step would become the governing step and degradation increased slowly with concentration until finally a virtually constant degradation was obtained. From Figure 5, it is clearly observed that the performance of TiO_2 supported on glass beads was relatively poor compared to the other two supported photocatalysts.

(b) Half-Life Time, $t_{1/2}$. Table 2 presents the value of half-life time, $t_{1/2}$, of phenol degradation for TiO_2 supported on quartz sand, silica gel, and glass beads. From the table, it is observed that the half-life time increased in this order: TiO_2/quartz sand < TiO_2/silica gel < TiO_2/glass beads. The half-life time for TiO_2/quartz sand and TiO_2/silica gel were quite close. However, the value of the half-life time for TiO_2/glass beads was significantly higher.

(c) Effect of Phenol Concentration on Reaction Rate. Figure 6 shows the relationship between the initial degradation rate against initial phenol concentration for TiO_2 supported on quartz sand, silica gel, and glass beads. The figure suggests that when the value of initial phenol concentration exceeded 50 mg/L, the initial degradation rate increment was very small and almost constant for TiO_2/quartz sand and TiO_2/silica gel. However, with TiO_2/glass beads, a slight decrease in initial rate of reaction was observed after 50 mg/L. This behavior clearly suggested the dependence of initial degradation rate on initial concentration of phenol at lower concentration.

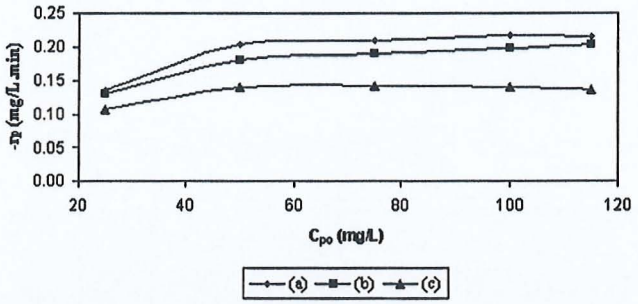


Figure 6. Plots of initial degradation rate against initial phenol concentration by supported TiO_2 on (a) quartz sand, (b) silica gel, and (c) glass beads. (Reaction time = 60 min.)

The lower rate of reaction at low phenol concentration (25 mg/L) was attributed to external mass transfer effects, and higher concentration led to higher reaction rate.[6] At phenol concentration higher than 50 mg/L, the increase in the rate of the photocatalytic reaction was generally impaired. This was due to high concentration of phenol beyond what that amount of photocatalyst was capable of degrading. Thus, an almost constant reaction rate was achieved.

Dobosz et al.[23] also reported that there were at least two reasons for the observed rate reduction. First, higher substrate concentration could favor the zero-order photocatalytic reaction kinetics (e.g., when phenol adsorption was not concentration dependent), and second, fast formation of some reaction intermediates at the very beginning of the process could result in formation of compounds such as polyphenols which would adsorb strongly onto the titania surface and block a significant part of photoreactive sites. In this study, both phenomena influenced the photoreaction rate when the concentration of phenol was higher. Therefore, under the experimental conditions, the highest removal was achieved with an initial phenol concentration of 50 mg/L.

3.2.2. Effect of pH. The effect of pH on phenol degradation using various supported TiO_2 photocatalysts was investigated in the range of pH 5.0−9.0. The results show that the phenol degradation depends significantly on the surface characteristics of the TiO_2 particles. As shown in Figure 7, TiO_2/glass beads gave the lowest removal and the phenol degradation order for the photocatalyst is as follows: TiO_2/quartz sand > TiO_2/silica gel > TiO_2/glass beads. The significant effect of pH on phenol degradation was observed, and the higher degradation was obtained at pH 5. Bouzaide et al.[24] and Parra et al.[25] reported that the point of zero charge for TiO_2 is around pH 6.8. TiO_2 particles were positively charged at lower than pH 6.8, while they carried negative charge above that pH.

It has been reported that the degradation is greatly influenced by the reaction pH. TiO_2 has amphoteric behavior that can change its surface charge properties when the pH of the solution changes. When the phenol solution is acidic, an attraction between TiO_2 photocatalyst and phenol molecules occurs and leads to an increase in the amount of phenol adsorbed on the positively charged surface of TiO_2 photocatalyst. For solution pH greater than 6.8, the groups with negative charge on the TiO_2 photocatalyst surface are assumed to increase gradually. Thus, it can be concluded that low pH values can facilitate the adsorption of the phenol molecule on the surface of supported TiO_2 photocatalyst, resulting in the enhancement of phenol degradation.

3.2.3. Effect of Hydrogen Peroxide (H_2O_2). One strategy to inhibit electron−hole pair recombination is by adding an external oxidant as an electron acceptor to the reaction. A

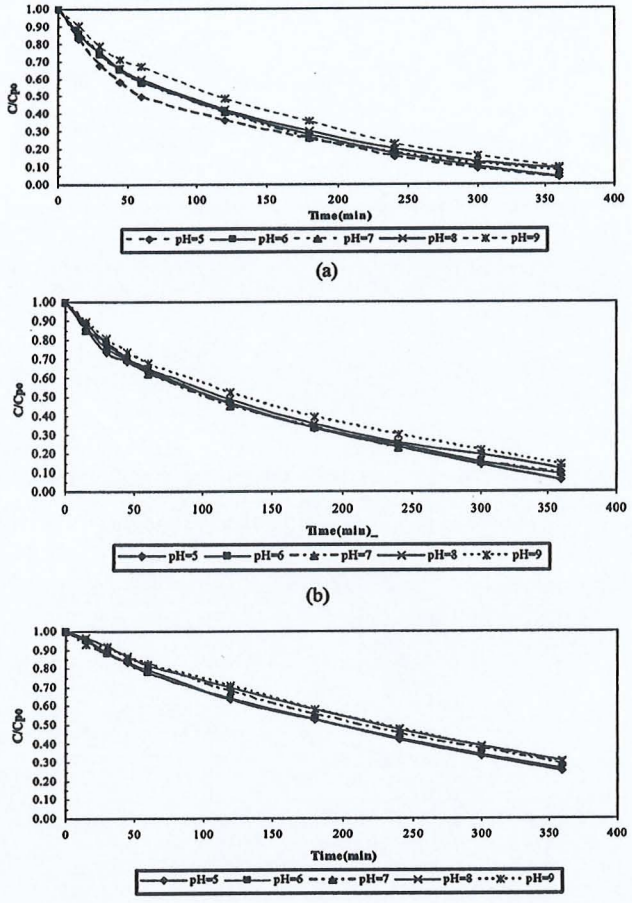


Figure 7. Effect of pH on phenol degradation by supported TiO_2 on (a) quartz sand, (b) silica gel, and (c) glass beads. (C_{po} = 50 mg/L and T = 30 °C.)

common oxidant that has been previously used to enhance the photocatalytic degradation is hydrogen peroxide (H_2O_2).[15,26] In the present study, the reaction behavior of the photocatalysts developed in the presence of H_2O_2 was studied for this role. However, as the holes were not created without the photocatalyst, the H_2O_2 had no role to play in this respect. For confirmation, this aspect was actually investigated earlier and, as expected, no significant difference was detected in the result when compared with the blank photocatalytic run (i.e., UV-C with TiO_2). Thus, the result was omitted for clarity of the data presentation in Figure 8, which shows the phenol degradation at various H_2O_2 concentrations using TiO_2/quartz sand, TiO_2/silica gel, and TiO_2/glass beads photocatalysts.

It can be seen in Figure 8 that phenol degradation increased in the presence of H_2O_2 concentration up to 200 mg/L. At this concentration, complete degradation of phenol was achieved at 3 h for TiO_2/quartz sand and TiO_2/silica gel while it was 5 h for TiO_2/glass beads. Compared to the phenol degradation in the absence of H_2O_2, this value was about 50% for TiO_2/quartz sand and TiO_2/silica gel and 38% for TiO_2/glass beads. Further increase in the concentration of H_2O_2 after this point did not increase the phenol degradation; instead, it caused the significant inhibition of phenol degradation.

H_2O_2 is suitable for trapping electrons by preventing the recombination of electron (e^-) and photogenerated hole (h^+) pairs. At the same time, the chances of formation of hydroxyl radical ($^{\bullet}OH$) on the surface of photocatalyst are also increased. However, in the presence of excess H_2O_2, the phenol degradation

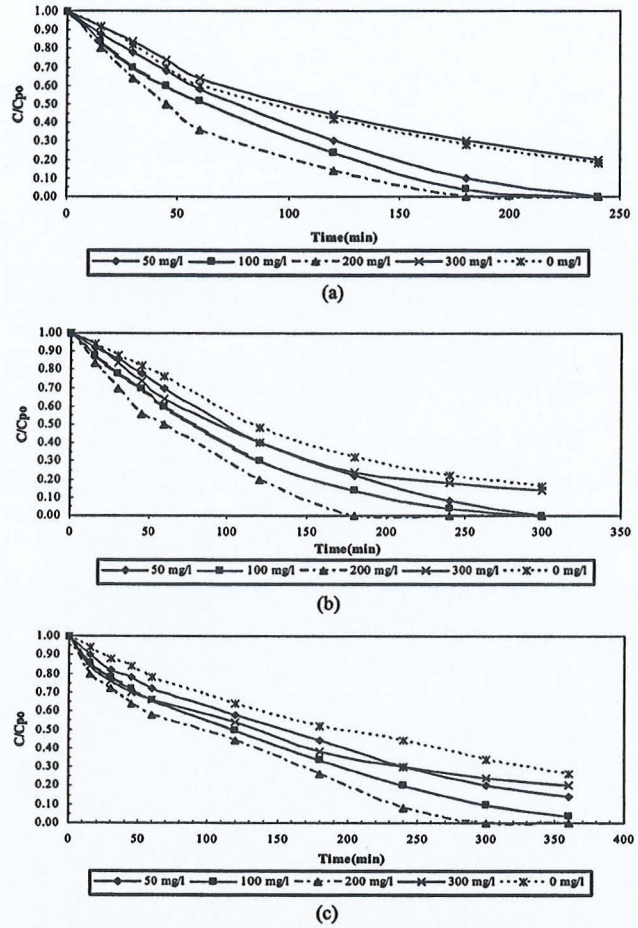


Figure 8. Phenol degradation at various H_2O_2 concentrations by supported TiO_2 on (a) quartz sand, (b) silica gel, and (c) glass beads. (C_{po} = 50 mg/L, pH 7, and T = 30 °C.)

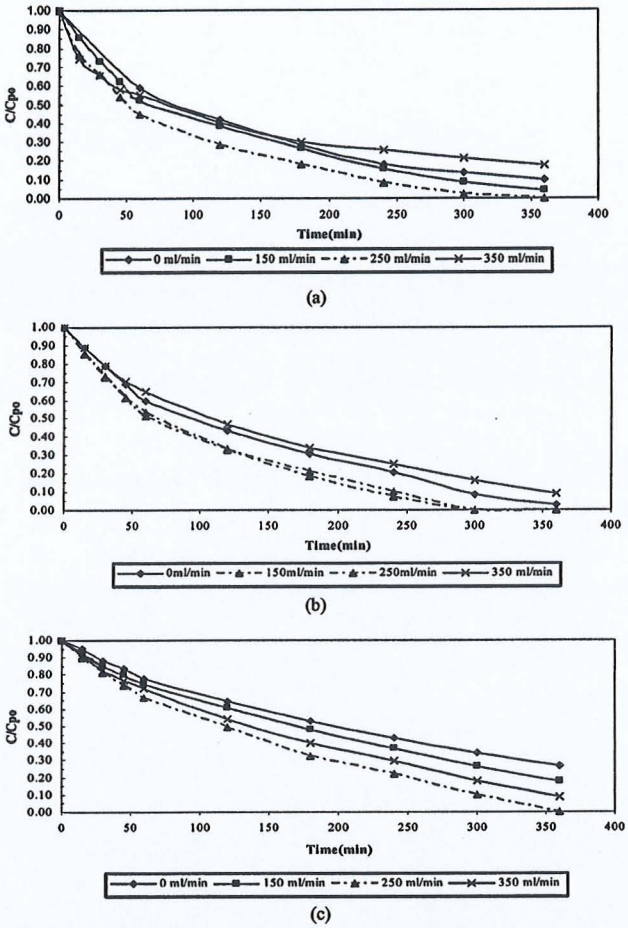


Figure 9. Phenol degradation at different air flow rates by supported TiO_2 on (a) quartz sand, (b) silica gel, and (c) glass beads. (C_{po} = 50 mg/L, pH 7, and T = 30 °C.)

decreased due to the consumption of •OH radicals and the formation of proxyl radicals (HO_2•). Therefore, it can be observed that the degradation decreased due to the consumption of •OH radicals and formation of HO_2• radicals, which were significantly less reactive than •OH radicals. Thus, the addition of H_2O_2 with a suitable concentration could assist the photocatalytic reaction in enhancing the degradation by preventing the recombination of e^- and h^+.[27]

3.2.4. Effect of Air Flow Rate. The cheapest and simplest way to supply a sufficient amount of oxygen (O_2) is by introducing air into the photocatalytic reactor. In this study, the air flow rate was varied to vary the rate at which oxygen was introduced into the reaction system. Basically, the corresponding oxygen supply rate was the actual reaction parameter. Based on 20.8% content of oxygen in purified air, the corresponding oxygen flow rates under the experimental conditions were 0, 31.2, 52.0, and 72.8 mL/min. The balance gas, i.e., nitrogen, did not participate in any reaction. Despite creating additional turbulence in the reaction vessel, no additional advantage was expected in the rate of external mass transfer as the system was already operating under the reaction-controlling regime even without air (oxygen) supplementation.

The effect of air flow rate on the photocatalytic degradation of phenol with supported TiO_2 photocatalysts is illustrated in Figure 9. From the figure, it is noted that initially, when the air flow rate was increased, the phenol degradation increased. However, when the air flow rate was further increased from 250 to 350 mL/min, the phenol degradation decreased. At the higher air flow rate, the bed expanded as the volume fraction of bubbles increased with air flow rate. Also, the larger number of bubbles might hinder absorbance of UV light to the photocatalyst.[28] Therefore, it can be concluded that the optimum value of air flow rate was 250 mL/min. The actual dissolved oxygen was measured to be 5−6 mg/L at this air flow rate. The dissolved oxygen improved the efficiency of the degradation by enhancing the separation of photogenerated electron−hole pairs, thereby increasing •OH radical concentration. The molecular oxygen adsorbed on the TiO_2 surface would trap the conduction band electrons to form the superoxide ions ($O_2^{\bullet -}$), so more •OH radicals were formed to result in the increase in the phenol degradation. The mechanistic pathway is as follows:

$$O_2(\text{ads}) + e^- \rightarrow O_2^{\bullet -} \xrightarrow{H^+} HO_2^{\bullet} \xrightarrow{HO_2^{\bullet}} O_2 + H_2O_2 \xrightarrow{e^-} O_2 + {}^{\bullet}OH + OH^-$$

The mechanism indicates that O_2 allows the increase of hole lifetime through its reaction with an electron to consequently result in the formation of oxidizing species •OH radicals.[29]

It is also shown in Figure 9 that phenol degradation was completed after 300 min at 250 mL/min air flow rate on TiO_2/quartz sand and TiO_2/silica gel. However, it was achieved only after 350 min with TiO_2/glass beads. Additionally, phenol degradation was the highest with TiO_2/quartz sand compared to the TiO_2/silica gel and TiO_2/glass beads. Besides, the concentration of phenol was the highest at 350 mL/min air flow

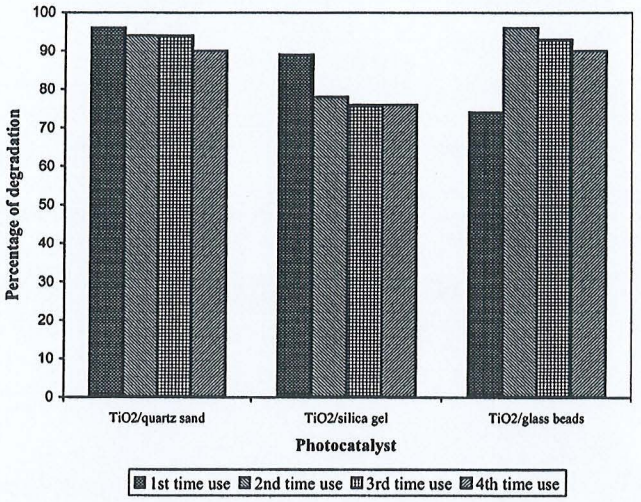


Figure 10. Comparison of photocatalytic activity of TiO_2 supported on quartz sand, silica gel, and glass beads for four times used. (C_{po} = 45 mg/L.)

Table 3. Effect of H_2O_2 Addition and Air Flow on the Half-Life Time, $t_{1/2}$, for Various Photocatalysts

	half-life time, $t_{1/2}$ (min)	
photocatalyst	H_2O_2 (200 mg/L)	O_2 (250 mL/min)
TiO_2/quartz sand	44	55
TiO_2/silica gel	60	74
TiO_2/glass beads	104	118

rate with TiO_2/quartz sand and TiO_2/silica gel. Thus, the phenol degradation from 0 to 150 mL/min was comparable with TiO_2/quartz sand and TiO_2/silica gel. However, it was significantly different with TiO_2/glass beads.

3.2.5. Effect of H_2O_2 and Air Flow. For a comparison between the effect of H_2O_2 concentration and air flow rate (dissolved oxygen supply rate), both were studied at their optimum values, i.e., 200 mg/L and 250 mL/min for H_2O_2 concentration and air flow rate, respectively. The results for these three supported TiO_2 photocatalyst are presented in Table 3. The data show the value of half-life time for the photocatalytic degradation of phenol using different supported TiO_2 photocatalysts. It is noted that the addition of H_2O_2 on the system was more effective than that of air. The addition of H_2O_2 in the phenol solution resulted in a shorter time for a complete degradation of phenol. Therefore, H_2O_2 was a better electron accepter than molecular oxygen. This was due to the minimum energy requirement to produce $^{\bullet}OH$, i.e., 3.0 eV for air flow rate while it was 2.2 eV for H_2O_2. H_2O_2 might produce $^{\bullet}OH$ radicals by photolytic splitting depending on the wavelength of the incident radiation. H_2O_2 is photosensitive, and the wavelength, $\lambda \sim 252$ nm, is needed to produce $^{\bullet}OH$ radicals.[7]

3.3. Performance of Recycled Supported TiO_2. In this study, spent supported TiO_2 photocatalyst was recycled to investigate its performance after repeated usage. After each run, the photocatalysts were calcined again at 600 °C for TiO_2/quartz sand and TiO_2/silica gel, while it was 700 °C for TiO_2/glass beads. Figure 10 shows the reusability of TiO_2 supported on quartz sand, silica gel, and glass beads obtained after four experimental runs. A reaction time of 6 h, an initial phenol concentration of 45 mg/L, and 0.25 g of each photocatalyst were chosen for each run. From the figure, it can be observed that the trend for percentage degradation of phenol was almost the same for TiO_2 supported on quartz sand and silica gel. It clearly shows that, for the TiO_2/quartz sand, the percentage of degradation for the second and third runs were only slightly lower than that in the first run and for the fourth time it was also slightly lower than for the earlier runs. For the TiO_2/silica gel, the percentage of degradation significantly decreased after the first time recycling. As for TiO_2/glass beads, the result was noticeably different. After the first run, the percentage of degradation increased significantly from 74% to 96% and then decreased slightly. This behavior was very much like the performance of TiO_2/quartz sand and TiO_2/silica gel after being recycled three and two times, respectively. TiO_2/glass beads were reactivated when it was calcined again. The possibility of a higher yield of anatase might be obtained, and this was the reason for such a good performance by TiO_2/glass beads when used for the second time.

After each run, it was observed that the color of the supported TiO_2, especially silica gel, gradually turned dark brown. The accumulation of intermediates with a poisoning effect on the surface of TiO_2/silica gel seemed higher, and this contributed to the low performance of photocatalytic activity when it was reused. The percentage degradation decreased to 78% in the second use compared to the first time use, which was 89%. The decrease in percentage of degradation was the highest for TiO_2/silica gel compared to the other two supports. However, after being regenerated at 600 °C for TiO_2/quartz sand and TiO_2/silica gel while at 700 °C for TiO_2/glass beads, all photocatalysts returned to their original color. Therefore, the deactivated photocatalyst can be regenerated by burning out all the carbon species.

This result was very encouraging that the photocatalyst activity could be recovered by a certain regeneration process. TiO_2/quartz sand and TiO_2/glass beads gave very good performances in the degradation of phenol in terms of their reusability. The result clearly suggests that supported TiO_2 photocatalysts used in this study were quite stable for repeated use. In the case of TiO_2/silica gel, the percentage of degradation decreased to about 11% when used for the second time. However, the percentage of degradation decreased slightly when reused again in the third and fourth runs.

4. Conclusion

TiO_2 photocatalysts supported on quartz sand, silica gel, and glass beads were successfully synthesized using the sol−gel method. XRD analyses confirmed the existence of crystallized anatase TiO_2 phase with some minor rutile phase as well. Different calcination temperatures were needed to obtain the anatase phase: 600 °C for TiO_2/quartz sand and TiO_2/silica gel, while TiO_2/glass beads need 700 °C. SEM pictures of the catalysts showed signs of cracks on silica gel and quartz sand, whereas only minor cracks appeared on the glass beads. The performance study of the synthesized supported TiO_2 photocatalysts under UV-C irradiation was performed in a batch reactor for the degradation of phenol. A series of experiments were conducted to investigate the effects of initial phenol concentration, solution pH, H_2O_2 concentration, and air flow rate (oxygen supply rate). The most suitable initial concentration of phenol was found to be 50 mg/L. Acidic conditions favored phenol degradation reaction. The addition of H_2O_2 and air flow increased the phenol degradation. The optimum values of H_2O_2 concentration and air flow rate were found to be 200 mg/L and 250 mL/min, respectively. After four times of repeated use, the system showed only a slight decrease in activity for TiO_2/quartz sand and TiO_2/silica gel. As for the TiO_2/glass beads, there was an increase in activity after it was regenerated. Therefore, the supported photocatalysts synthesized in this study have been proven to be stable for repeated usage.

Acknowledgment

The authors gratefully acknowledge the Universiti Sains Malaysia and Ministry of Science, Technology and Innovation Malaysia for funding this project in the form of a short-term grant (No. 6035220) and IRPA Grant (No. 6012806), respectively.

Literature Cited

(1) Wang, Z.; Cai, W.; Hong, X.; Zhao, X.; Xu, F.; Cai, C. Photocatalytic Degradation of Phenol in Aqueous Nitrogen-doped TiO_2 Suspensions with Various Light Sources. *Appl. Catal., B* **2005**, *57*, 223.

(2) Hongfei, L.; Kalliat, T. V. An Optical Fiber Monolith Reactor for Photocatalytic Wastewater Treatment. *AIChE J.* **2006**, *52*, 2271.

(3) Baolong, Z.; Baishun, C.; Keyu, S.; Shangjin, H.; Xiaodong, L.; Zongjie, D.; Kelian, Y. Preparation and Characterization of Nanocrystal Grain TiO_2 Porous Microspheres. *Appl. Catal., B* **2003**, *40*, 253.

(4) Moonsiri, M.; Rangsunvigit, P.; Chavadej, S.; Gulari, E. Effects of Pt and Ag on the Photocatalytic Degradation of 4-Chlorophenol and Its by-Products. *J. Chem. Eng.* **2004**, *97*, 241.

(5) Kolen'ko, Y. V.; Garshev, A. V.; Churagulov, B. R.; Boujday, S.; Portes, P.; Colbeau-Justin, C. Photocatalytic Activity of Sol-gel Derived Titania Converted into Nanocrystalline Powders by Supercritical Drying. *J. Photochem. Photobiol., A* **2005**, *172*, 19.

(6) Senthilkumaar, S.; Porkodi, K.; Gomathi, R.; Geetha Maheswari, A.; Manonmani, N. Sol-gel Derived Silver Doped Nanocrystalline Titania Catalyzed Photodegradation of Methylene Blue from Aqueous Solution. *Dyes Pigm.* **2006**, *69*, 22.

(7) Grzechulska, J.; Morawski, A. W. Photocatalytic Labyrinth Flow Reactor with Immobilized P25 TiO_2 Bed for Removal of Phenol from water. *Appl. Catal., B* **2003**, *46*, 415.

(8) Matthews, W. R. Photooxidative Degradation of Colored Organics in Water using Supported Catalysts TiO_2 on Sand. *Water Res.* **1991**, *25*, 1169.

(9) Pozzo, R. L.; Giombi, J. L.; Baltanas, M. A.; Cassano, A. E. The Performance in a Fluidized Bed Reactor of Photocatalysts Immobilized onto Inert Supports. *Catal. Today* **2000**, *62*, 75.

(10) Balasubramanian, G.; Dionysiou, D. D.; Suidan, M. T.; Baudin, I.; Laine, J. M. Evaluating the Activities of Immobilized TiO_2 Powder Films for the Photocatalytic Degradation of Organic Contaminants in Water. *Appl. Catal., B* **2004**, *47*, 73.

(11) Xie, Y.; Yuan, C. Photocatalytic Activity and Recycle Application of Titanium Dioxide Sol for X-3B Photodegradation. *J. Mol. Catal. A* **2003**, *206*, 419.

(12) Yun, Y. J.; Chung, J. S.; Kim, S.; Hahn, S. H.; Kim, E. Low Temperature Coating of Sol-gel Anatase Thin Films. *J. Mater. Lett.* **2004**, *58*, 3703.

(13) Chao, H. E.; Yun, Y. U.; Xingfang, H. U.; Larbot, A. Effect of Silver Doping on the Phase Transformation and Grain Growth of Sol-gel Titania Powder. *J. Eur. Ceram. Soc.* **2003**, *23*, 1457.

(14) Byrne, J. A.; Eggins, B. R.; Brown, N. M. D.; McKinney, B.; Rouse, M. Immobilization of TiO_2 Powder for the Treatment of Polluted water. *Appl. Catal., B* **1998**, *17*, 25.

(15) Ling, C. M.; Mohamed, A. R.; Bhatia, S. Performance of Photocatalytic Reactors using Immobilized TiO_2 Film for the Degradation of Phenol and Methylene Blue Dye Present in Water Stream. *Chemosphere* **2004**, *57*, 547.

(16) Balasubramaniam, G.; Dionysiou, D. D.; Suidan, M. T.; Subramanian, V.; Baudin, I.; Laine, J. M. Titania Powder Modified Sol-gel Process for Photocatalytic Applications. *J. Mater. Sci.* **2003**, *38*, 823.

(17) Exarhos, J.; Hess, N. Spectroscopic Measurements of Stress Relaxation during Thermally Induced Crystallization of Amorphous Titania Films. *Thin Solid Films* **1992**, *220*, 254.

(18) Qiu, W.; Zheng, Y. A Comprehensive Assessment of Supported Titania Photocatalysts in a Fluidized Bed Photoreactor: Photocatalytic Activity and Adherence Stability. *Appl. Catal., B* **2007**, *71*, 151.

(19) Guillard, C.; Beaugiraud, B.; Dutriez, C.; Herrmann, J. M.; Jaffrezic, H.; Renault, N. J.; Lacroix, M. Physicochemical Properties and Photocatalytic Activities of TiO_2-films Prepared by Sol-gel Methods. *Appl. Catal., B* **2002**, *39*, 331.

(20) Alapi, T.; Dombi, A. Comparative Study of the UV and UV/VUV-induced Photolysis of Phenol in Aqueous Solution. *J. Photochem. Photobiol., A* **2007**, *188*, 409.

(21) Sobczynski, A.; Duczmal, L.; Zmudzinski, W. Phenol Destruction by Photocatalysis on TiO_2: an Attempt to Solve the Reaction Mechanism. *J. Mol. Catal. A* **2004**, *213*, 225.

(22) Chen, D. Ray, A. K. Photocatalytic Kinetics of Phenol and its Derivatives over UV Irradiated TiO_2. *Appl. Catal., B* **1999**, *23*, 143.

(23) Dobosz, A.; Sobczynski, A. The Influence of Silver Additives on Titania Photoactivity in the Photooxidation of Phenol. *Water Res.* **2003**, *37*, 1489.

(24) Bouzaide, I.; Ferronato, C.; Chovelon, J. M.; Rammah, M. E.; Herrmann, J. M. Heterogeneous Photocatalytic Degradation of the Anthraquinonic Dye, Acid Blue 25 (AB25): a Kinetic Approach. *J. Photochem. Photobiol., A* **2004**, *168*, 107.

(25) Parra, S.; Sanca, S. E.; Guasaquillo, I.; Thampi, K. R. Photocatalytic Degradation of Atrazine using Suspended and Supported TiO_2. *Appl. Catal., B* **2004**, *51*, 107.

(26) Irmak, S.; Kusvuran, E.; Erbatur, O. Degradation of 4-Chloro-2-Methylphenol in Aqueous Solution by UV Irradiation in the Presence of Titanium Dioxide. *Appl. Catal., B* **2004**, *54*, 85.

(27) Konstantinou, I. K.; Albanis, T. A. TiO_2-assisted Photocatalytic Degradation of Azo Dyes in Aqueous Solution: Kinetic and Mechanistic Investigations A review. *Appl. Catal., B* **2004**, *49*, 1.

(28) Nam, W.; Kim, J.; Han, G. Photocatalytic Oxidation of Methyl Orange in a Three-phase Fluidized Bed Reactor. *Chemosphere* **2002**, *47*, 1019.

(29) Chhor, K.; Bocquet, J. F.; Colbeau-Justin, C. Comparative Studies of Phenol and Salicylic Acid Photocatalytic Degradation: Influence of Adsorbed Oxygen. *Mater. Chem. Phys.* **2004**, *86*, 123.

Received for review February 24, 2007
Revised manuscript received September 18, 2007
Accepted October 1, 2007

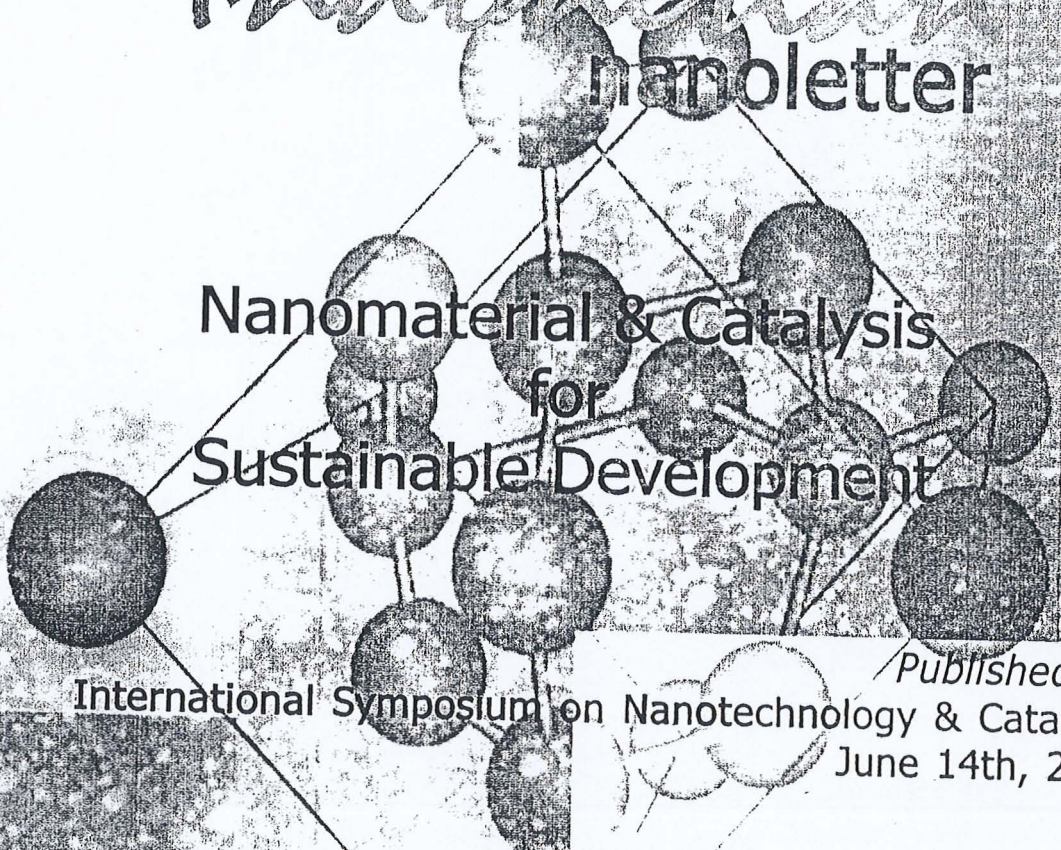
IE070284X

Vol. 2, No.1, Juni 2007

ISSN 1907-803X

Indonesian nanoletter

Nanomaterial & Catalysis for Sustainable Development



Published at:
International Symposium on Nanotechnology & Catalysis
June 14th, 2007

NanoTech Indonesia

Publisher:
Indonesian Society for Nanotechnology

The Effects of Catalytic Nanoparticles on the Growth of Single-walled Carbon Nanotubes and Photo-Degradation of Phenol

Abdul Rahman Mohamed*, Shwu-Miin Tan, Minoo Tasbihi, Siang-Piao Chai

School of Chemical Engineering, Engineering Campus, Universiti Sains Malaysia, Seri Ampangan, 14300 Nibong Tebal, S.P.S. Pulau Pinang, Malaysia.
*Email: chrahman@eng.usm.my

Catalysts are usually nanoparticles composed of clusters of atoms, often metals or metal oxides, with particle size varying between 1 – 100 nm. Nanoparticle catalysts are highly active since most of the particle surfaces can be available to catalysis. Modern surface science studies reveal that chemisorption and catalytic reaction involve the adsorbed molecules binding to the active metals, breaking the surface chemical bonds and weakening metal-metal bonds as the particles restructure. Since the atoms in nanoparticles have low coordination, such adsorbate-induced restructuring is facile. Owing to the highly effectiveness of nanoparticles in catalysis, many of them have found applications in ammonia synthesis, environmental protection, photocatalysis, waste removal, fiber and mechanical industries. Catalysis can play two principal roles in nanoscience, including (1) catalysts can be involved in some methods for preparing nanomaterials such as nanotubes; (2) some nanostructures themselves can serve as catalysts for improved chemical reactions. Both aspects are highlighted, covering the topics of the use of catalysts for synthesizing carbon nanotubes (CNTs) and nano-TiO_2 as catalyst for photocatalytic degradation of phenol.

Single-walled carbon nanotubes (SWNTs), demonstrating unique structural, mechanical, and electrical properties [1], are novel nanomaterials that possess many new important applications such as the quantum wires, field-effect transistors, field emitters, diodes, gas sensor, electric power storage, targeted drug delivery, catalyst support, reinforcing elements in composites, etc. [2]. They consist of only a single-graphene sheet, which are the most valuable type of CNTs, and hardly to be synthesized. In this study, various Co-, Ni-, and Fe-

based catalysts were developed using conventional impregnation method at different calcination temperatures. The detailed experimental setup and procedures have been reported previously [3-5]. These catalysts were tested in methane decomposition for synthesizing SWNTs. The experimental results show that SWNTs had been successfully synthesized from methane decomposition over FeO_x/Al_2O_3 catalysts which were calcined at 300 °C, 600 °C and 850 °C as well as over CoO_x/Al_2O_3 catalysts which were calcined at 600 °C and 850 °C. Further discussion on the findings will be elaborated. Besides this, the synthesis of other types of CNTs, including multi-walled CNTs (MWNTs) and Y-junction CNTs, will be discussed too.

Photocatalysis of nanocrystalline TiO_2 has many of advantages on phenolic wastewater treatment, such as high catalysis efficiency, energy-saving, non-pollution and can degrade all kinds of organic pollutants from water effectively. A way to increase photocatalytic activity is the preparation of a nanostructural to get a high surface area that is directly related with catalytic activity. In this study, nano-TiO_2 has been developed for photocatalytic degradation of phenol. In order to evaluate the photoactivity of prepared nano-TiO_2 catalyst, the experiment was conducted in a batch reactor. The findings from the experimental work show that the degradation of phenol using prepared nano-TiO_2 is higher than the Degussa P25, a commercial catalyst. The results further indicate that the prepared nano-TiO_2 has larger surface area, higher porosity and is of smaller particle size than the Degussa P25. This is the reason why the prepared nano-TiO_2 is more active than the commercial TiO_2 powder for photocatalytic degradation of phenol.

References

[1] S.G. Louie, in: M.S. Dresselhaus, G. Dresselhaus, P. Avouris (Eds.), Carbon Nanotubes: Synthesis, Structure, Properties, and Applications, Springer, New York, 2001, pp. 113-145.

[2] R.H. Baughman, A.A. Zakhidov, W.A. de Heer, Science 297 (2002) 787-792.

[3] S.P. Chai, S.H.S. Zein, and A.R. Mohamed, Chem. Phys. Lett. 426 (2006) 345-350.

[4] S.P. Chai, S.H.S. Zein, and A.R. Mohamed, Carbon 45 (2007) 1535-1541.

[5] S.P. Chai, S.H.S. Zein, and A.R. Mohamed, Applied Catalysis A: General, (In Press).

Bulletin of Chemical Reaction Engineering & Catalysis, x(x), 2007, xx-xx

Advances in Nanocatalysis Research for Carbon Nanotubes Formation and Photocatalytic Degradation of Phenol

Abdul Rahman Mohamed *, Minoo Tasbihi, Siang-Piao Chai

School of Chemical Engineering, Engineering Campus, Universiti Sains Malaysia, Seri Ampangan, 14300 Nibong Tebal, S.P.S. Pulau Pinang, Malaysia

Selected paper from Congress and Symposium of MKICS 2007 (18-19 April 2007)

Introduction

Catalysts daily accelerate and boost thousands of different chemical reactions, and thereby form the basis for the multibillion dollar chemical industry worldwide and indispensable environmental protective technologies. Research in nanotechnology and nanoscience is expected to have a great impact on the development of new catalysts. The detailed understanding of chemistry of nanostructures and the ability to control materials on the nanometer scale will ensure a rational and cost-efficient development of new and more capable catalysts for a chemical process.

Recently, countries in Asia are setting up nanotechnology initiatives. Some of the major initial advances are expected to come in areas of increasing rates of reaction using nanocatalysts in catalytic processes. Although most production by catalysis is performed in large-scale reactors, the reaction that actually takes place in the catalyst occurs on the surface of highly dispersed metallic particles with typical dimensions of 1 – 100 nm (Fig. 1). Catalysts are perhaps the first industrial nanotechnology. It is well known that the catalytic activity of supported metal catalysts is strongly dependent on the size and shape of the metal particles. Nanoparticle catalysts are highly active since most of the particle surfaces can be available to catalysis. Many of the nanocatalysts have found applications in ammonia synthesis, environmental protection, photocatalysis, waste removal, fiber and mechanical industries.

Catalysis can play two principal roles in nanoscience, including (1) catalysts can be involved in some methods for preparing nanomaterials such as nanotubes; (2) some nanostructures themselves can serve as catalysts for additional chemical reactions. Both nanocatalysis aspects are highlighted in this paper, covering the topics of the use of nanocatalyst for photocatalytic degradation of phenol and methane decomposition into carbon nanotubes (CNTs).

1. Formation of CNTs via catalytic decomposition of methane

Carbon nanotubes (CNTs), demonstrating unique structural, mechanical, and electrical properties [1], possess many new important applications such as the quantum wires, field-effect transistors, field emitters, diodes, gas sensor, electric power storage, targeted drug delivery, catalyst support, reinforcing elements in composites, etc. [2-4]. This section highlights the tailor-making of CNTs with desirable morphologies through manipulating the nano-active metals and support of a catalyst.

Fig. 2 shows the TEM images of NiO/SiO_2 and NiO/Al_2O_3 catalysts prepared via conventional impregnation method. The dark spots are NiO crystallites (indicated by arrows), and the shallow matters around these crystallites are assigned to the catalyst supports. It can be noted that NiO supported on SiO_2 is of larger size. Apparently, very

* Corresponding Author.
E-mail address: chrahman@eng.usm.my (Abdul Rahman Mohamed)

Copyright © 2007, BCREC, ISSN 1978-2993

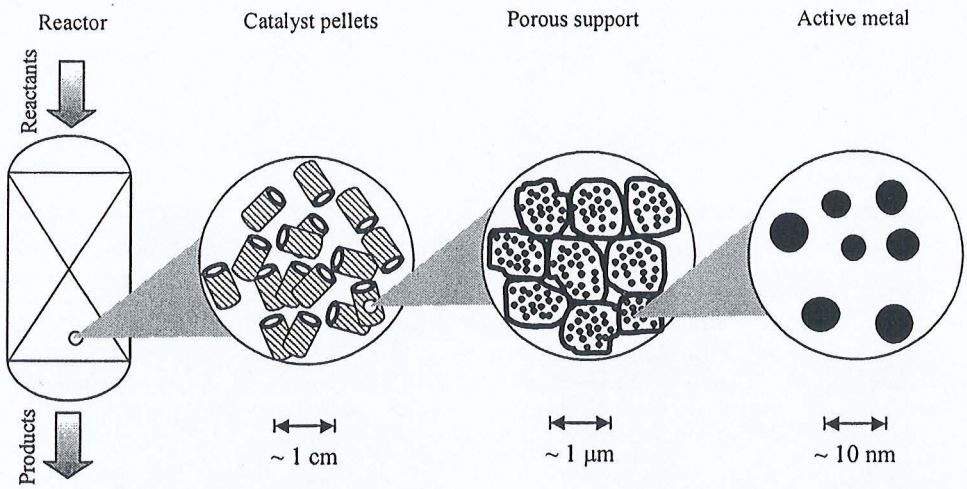


Fig. 1. Schematic diagram showing the typical catalyst structure used in a chemical process.

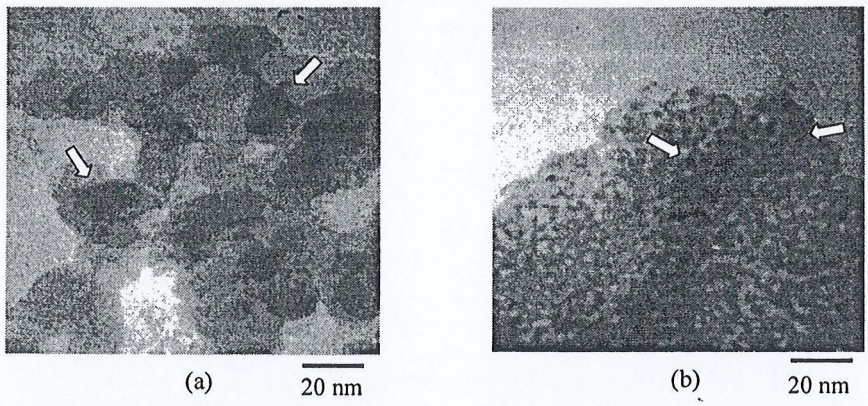


Fig. 2. TEM images of catalysts. (a) NiO/SiO_2 and (b) NiO/Al_2O_3 [5]

small size NiO crystallites are formed on Al_2O_3 support. The formation of smaller size NiO crystallites on alumina support is because of NiO/Al_2O_3 catalyst possesses stronger metal-support interaction (MSI) effect. This helps in the dispersion of NiO crystallites, preventing their agglomeration to form larger cluster. On the contrary, NiO crystallites of larger size are formed on silica support. This is due to the lower MSI of NiO/SiO_2 catalyst [5]. This finding shows that the size of the active metals can be controlled by doping them on different catalyst supports [6,7].

Fig. 3 shows the TEM images of the NiO/SiO_2 and NiO/Al_2O_3 catalysts after 1 h reaction with methane at 700°C. It was noted that CNTs were grown on both catalysts. The size of CNTs formed on NiO/SiO_2 was larger than that on NiO/Al_2O_3. For NiO/SiO_2 catalyst, only multi-walled CNTs (MWNTs) were formed. Interestingly, a mixture of MWNTs and single-walled CNTs (SWNTs) were grown on NiO/Al_2O_3 catalyst at 700°C, shown in Fig. 3b-d and indicated by arrow A1,2 and arrow B, respectively. From the TEM analysis, we noticed that the synthesized SWNTs appeared in two forms, i.e. isolated (arrow A1) and bundles (arrow A2). The Raman spectrum (not shown in this paper) shows strong intensity at radial breathing mode (RBM), indicating that the occurrence of SWNTs was dominant. This analysis also reveals that the synthesized SWNTs have a diameter in the range from 0.58 nm to 2.02 nm [8].

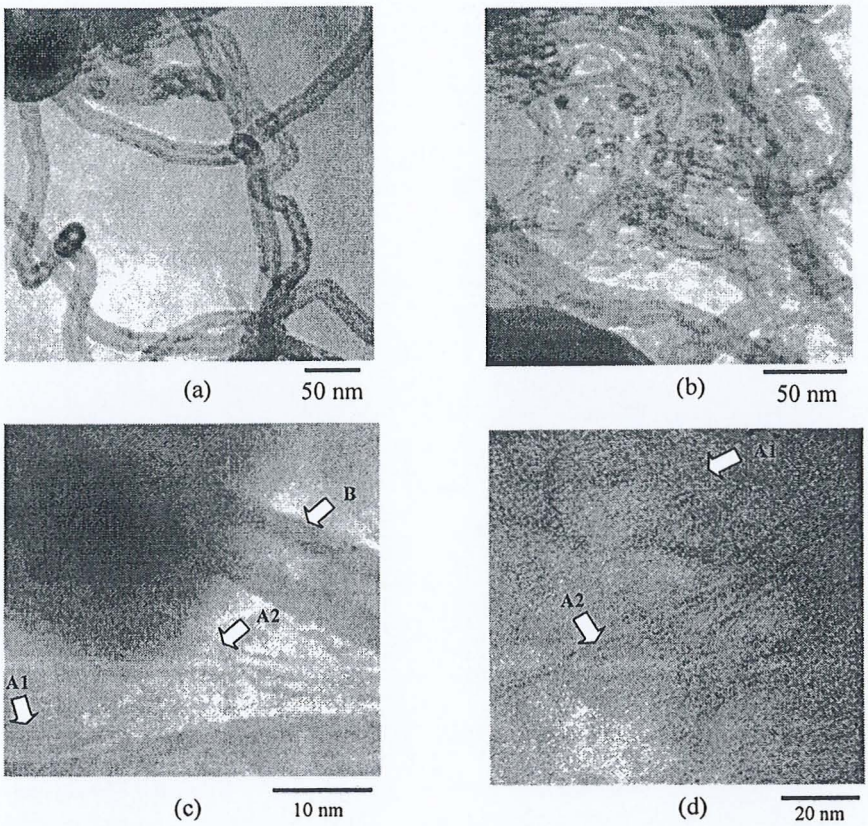


Fig. 3. TEM images of CNTs formed on the catalysts after 1hr reaction with methane. (a) NiO/SiO_2 and (b-d) NiO/Al_2O_3 [8].

To arrive at the understanding why SWNTs were formed on NiO/Al_2O_3 catalyst, we have to know the nature of the catalyst structure. It is well accepted that the formation of CNTs is governed by the size of the active metal particles. The formation of SWNTs on NiO/Al_2O_3 catalyst did reveal that very small size of NiO were formed on Al_2O_3 support and this size was small enough for growing SWNTs. As what we believe, the formation of these ultra-small NiO nanoparticles was mainly induced by the strong MSI effect between the NiO and the Al_2O_3 support, as previously mentioned. This is because strong MSI allowed high NiO dispersion and prevented NiO from agglomerating and forming larger clusters. Probably, some adjacent NiO particles might combine/sinter during the calcination and reaction stages to form larger NiO particles and these particles led to the formation of MWNTs as observed in the TEM image.

Fig. 4a shows the TEM image of CoO-MoO/Al_2O_3 catalyst. The dark spots represent the active metals (indicated by arrows) and the shallow matter is the alumina support. The active metals are the catalyst component subjected to methane decomposition and the growth of CNTs. Fig. 4b shows the TEM image of MWNTs grown on CoO-MoO/Al_2O_3 catalyst from methane decomposition at 700°C. The high degree of diameter control and uniformity of the synthesized MWNTs can be seen clearly in the TEM image. In addition, the TEM analysis shows that out of total 156 MWNTs measured, more than 98% had diameters ranging from 6 nm to 12 nm. The calculated average diameter and standard deviation were 9.0 nm and 1.4 nm, respectively. This indicates that the formed MWNTs were of higher uniform diameter.

Although many effective ways in producing CNTs with nearly uniform diameters have been suggested in the literature, this study represents a simple and convenient way to achieve this objective. This also reflects a real possibility to produce

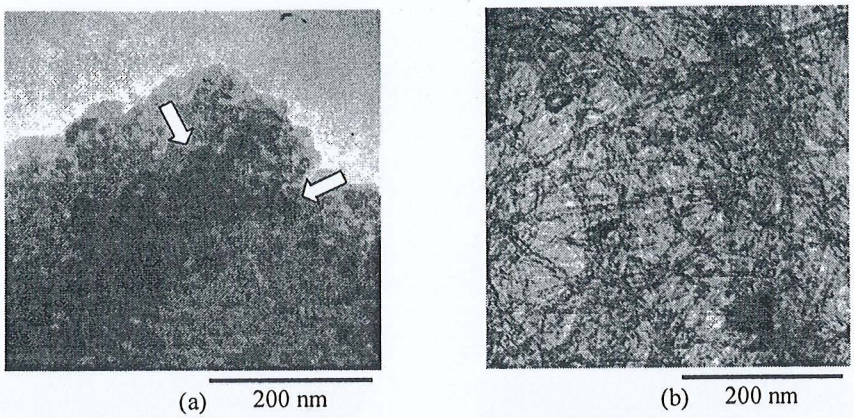


Fig. 4. TEM images of (a) CoO-MoO/Al_2O_3 catalyst, and (b) CNTs formed on the catalyst after 2 hrs methane decomposition [9]

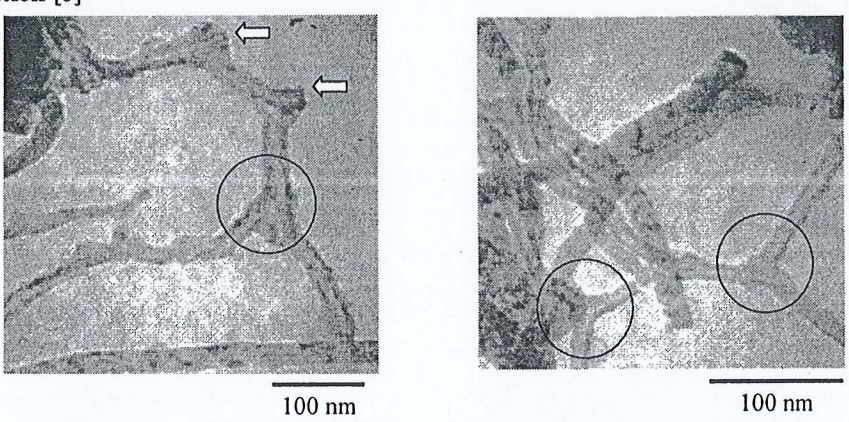


Fig. 5. TEM images of Y-junction CNTs grown on NiO-CuO-MoO/SiO_2 catalyst [10].

CNTs of uniform diameter by means of a simpler and cheaper approach in the near future, i.e. through controlling the size of the active metals [9].

Fig. 5 shows the TEM images of Y-junction CNTs grown on the complex NiO-CuO-MoO/SiO_2 catalyst from methane decomposition at 700oC. The circles drawn in Fig. 5 indicate the junction part of CNTs. One can notice that three joining tubes branch out from the junction, forming a Y structure. We suggest that Mo is the important factor for the growth of Y-junction CNTs. A small amount of MoO added to NiO-CuO enhances the growth of Y-junction CNTs. A growth model of this special structure is proposed based on the observation of the CNTs' stem and branch. Fig. 6 shows the proposed sequential growth mechanism of straight and Y-junction CNTs [10].

The diagram shown in Fig. 6 illustrates the conditions of the NiO–CuO–MoO/SiO_2 catalyst before and after CVD reaction. The black dots represent active metals and white circles represent the catalyst support. We expected that not all the added MoO incorporated with NiO–CuO on the SiO_2 support. MoO-free NiO–CuO catalyst would grow straight CNTs, indicated by (i), and (ii) in Fig. 6, whereas MoO-incorporated NiO–CuO led to the growth of CNT stems and branches. Their possible growth mechanism is represented by (iii), and (iv) in Fig. 6. It is likely that the addition of a small amount of MoO to NiO–CuO acts as nucleation sites, seeding the growth of CNT branches. We believe that, after some time, the surface carbons deposited on the active metals will join the graphitic layers for both CNT stems and branches, forming a poorly graphitized junction part. This is evident when most of the junction parts observed under the TEM exhibit poor crystalline wall structure. The continuous growth of a CNT stem forms the Y-

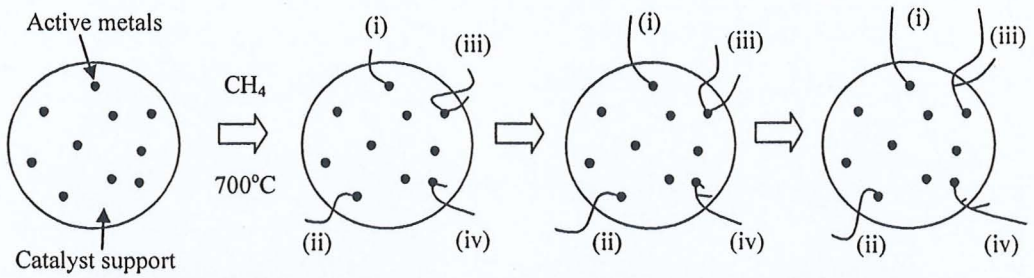


Fig. 6. Schematic diagrams showing the proposed sequential growth mechanism of straight (i, ii) and Y-junction (iii, iv) CNTs [10].

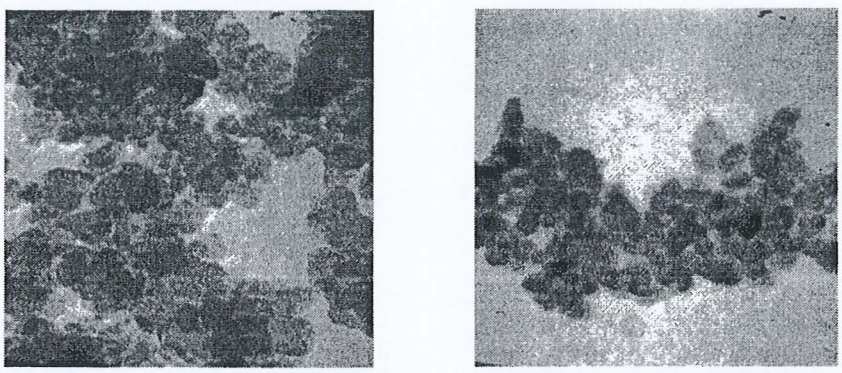


Fig. 7. TEM images of nanocrystalline TiO_2 prepared using sol-gel method

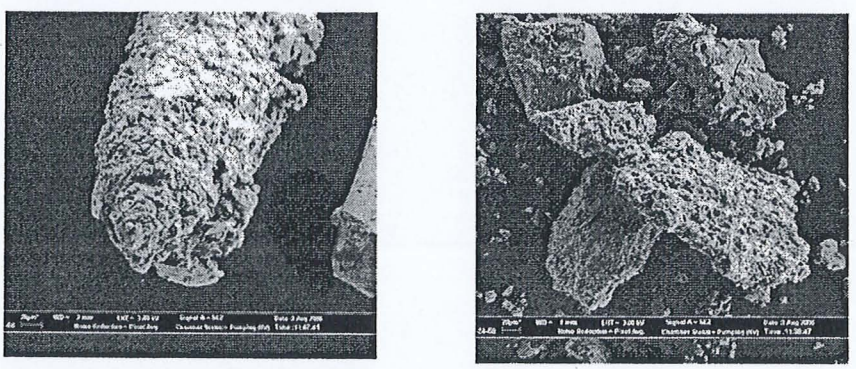


Fig. 8. SEM images of nanocrystalline TiO_2 using sol-gel method support

junction structure. In the process that follows, other branches could also be formed on the Y-junction CNT stem. The growth mechanism of a second CNT branch is indicated by arrows in Fig. 5 and represented by (iv) in Fig. 6. Y-junction CNTs without short branches, indicated by circles in Fig. 5 were grown on the catalyst, following the mechanism represented by (iii) in Fig. 6 .

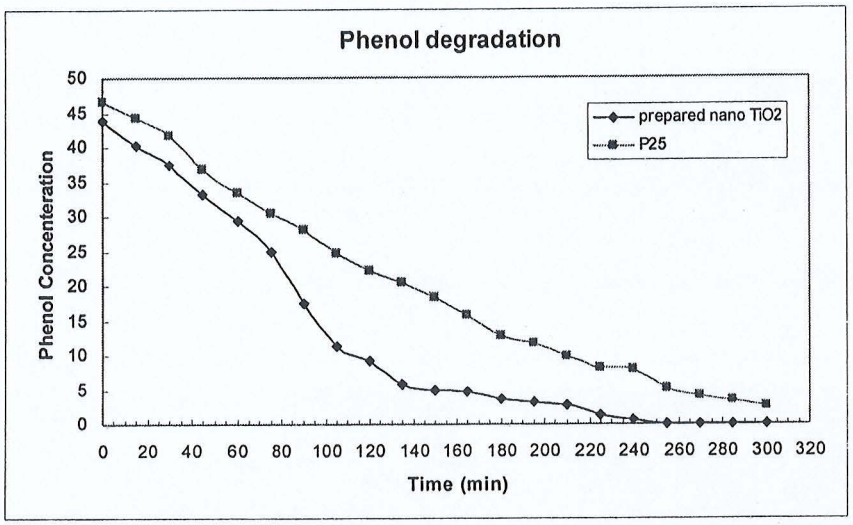


Fig. 9. Photocatalytic degradation of phenol, catalyst 0.6 g, initial phenol concentration of 50 ppm

2. Nano TiO_2 for photocatalytic degradation of phenol

Phenol and substituted phenols are widely distributed at low concentration in natural waters, including algal secretion, hydrolyzable tannins and flavanoids and humification processes, and at high concentrations in some industrial wastewater discharge and agricultural activities [11]. Treating phenolic wastewater to harmless level is an arduous process for many biological and chemical processes due to its high solubility and stability in water.

Although a wide range of catalyst has been tested, titania (TiO_2) seems to be the most widely used catalyst because of its photocatalytic, conservative nature, low cost, low toxicity, corrosion resistant [12] and high stability to light illumination. A way to increase photocatalytic activity is the preparation of a nanostructural to get a high surface area that is directly related with catalytic activity [13]. Moreover, photocatalysis of nanocrystalline TiO_2 has many of advantages on wastewater treatment, such as high catalysis efficiency, energy-saving, non-pollution and can degrade all kinds of organic pollutants from water effectively. All of these merits make photocatalysis of TiO_2 a fine and attractive method in the research of water treatment and it is supposed to be used widely in future.

Fig. 7 shows the TEM images of the prepared nano TiO_2 catalyst. The TEM images data revealed that the catalyst consists of uniform and spherical particles with an average nanoparticles size of 11.50 nm. The SEM images of the catalyst are shown in Fig. 8. It was noted that the catalyst consisting of fine irregular TiO_2 particles agglomerated to form a porous structure.

In order to evaluate photoactivity of prepared nano TiO_2 catalyst, the photocatalytic degradation of phenol in a batch reactor was studied. Fig. 9 shows the photoactivity of the prepared nano TiO_2 catalyst and commercialized TiO_2 powder (Degussa P25). The figure obviously indicates that the phenol concentration decreases with the increase of reaction time. The degradation of phenol using prepared nano TiO_2 is higher than the Degussa P25. It is well known that the higher efficiency of prepared nano TiO_2 is influenced by many factors such as particle size and surface area. In this study, the findings show that the prepared nano TiO_2 has larger surface area, higher porosity and is of smaller particle size than the Degussa P25. This is the reason why the prepared nano TiO_2 is more active than the commercialized TiO_2 powder for photocatalytic degradation of phenol.

Acknowledgements

The authors would like to acknowledge the financial support provided by the Academic Sciences of Malaysia and the Ministry of Science, Technology and Innovation Malaysia under Scientific Advancement Grant Allocation (SAGA) (Project: A/C No. 6053001), IRPA Long-Term Grant (Project: A/C No. 6012806) and IRPA Short-Term Grant (Project: A/C No. 6035220) .

References

[1] S.G. Louie, in: M.S. Dresselhaus, G. Dresselhaus, P. Avouris (Eds.), Carbon Nanotubes: Synthesis, Structure, Properties, and Applications, Springer, New York, 2001, pp. 113-145.

[2] R.H. Baughman, A.A. Zakhidov, W.A. de Heer, Science 297 (2002) 787-792.

[3] P. Calvert, in: T.W. Ebbesen (Eds.), Carbon Nanotubes: Preparation and Properties, CRC, New York, 1997, pp. 277-292.

[4] A.G. Mamalis, L.O.G. Vogtländer, A. Markopoulos, Precis. Eng. 28 (2004) 16-30.

[5] S.P. Chai, S.H.S. Zein, A.R. Mohamed, Diam. & Relat. Mater. (In Press, Accepted Manuscript).

[6] S.H.S. Zein, A.R. Mohamed, and S.P. Chai, Stud. Surf. Sci. Catal. 159 (2006) 725-728.

[7] S.P. Chai, S.H.S. Zein, and A.R. Mohamed, Chem. Phys. Lett. 426 (2006) 345-350.

[8] S.P. Chai, S.H.S. Zein, and A.R. Mohamed. Mater. Lett. (In Press, Corrected Proof).

[9] S.P. Chai, S.H.S. Zein, and A.R. Mohamed, Carbon (In Press, Accepted Manuscript).

[10] S.P. Chai, S.H.S. Zein, and A.R. Mohamed, Solid State Commun. 140 (2006) 248-250.

[11] A. Sobczynski, L. Duczmal, W. Zmudzinski, J. Mol. Catal. A: Chemical 213 (2004) 225-230.

[12] M. Moonsiri, P. Rangsunvigit, S.Chavadej & E.Gulari, Chem. Eng. J. 97 (2004) 241-248.

[13] Y. Hwu, Y. D Yao, N. F. Cheng, C. Y. Tung & H. M. Lin, Nanostructured Materials 9 (1997) 355-358

DEVELOPMENT OF SUPPORTED TiO_2 PHOTOCATALYST BASED ADSORBENT FOR PHOTOCATALYTIC DEGRADATION OF PHENOL

NOR FAUZIAH ZAINUDIN, AHMAD ZUHAIRI ABDULLAH and ABDUL RAHMAN MOHAMED*

School of Chemical Engineering, Engineering Campus,
Universiti Sains Malaysia, Seri Ampangan, 14300 Nibong Tebal,
Pulau Pinang, Malaysia.
*Corresponding author. Tel: (+06)-045996410, Fax: (+06)-045941013
Email: chrahman@eng.usm.my

The presence of harmful organic compounds such as phenols and their derivatives in water supplies and from industrial effluents is a topic of global concern. In recent years, it has received considerable attention as an alternative for treating industrial waste water. Photocatalysis is an emerging promising technology as it will completely oxidize harmful organic compounds present in the waste stream without leaving behind any hazardous residues. In the present study, photocatalytic degradation of phenol was investigated using supported TiO_2 photocatalyst based adsorbent as a semiconductor photocatalyst in a batch reactor. The synthesized photocatalyst composition was developed using TiO_2 as photoactive component and zeolite as the adsorbents, all supported on silica gel using colloidal silica gel binder. The project included the search for the optimum composition of the supported catalyst and to study the reusability of prepared catalyst. The optimum formulation of supported catalyst was found to be (TiO_2:ZSM-5:silica gel:colloidal silica gel=5:3:5:3) which gave the highest efficiency with 98% degradation of 50 mg/L phenol solution in six hours. The supported TiO_2 was found to be stable for repeated use.

Keywords: Photocatalysis; phenol; supported TiO_2; adsorbent; binder

INTRODUCTION

The release of those phenols and their derivatives in the environment is an ever increasing problem for the global concern. Due to their high solubility and stability in water, it is an onerous process to treat phenolic water to innocuous levels for many biological and chemical processes. Conventional water treatment technologies such as solvent extraction, activated carbon adsorption, and chemical treatment process such as oxidation by ozone (O_3) often produce hazardous by-products and generate large amount of solid wastes, which require costly disposal or regeneration method [1,2]. Due to these reasons, considerable attention has been focused on complete oxidation of organic compounds to harmless products such as CO_2 and H_2O by the advanced oxidation process (AOP) and appears as the most emerging promising technologies. A great deal of attention has been devoted to titanium dioxide (TiO_2) for use as photocatalysts due to the stability of its chemical structure, biocompatibility, physical, nontoxicity, low cost and it possesses high oxidizing power [3,4]. However, from an engineering point of view the immobilization of TiO_2 onto support is preferable compare to the slurry system as to avoid costly and difficult separation and the recycling of the photocatalyst [5,6]. Among the various supports, silica gel is very promising as a support, since it has been used widely in the industry and it possesses good light transmission and adsorption of pollutants [7].

Nevertheless, there are problems that limit the TiO_2 photocatalysis potential as wastewater treatment. According to Haque *et. al.* [8], the requirement for near UV light and a high energy is

required to drive lamps as the intrinsic quantum yields of titania are low. We attempt to solve these problems by dispersing TiO_2 onto a good adsorbent, since reactions predominantly occur on the surface. The adsorbents collect pollutants, even in the dark to the photocatalyst surface, which reducing the requirement of a high energy [9-11]. Among the various adsorbents, zeolite (ZSM-5) has been chosen for the several reasons: its unique Al-O units in zeolite framework are the photocatalytic active sites, it can delocalize band gap excited electrons of TiO_2, thus reduce electron-hole recombination process on the surface and adsorption of intermediates [12,13].

With this goal in mind, special attention was given in this research in order to obtain the optimum composition of each component in this supported catalyst and to study the reusability of prepared catalyst. The prepared catalyst consists of the mixture of ZSM-5 and TiO_2 supported onto the silica gel using colloidal silica gel as binder.

MATERIALS AND METHODS

Materials. Phenol (≥99.5 %) was selected as a model organic compound in the present study. It was purchased from Fisher Scientific and used as received. Powdered particles of Zeolite ZSM-5 (425 m^2/g and Si/Al= 23) was purchased from Zeolyst International was treated by calcined at 500 °C for an hour. Silica gel with a particle size of 0.2-0.5 mm was purchased from Acros Organic. Colloidal silica gel (30 wt. % silica suspension in water) was purchased from Sigma Aldrich and used as received. For the preparation of the TiO_2, Titanium (IV) Isopropoxide (TTIP, 98 %) and ethanol (C_2H_5OH 95 %) were purchased from Acros Organic and TiO_2 Degussa P25 powder (50 m^2/g; 15-30 % rutile + 85-70% anatase) was purchased from Degussa, Germany. All the solutions were prepared using deionized water from Milli-Q system and controlled by its resistivity (18.2 MΩ).

Preparation of Catalyst. TiO_2 nanoparticle was synthesized using sol-gel method as reported [14]. A mixture of 1 TTIP:2 C_2H_5OH:5 H_2O was prepared for the sol-gel solution. A solution of TTIP in ethanol was prepared with molar ratio TTIP/C_2H_5OH = 1/2. The solution was stirred at room temperature for an hour. Subsequently water was added drop by drop under vigorous stirring. A molar ratio of H_2O/TTIP = 5 was used. The gel obtained was dried at 80°C for 24 hours. The modified sol-gel solution was prepared by addition of a calculated amount of TiO_2 Degussa P25 to the sol solution before dried in the oven at 80°C for 24 hours. The powder was added slowly with vigorous stirring to prevent the formation of agglomerates. The TiO_2 obtained then was immobilized according to literature method [8]. A known weight of TiO_2 and ZSM-5 were mixed in the appropriate amount of colloidal silica gel. A known weight of silica gel then magnetically stirred into the mixture for about 30 minutes. The mixture was dried at ambient conditions and then dried in the oven at 100°C. The granules obtained were gently crushed and screened, followed by washing with deionized water for several times. After the impregnation process have finished, the catalyst was calcined in the furnace at 600°C for three hours.

Experimental set up. Figure 1 shows the schematic diagram of the experimental set up. The batch photocatalytic reactor consists of a pyrex glass jacketed reactor with dimensions of 23 x 10 cm x 8 cm (height x outside diameter x inside diameter) and at the top portion has ports for sampling, gas purging, thermocouple and UV lamp. The lamp and reactor were placed inside a wooden box painted black so that no stray light can enter the reactor. The reactor was placed on a magnetic stirrer for thorough mixing. A 15 W low pressure mercury lamp (PCQ lamp, UVP,

Inc) was located in the center of the reactor. A 1 cm diameter of quartz tube protected the lamp from solution contact. In order to conduct experiments at the controlled temperature and protect the lamp from overheating, the reactor was surrounded with a cooling jacket and a fan.

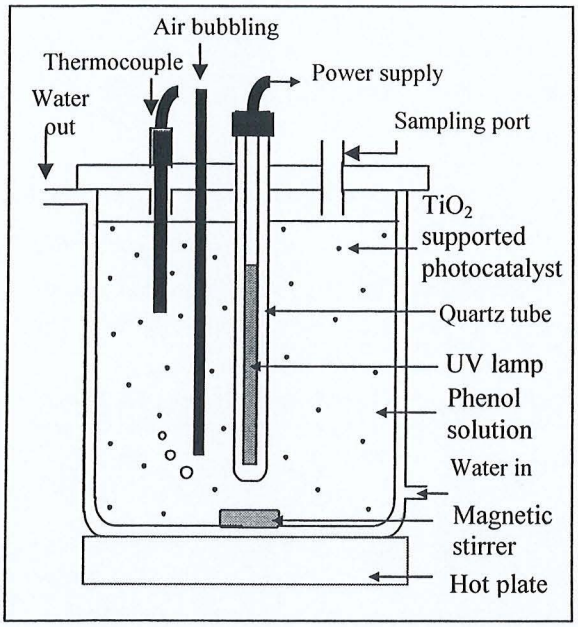


Figure 1: Schematic diagram of batch photocatalytic reactor (cross section view).

Photocatalytic Degradation of Phenol. An aqueous suspension of phenol (50 mg/l, 500 ml) containing the required quantity of supported photocatalyst was stirred for about 30 min in the dark to reach the adsorption/desorption equilibrium, followed by UV lamp illumination for degradation of phenol. During experiments, air was bubbled into the phenol solutions at a constant flow rate of 2 ml/min. This is the cheapest and simplest way to supply a sufficient amount of oxygen (O_2) into the photocatalytic reactor. All reaction was carried out at atmospheric pressure and at room temperature. A base supported catalyst composition consisting of mixture of TiO_2 and ZSM-5 supported on silica gel using colloidal silica gel as binder (TiO_2:ZSM-5:silica gel:colloidal silica gel=1:1:1:2) was used as reference point in order to evaluate the optimum loading for each of the catalyst component. Samples of the suspension were removed at specific time intervals for analysis. The residual phenol concentration was monitored using a high-performance liquid chromatography (HPLC). The HPLC system used in the experiment comprised of Perkin-Elmer UV/VIS 200 HPLC Detector, a Luna 5 μm C18 (2) 100A column and a Perkin-Elmer 200 HPLC pump with an injector port. The mobile phase in this HPLC system consisted of 40 % acetonitrile and 60 % deionized water. The flow rate was adjusted to 1 ml/min. Full loop injection at 20 μL was conducted and the retention time of phenol was 3.81 min. Before HPLC analysis, all samples were filtered using WHATMAN filter (PTFE-membrane, 0.45 μm).

RESULTS AND DISCUSSION

Optimum Composition of Supported Photocatalyst. Selection of optimum catalyst composition is important in order to minimize excess of catalyst and for economic effect. Thus, each component loading in the supported photocatalyst were investigated.

TiO_2 Loading. Experiment was carried out with different TiO_2 loading; 0.05 g, 0.15 g, 0.25 g, 0.35 g and 0.45 g, at fixed phenol concentration (50 mg/L). It was believed that increased in TiO_2 loading, the photodegradation rate should be increased as well, owing to the higher holes and hydroxyl radicals were generated. However, it remains almost constant beyond certain level as shown in Figure 2. This performance is due to the fact that number of photons absorbed and the number of phenol molecules adsorbed were increased as the amount of TiO_2 loading increased. After above a certain level, excess of TiO_2 particles occur. Thus, the UV light penetration was hindering by photocatalyst itself [15,16]. Besides, as the TiO_2 loading increase, it could cause greater aggregation of TiO_2 particles on the catalyst surface. Hence, reducing the specific surface area, consequently reduces the photodegradation efficiency.

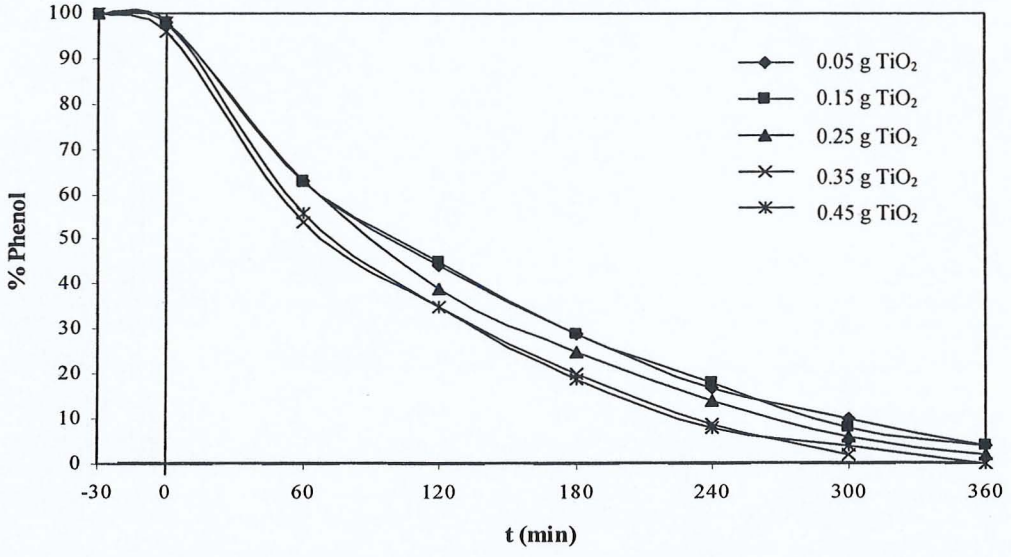


Figure 2: Degradation of phenol at different TiO_2 loading. Conditions; air flow rate=2 L/min, initial concentration=50 mg/L).

Adsorbent Loading. The composition of adsorbent loading were varied from 0.05 g, 0.15 g, 0.25 g, 0.35 g to 0.45 g of ZSM-5. Figure 3 shows that 0.15 g of ZSM-5 exhibits the optimum adsorbent loading. At first 30 min in the dark, increase in the ZSM-5 loading will lead to increase in phenol degradation. After the illumination of UV lamp, the photodegradation take place which indicates that increase the addition of ZSM-5 over 0.25 g will reduce the degradation of phenol. Degradation of phenol become slower since the surface of ZSM-5 increase, thus increase the diffusion pathway for phenol molecules [17].

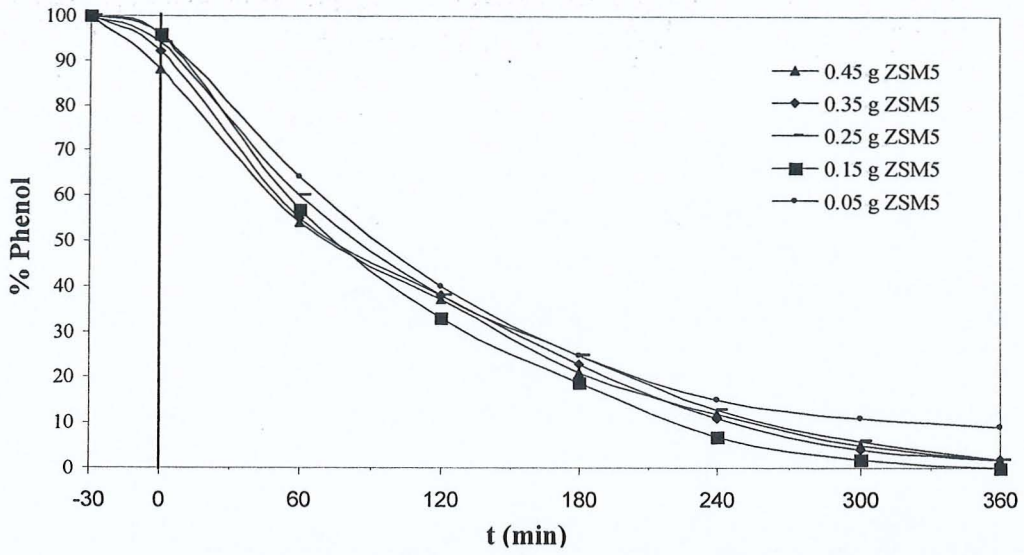


Figure 3: Degradation of phenol at different adsorbent loading. Conditions; air flow rate=2 L/min, initial concentration=50 mg/L).

Binder Loading. One approach to immobilize the photocatalyst is by a binding method. The important needs for binder is it possess a good adherence between the catalyst and support over a prolonged period of time without losing its photocatalytic activity. According to the result studied by Haque *et.al.* [8], colloidal silica gel binder exhibits the best contaminant degradation efficiency. Figure 4 demonstrates the reusability of the prepared catalyst on the different amount of colloidal silica gel binder obtained after four experimental runs. After each run, it was observed that the color of the supported catalyst turned to dark brown. The change in color of photocatalyst is due to the accumulation of intermediates on the active sites of TiO_2 surface [18]. Hence, attribute to the reducing of photocatalytic activity in reuse catalyst. The result in Figure 4 indicates that the reusability of the supported catalyst with 0.25 and 0.50 g colloidal silica gel can almost execute as well as that with 0.75 g colloidal silica gel. Nevertheless, increase the amount binder beyond that limit cause the decreasing in the photocatalytic activity. Since the result revealed that the photocatalytic activity among 0.25 to 0.75 g of colloidal silica gel are slightly differ each other, 0.25 g amount has been chosen as an essential aspect of the cost effectiveness.

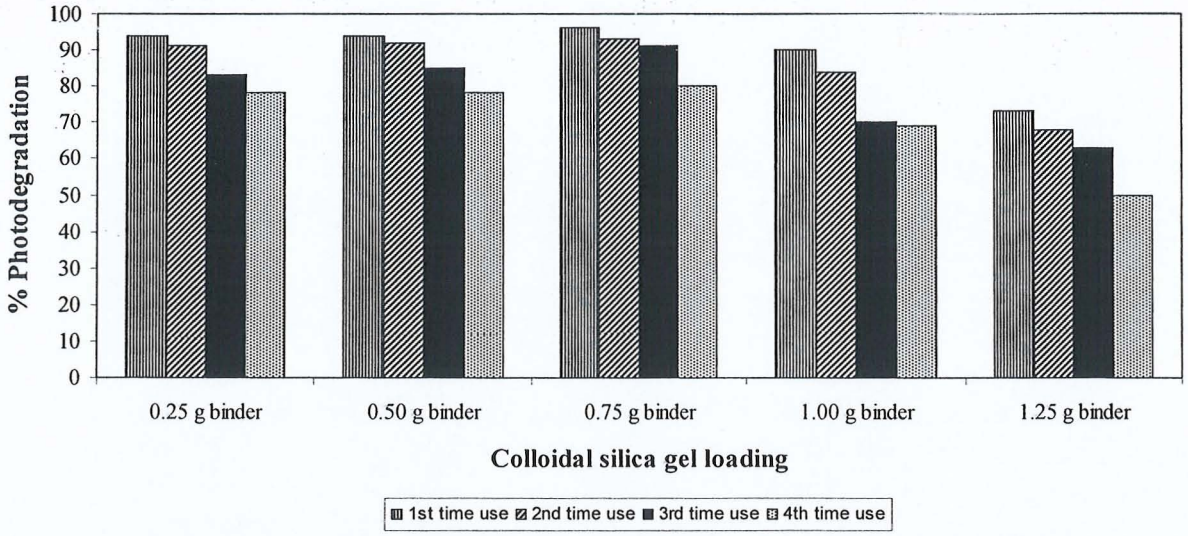


Figure 4: Comparison of photocatalytic activity of supported catalyst at different loading of binder for four times used. Conditions; air flow rate= 2 L/min, initial concentration=50 mg/L)

Support Loading. To evaluate the effect of support loading on the degradation of phenol, several kinds of catalyst were prepared; 0.05 g, 0.15 g, 0.25 g, 0.35 g and 0.45 g silica gel was used. The other compositions were fixed with the base supported catalyst composition. According to the Figure 5, the adsorption of phenol on the catalyst in the dark increased with the increase of silica gel content in the catalyst. However, under the illumination, increase the silica gel loading lead to the improvement in of the phenol degradation until it reaches an optimum level at 0.15 g silica gel. Further addition of silica gel decreases the phenol degradation. Silica gel also possesses the adsorption ability of the contaminant [7]. This is also consistent with our earlier report in the adsorbent loading section that increase in the adsorption will lead to the decrease in the photocatalytic degradation.

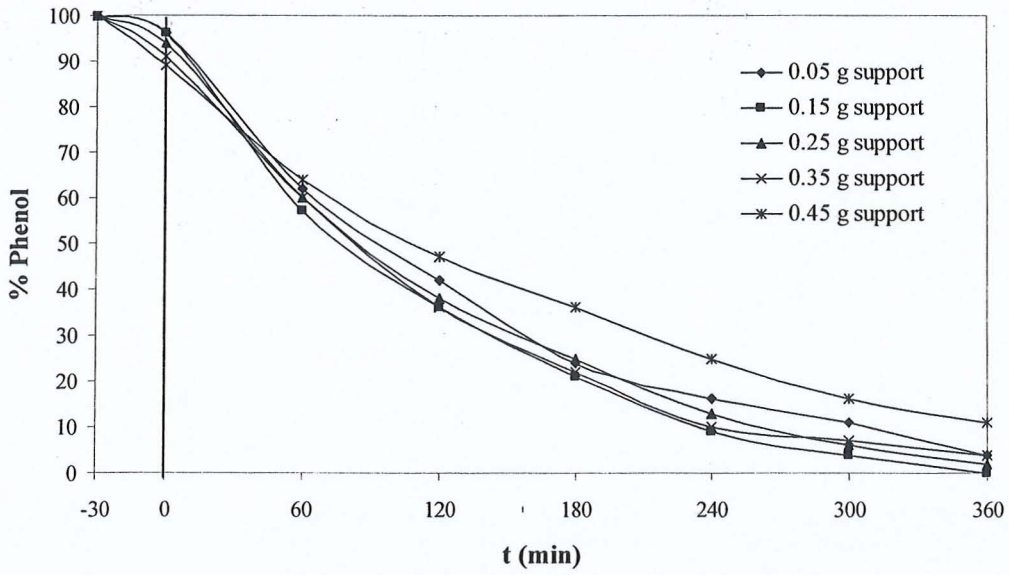


Figure 5: Degradation of phenol at different support loading. Conditions; air flow rate=2 L/min, initial concentration=50 mg/L)

CONCLUSIONS

TiO_2 supported photocatalyst was successfully synthesized using the sol-gel method. The performance study of the synthesized photocatalyst under UV irradiation was performed in a batch reactor for the degradation of phenol. A series of experiments were conducted to investigate the optimum composition for each component in this catalyst. The optimum formulation for the synthesized photocatalyst which consist the mixture of TiO_2 and ZSM-5 supported on silica gel using colloidal silica gel as binder was found to be (TiO_2:ZSM-5:silica gel:colloidal silica gel=5:3:5:3). After four times of repeated use, the system showed only a slight decrease in activity. Therefore, the supported photocatalyst synthesized in this study have been proven to be stable for repeated usage.

ACKNOWLEDGEMENT

The authors gratefully acknowledge the Universiti Sains Malaysia and Ministry of Science, Technology and Innovation Malaysia for funding this project in the form of a USM Short-Term Grant (No. 6035220) and E-ScienceFund Grant (No. 6013338), respectively.

REFERENCES

[1] Gondal M.A., Sayeed, M.N. and Seddigi, Z., Laser enhanced photo-catalytic removal of phenol from water using p-type NiO semiconductor catalyst, *Journal of Hazardous Materials*, doi:10.1016/j.jhazmat.2007.11.066.

[2] Kabir, M.F., Vaisman, E., Langford, C.H. and Kantzas, A., Effects of hydrogen peroxide in a fluidized bed photocatalytic reactor for wastewater purification, *Chemical Engineering Journal*, Vol. 118, 2006, pp. 207-212.

[3] Yahiro, H., Miyamoto, T., Watanabe, N. and Yamaura, H., Photocatalytic partial oxidation of a-methylstyrene over TiO_2 supported on zeolites, *Catalysis Today*, Vol. 120, 2007, pp. 158–162.

[4] Yu, Y., Preparation of nanocrystalline TiO_2-coated coal fly ash and effect of iron oxides in coal fly ash on photocatalytic activity, *Powder Technology*, Vol. 146, 2004, pp. 154–159.

[5] Xie, C., Xu, Z., Yang, Q. and Xue, B., Du, Y. and Zhang, J., Enhanced photocatalytic activity of titania–silica mixed oxide prepared via basic hydrolyzation, *Materials Science & Engineering B*, Vol. 112, 2004, pp. 34–41.

[6] Gelover, S., Mondragon, P. and Jimenez, A., Titanium dioxide sol-gel deposited over glass and its application as a photocatalyst for water decontamination, *Journal of Photochemistry and Photobiology A: Chemistry*, Vol. 165, , 2004, pp. 241-246.

[7] Wang, Y.M., Liu, S.W., Xiu, Z., Jiao, X.B., Cui, X.P. and Pan, J., Preparation and photocatalytic properties of silica gel-supported TiO_2, *Materials Letters*, Vol. 60, 2006, pp. 974–978.

[8] Haque, F., Vaisman, E., Langford, C. H., and Kantzas, A., Preparation and performance of integrated photocatalyst adsorbent (IPCA) employed to degrade model organic compounds in synthetic wastewater, *Journal of Photochemistry and Photobiology A: Chemistry*, Vol. 169, No. 1, 2005, pp. 21-27.

[9] Bhattacharyya, A., Kawi, S. and Ray M.B., Photocatalytic degradation of orange II by TiO_2 catalysts supported on adsorbents, *Catalysis Today*, Vol. 98, 2004, pp. 431–439.

[10] Yamaguchi, K., Inumaru, K., Oumi, Y., Sano, T. and Yamanaka, S., Photocatalytic decomposition of 2-propanol in air by mechanical mixtures of TiO_2 crystalline particles and silicalite adsorbent: The complete conversion of organic molecules strongly adsorbed within zeolitic channels, *Microporous and Mesoporous Materials*, 2008, doi:10.1016/j.micromeso.2008.07.009.

[11] Yoneyama, H. and Torimoto, T., Titanium dioxide/adsorbent hybrid photocatalysts for photodestruction of organic substances of dilute concentrations, *Catalysis Today*, Vol. 58, 2000, pp. 133–140.

[12] Shankar, M.V., Anandan, S., Venkatachalam, N., Arabindoo, B. and Murugesan, V., Fine route for an efficient removal of 2,4-dichlorophenoxyacetic acid (2,4-D) by zeolite-supported TiO_2, *Chemosphere*, Vol. 63, 2006, pp. 1014–1021.

[13] Yan, G., Wang, X., Fu, X. and Li, D., A primary study on the photocatalytic properties of HZSM-5 zeolite, *Catalysis Today*, 93–95, 2004, pp. 851–856.

[14] Gennequin, C., Lamallem, M., Cousin, R., Siffert, S., Aı¨ssi, F. and Aboukaı¨s, A., Catalytic oxidation of VOCs on Au/Ce-Ti-O, *Catalysis Today*, Vol. 122, 2007, pp. 301–306.

[15] Lu, M.C., Chen, J.N. and Chang, K.T., Effect of adsorbents coated with titanium dioxide on the photocatalytic degradation of propoxur, *Chemosphere*, Vol. 38, No. 3, 1999, pp. 617-627.

[16] Nam, W., Kim, J. and Han, G., Photocatalytic oxidation of methyl orange in a three-phase fluidized bed reactor, *Chemosphere*, Vol. 47, 2002, pp. 1019-1024.

[17] Noorjahan, M., Kumari, V.D., Subrahmanyama, M. and Boule, P., A novel and efficient photocatalyst: TiO_2-HZSM-5 combinate thin film, *Applied Catalysis B: Environmental*, Vol. 47, 2004, pp. 209–213.

[18] Tasbihi, M., Ngah, C.R., Aziz, N., Mansor, A., Abdullah, A.Z., Lee, K.T. and Mohamed, A.R., Lifetime and regeneration studies of various supported TiO_2 photocatalysts for the degradation of phenol under UV-C light in a batch reactor, *Ind. Eng. Chem. Res.*, Vol. 46, 2007, pp. 9006-9014.

Advances in Nanocatalysis Research for Carbon Nanotubes Formation and Photocatalytic Degradation of Phenol

Abdul Rahman Mohamed, Minoo Tasbihi, Siang-Piao Chai

School of Chemical Engineering, Engineering Campus, Universiti Sains Malaysia, Seri Ampangan, 14300 Nibong Tebal, S.P.S. Pulau Pinang, Malaysia.

Introduction

Catalysts daily accelerate and boost thousands of different chemical reactions, and thereby form the basis for the multibillion dollar chemical industry worldwide and indispensable environmental protective technologies. Research in nanotechnology and nanoscience is expected to have a great impact on the development of new catalysts. The detailed understanding of chemistry of nanostructures and the ability to control materials on the nanometer scale will ensure a rational and cost-efficient development of new and more capable catalysts for a chemical process.

Recently, countries in Asia are setting up nanotechnology initiatives. Some of the major initial advances are expected to come in areas of increasing rates of reaction using nanocatalysts in catalytic processes. Although most production by catalysis is performed in large-scale reactors, the reaction that actually takes place in the catalyst occurs on the surface of highly dispersed metallic particles with typical dimensions of 1 – 100 nm (Fig. 1). Catalysts are perhaps the first industrial nanotechnology. It is well known that the catalytic activity of supported metal catalysts is strongly dependent on the size and shape of the metal particles. Nanoparticle catalysts are highly active since most of the particle surfaces can be available to catalysis. Many of the nanocatalysts have found applications in ammonia synthesis, environmental protection, photocatalysis, waste removal, fiber and mechanical industries.

Catalysis can play two principal roles in nanoscience, including (1) catalysts can be involved in some methods for preparing nanomaterials such as nanotubes; (2) some nanostructures themselves can serve as catalysts for additional chemical reactions. Both nanocatalysis aspects are highlighted in this paper, covering the topics of the use of nanocatalyst for photocatalytic degradation of phenol and methane decomposition into carbon nanotubes (CNTs).

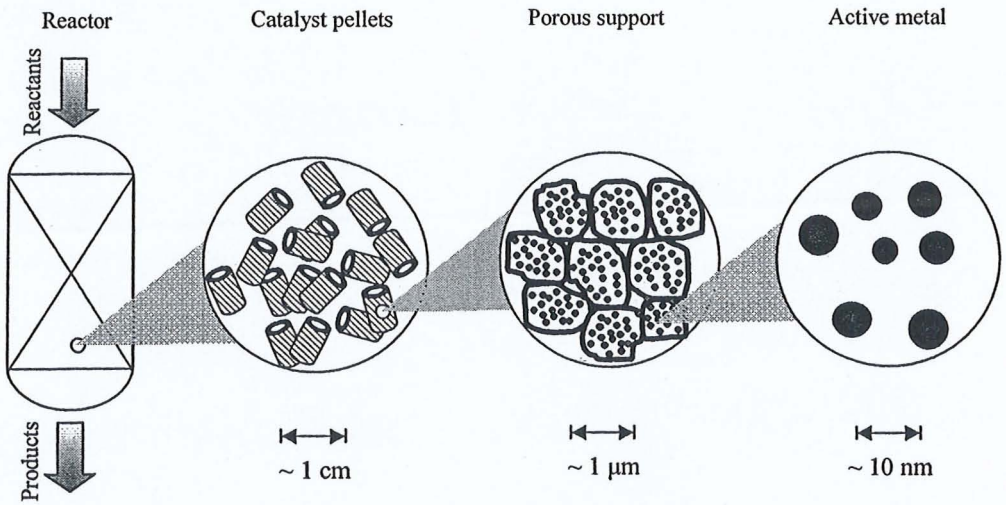


Fig. 1. Schematic diagram showing the typical catalyst structure used in a chemical process.

1. Formation of CNTs via catalytic decomposition of methane

Carbon nanotubes (CNTs), demonstrating unique structural, mechanical, and electrical properties [1], possess many new important applications such as the quantum wires, field-effect transistors, field emitters, diodes, gas sensor, electric power storage, targeted drug delivery, catalyst support, reinforcing elements in composites, etc. [2-4]. This section highlights the tailor-making of CNTs with desirable morphologies through manipulating the nano-active metals and support of a catalyst.

Fig. 2 shows the TEM images of NiO/SiO_2 and NiO/Al_2O_3 catalysts prepared via conventional impregnation method. The dark spots are NiO crystallites (indicated by arrows), and the shallow matters around these crystallites are assigned to the catalyst supports. It can be noted that NiO supported on SiO_2 is of larger size. Apparently, very small size NiO crystallites are formed on Al_2O_3 support. The formation of smaller size NiO crystallites on alumina support is because of NiO/Al_2O_3 catalyst possesses stronger metal-support interaction (MSI) effect. This helps in the dispersion of NiO crystallites, preventing their agglomeration to form larger cluster. On the contrary, NiO crystallites of larger size are formed on silica support. This is due to the lower MSI of NiO/SiO_2 catalyst [5]. This finding shows that the size of the active metals can be controlled by doping them on different catalyst supports [6,7].

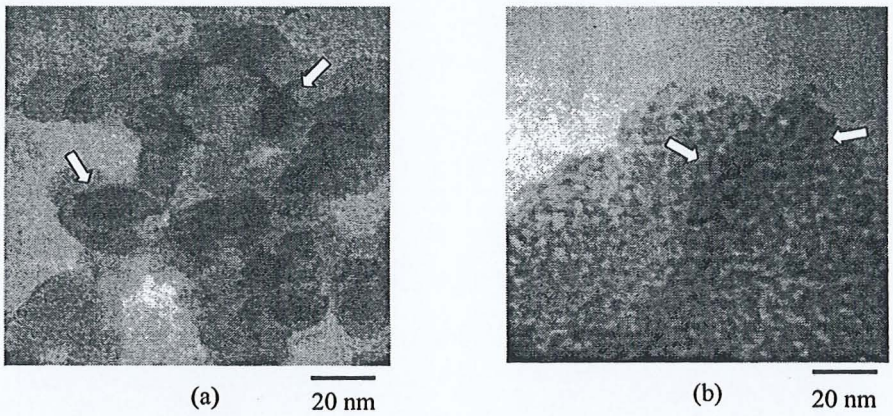


Fig. 2. TEM images of catalysts. (a) NiO/SiO_2 and (b) NiO/Al_2O_3 [5].

Fig. 3 shows the TEM images of the NiO/SiO_2 and NiO/Al_2O_3 catalysts after 1 h reaction with methane at 700°C. It was noted that CNTs were grown on both catalysts. The size of CNTs formed on NiO/SiO_2 was larger than that on NiO/Al_2O_3. For NiO/SiO_2 catalyst, only multi-walled CNTs (MWNTs) were formed. Interestingly, a mixture of MWNTs and single-walled CNTs (SWNTs) were grown on NiO/Al_2O_3 catalyst at 700°C, shown in Fig. 3b-d and indicated by arrow A1,2 and arrow B, respectively. From the TEM analysis, we noticed that the synthesized SWNTs appeared in two forms, i.e. isolated (arrow A1) and bundles (arrow A2). The Raman spectrum (not shown in this paper) shows strong intensity at radial breathing mode (RBM), indicating that the occurrence of SWNTs was dominant. This analysis also reveals that the synthesized SWNTs have a diameter in the range from 0.58 nm to 2.02 nm [8].

To arrive at the understanding why SWNTs were formed on NiO/Al_2O_3 catalyst, we have to know the nature of the catalyst structure. It is well accepted that the formation of CNTs is governed by the size of the active metal particles. The formation of SWNTs on NiO/Al_2O_3 catalyst did reveal that very small size of NiO were formed on Al_2O_3 support and this size was small enough for growing SWNTs. As what we believe, the formation of these ultra-small NiO nanoparticles was mainly induced by the strong MSI effect between the NiO and the Al_2O_3 support, as previously mentioned. This is because strong MSI allowed high NiO dispersion and prevented NiO from agglomerating and forming larger clusters. Probably, some adjacent NiO particles might combine/sinter during the calcination and reaction stages to form larger NiO particles and these particles led to the formation of MWNTs as observed in the TEM image.

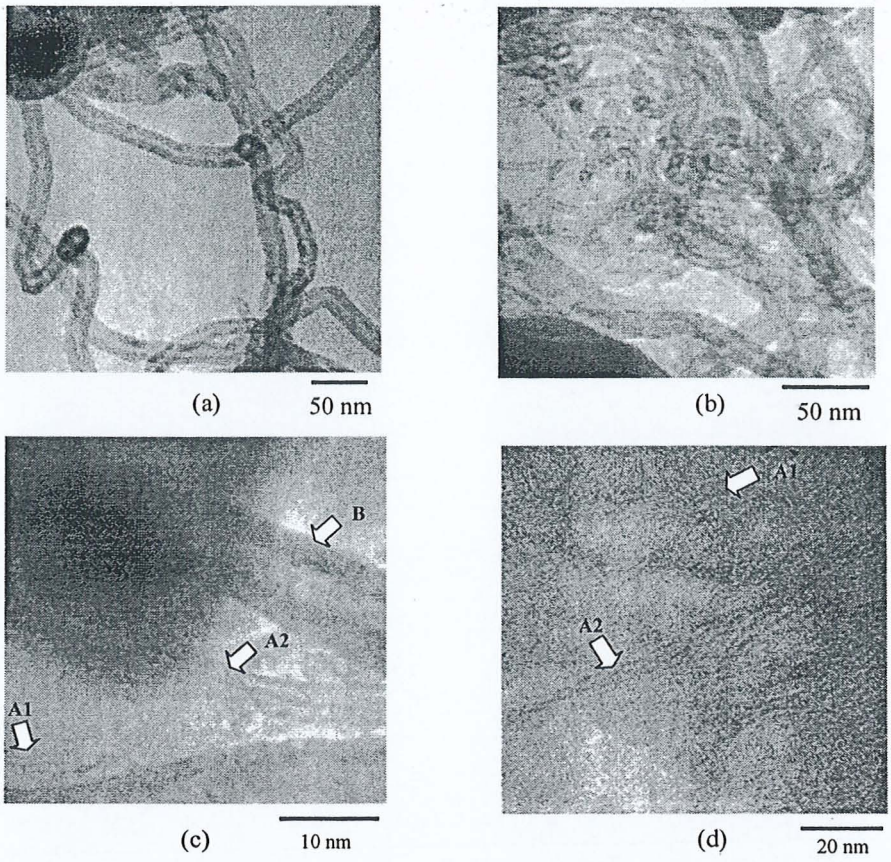


Fig. 3. TEM images of CNTs formed on the catalysts after 1hr reaction with methane. (a) NiO/SiO_2 and (b-d) NiO/Al_2O_3 [8].

Fig. 4a shows the TEM image of $CoO\text{-}MoO/Al_2O_3$ catalyst. The dark spots represent the active metals (indicated by arrows) and the shallow matter is the alumina support. The active metals are the catalyst component subjected to methane decomposition and the growth of CNTs. Fig. 4b shows the TEM image of MWNTs grown on $CoO\text{-}MoO/Al_2O_3$ catalyst from methane decomposition at 700°C. The high degree of diameter control and uniformity of the synthesized MWNTs can be seen clearly in the TEM image. In addition, the TEM analysis shows that out of total 156 MWNTs measured, more than 98% had diameters ranging from 6 nm to 12 nm. The calculated average diameter and standard deviation were 9.0 nm and 1.4 nm, respectively. This indicates that the formed MWNTs were of higher uniform diameter.

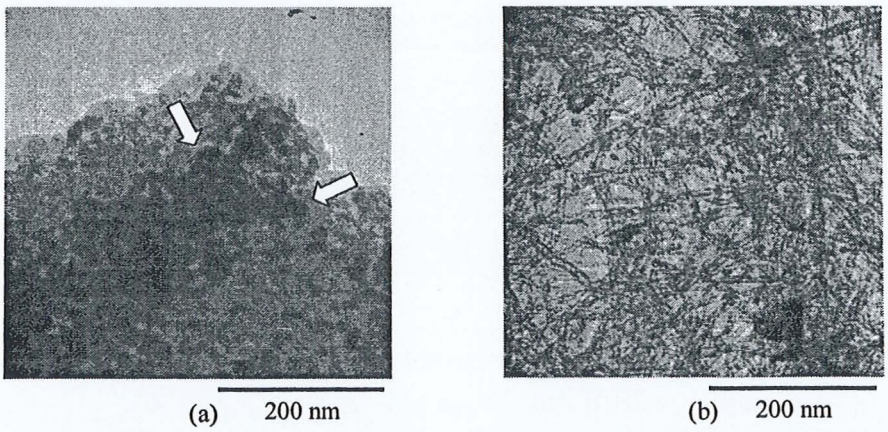


Fig. 4. TEM images of (a) $CoO\text{-}MoO/Al_2O_3$ catalyst, and (b) CNTs formed on the catalyst after 2 hrs methane decomposition [9].

Although many effective ways in producing CNTs with nearly uniform diameters have been suggested in the literature, this study represents a simple and convenient way to achieve this objective. This also reflects a real possibility to produce CNTs of uniform diameter by means of a simpler and cheaper approach in the near future, i.e. through controlling the size of the active metals [9].

Fig. 5 shows the TEM images of Y-junction CNTs grown on the complex NiO-CuO-MoO/SiO_2 catalyst from methane decomposition at 700°C. The circles drawn in Fig. 5 indicate the junction part of CNTs. One can notice that three joining tubes branch out from the junction, forming a Y structure. We suggest that Mo is the important factor for the growth of Y-junction CNTs. A small amount of MoO added to NiO-CuO enhances the growth of Y-junction CNTs. A growth model of this special structure is proposed based on the observation of the CNTs' stem and branch. Fig. 6 shows the proposed sequential growth mechanism of straight and Y-junction CNTs [10].

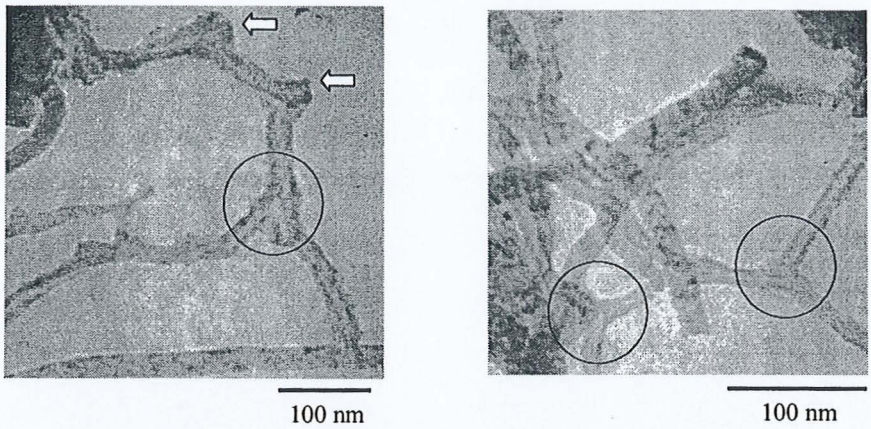


Fig. 5. TEM images of Y-junction CNTs grown on NiO-CuO-MoO/SiO_2 catalyst [10].

The diagram shown in Fig. 6 illustrates the conditions of the NiO–CuO–MoO/SiO_2 catalyst before and after CVD reaction. The black dots represent active metals and white circles represent the catalyst support. We expected that not all the added MoO incorporated with NiO–CuO on the SiO_2 support. MoO-free NiO–CuO catalyst would grow straight CNTs, indicated by (i), and (ii) in Fig. 6, whereas MoO-incorporated NiO–CuO led to the growth of CNT stems and branches. Their possible growth mechanism is represented by (iii), and (iv) in Fig. 6. It is likely that the addition of a small amount of MoO to NiO–CuO acts as nucleation sites, seeding the growth of CNT branches. We believe that, after some time, the surface carbons deposited on the active metals will join the graphitic layers for both CNT stems and branches, forming a poorly graphitized junction part. This is evident when most of the junction parts observed under the TEM exhibit poor crystalline wall structure. The continuous growth of a CNT stem forms the Y-junction structure. In the process that follows, other branches could also be formed on the Y-junction CNT stem. The growth mechanism of a second CNT branch is indicated by arrows in Fig. 5 and represented by (iv) in Fig. 6. Y-junction CNTs without short branches, indicated by circles in Fig. 5 were grown on the catalyst, following the mechanism represented by (iii) in Fig. 6.

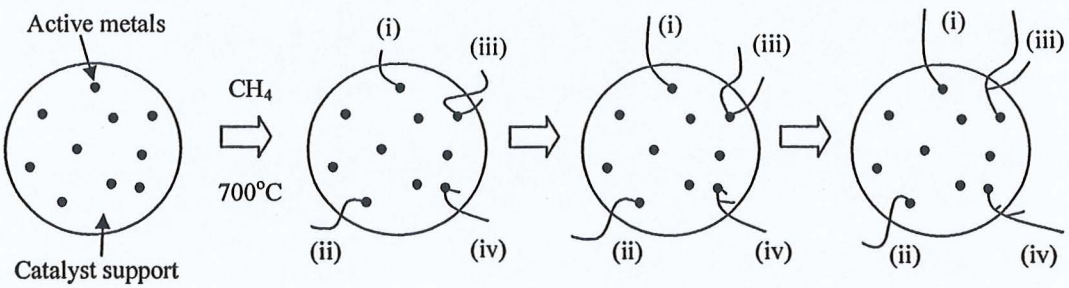


Fig. 6. Schematic diagrams showing the proposed sequential growth mechanism of straight (i, ii) and Y-junction (iii, iv) CNTs [10].

2. Nano TiO_2 for photocatalytic degradation of phenol

Phenol and substituted phenols are widely distributed at low concentration in natural waters, including algal secretion, hydrolyzable tannins and flavanoids and humification processes, and at high concentrations in some industrial wastewater discharge and agricultural activities [11]. Treating phenolic wastewater to harmless level is an arduous process for many biological and chemical processes due to its high solubility and stability in water.

Although a wide range of catalyst has been tested, titania (TiO_2) seems to be the most widely used catalyst because of its photocatalytic, conservative nature, low cost, low toxicity, corrosion resistant [12] and high stability to light illumination. A way to increase photocatalytic activity is the preparation of a nanostructural to get a high surface area that is directly related with catalytic activity [13]. Moreover, photocatalysis of nanocrystalline TiO_2 has many of advantages on wastewater treatment, such as high catalysis efficiency, energy-saving, non-pollution and can degrade all kinds of organic pollutants from water effectively. All of these merits make photocatalysis of TiO_2 a fine and attractive method in the research of water treatment and it is supposed to be used widely in future.

Fig. 7 shows the TEM images of the prepared nano TiO_2 catalyst. The TEM images data revealed that the catalyst consists of uniform and spherical particles with an average nanoparticles size of 11.50 nm. The SEM images of the catalyst are shown in Fig. 8. It was noted that the catalyst consisting of fine irregular TiO_2 particles agglomerated to form a porous structure.

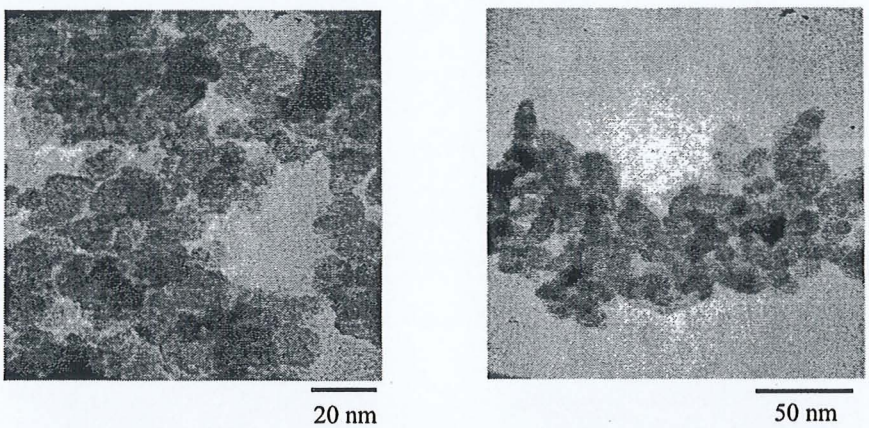


Fig. 7. TEM images of nanocrystalline TiO_2 prepared using sol-gel method

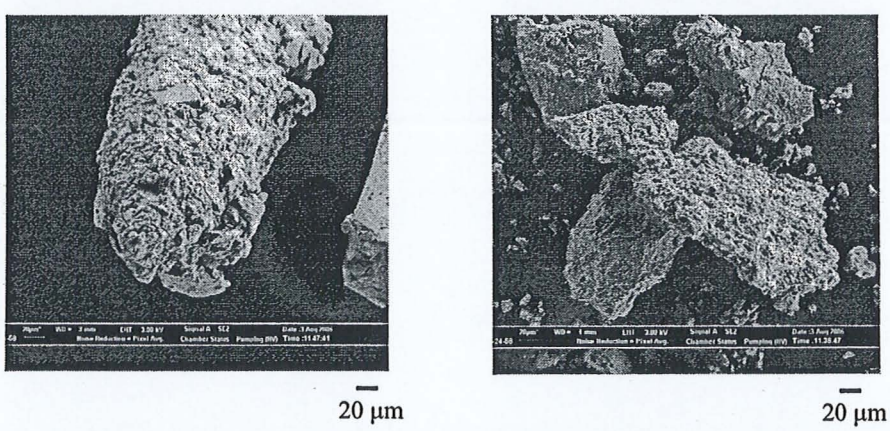


Fig. 8. SEM images of nanocrystalline TiO_2 using sol-gel method support

In order to evaluate photoactivity of prepared nano TiO_2 catalyst, the photocatalytic degradation of phenol in a batch reactor was studied. Fig. 9 shows the photoactivity of the prepared nano TiO_2 catalyst and commercialized TiO_2 powder (Degussa P25). The figure obviously indicates that the phenol concentration decreases with the increase of reaction time. The degradation of phenol using prepared nano TiO_2 is higher than the Degussa P25. It is well known that the higher efficiency of prepared nano TiO_2 is influenced by many factors such as particle size and surface area. In this study, the findings show that the prepared nano TiO_2 has larger surface area, higher porosity and is of smaller particle size than the Degussa P25. This is the reason why the prepared nano TiO_2 is more active than the commercialized TiO_2 powder for photocatalytic degradation of phenol.

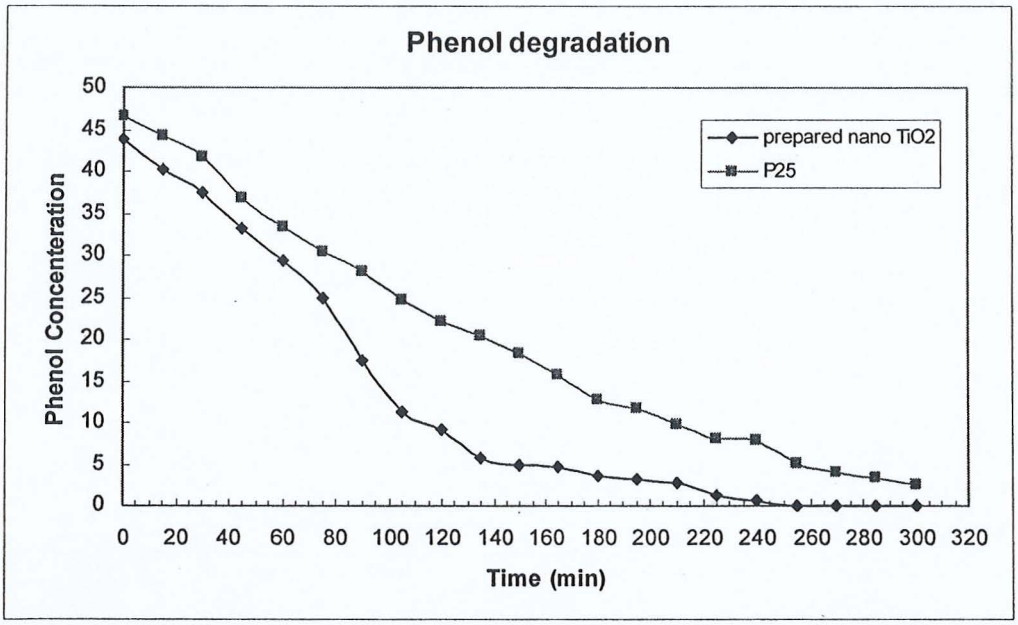


Fig. 9. Photocatalytic degradation of phenol, catalyst 0.6 g, initial phenol concentration of 50 ppm

Acknowledgements

The authors would like to acknowledge the financial support provided by the Academic Sciences of Malaysia and the Ministry of Science, Technology and Innovation Malaysia under Scientific Advancement Grant Allocation (SAGA) (Project: A/C No. 6053001), IRPA Long-Term Grant (Project: A/C No. 6012806) and IRPA Short-Term Grant (Project: A/C No. 6035220).

References

[1] S.G. Louie, in: M.S. Dresselhaus, G. Dresselhaus, P. Avouris (Eds.), Carbon Nanotubes: Synthesis, Structure, Properties, and Applications, Springer, New York, 2001, pp. 113-145.
[2] R.H. Baughman, A.A. Zakhidov, W.A. de Heer, Science 297 (2002) 787-792.
[3] P. Calvert, in: T.W. Ebbesen (Eds.), Carbon Nanotubes: Preparation and Properties, CRC, New York, 1997, pp. 277-292.
[4] A.G. Mamalis, L.O.G. Vogtländer, A. Markopoulos, Precis. Eng. 28 (2004) 16-30.
[5] S.P. Chai, S.H.S. Zein, A.R. Mohamed, Diam. & Relat. Mater. (In Press, Accepted Manuscript).
[6] S.H.S. Zein, A.R. Mohamed, and S.P. Chai, Stud. Surf. Sci. Catal. 159 (2006) 725-728.
[7] S.P. Chai, S.H.S. Zein, and A.R. Mohamed, Chem. Phys. Lett. 426 (2006) 345-350.
[8] S.P. Chai, S.H.S. Zein, and A.R. Mohamed. Mater. Lett. (In Press, Corrected Proof).
[9] S.P. Chai, S.H.S. Zein, and A.R. Mohamed, Carbon (In Press, Accepted Manuscript).
[10] S.P. Chai, S.H.S. Zein, and A.R. Mohamed, Solid State Commun. 140 (2006) 248-250.
[11] A. Sobczynski, L. Duczmal, W. Zmudzinski, J. Mol. Catal. A: Chemical 213 (2004) 225-230.
[12] M. Moonsiri, P. Rangsunvigit, S.Chavadej & E.Gulari, Chem. Eng. J. 97 (2004) 241-248.
[13] Y. Hwu, Y. D Yao, N. F. Cheng, C. Y. Tung & H. M. Lin, Nanostructured Materials 9 (1997) 355-358.

SYNTHESIS AND CHARACTERIZATION OF TiO_2 NANOCRYSTALLINE POWDER BY SOL-GEL PROCESS AND HYDRAZINE METHOD

M. TASBIHI, K. T. LEE, A. R. MOHAMED*

School of Chemical Engineering, Engineering Campus, Universiti Sains Malaysia,

Seri Ampangan, 14300 Nibong Tebal, Pulau Pinang, Malaysia.

Corresponding author: Phone: +604-5941012, Fax: +604-5941013

Email:chrahman@eng.usm.my

ABSTRACT

Recently, the use of titanium dioxide (TiO_2) as a photocatalyst has attracted considerable attention. This is mainly due to the characteristics of TiO_2 whereby it is chemically stable, highly endurance, good ultraviolet absorptivity, high photochemical activity and low production costs. TiO_2 is a polymorphic substance that is present in three crystalline phases: anatase, rutile and brookite with different properties and structures. It is well documented that anatase shows a higher photocatalytic activity than rutile and brookite. Since the photocatalytic activity is mostly confined to the surface of the photocatalytic material, its surface area must be increased to maximize the photocatalytic efficiency. One way to do this is to synthesis nano- sized TiO_2 particles to increase photocatalytic reaction sites on the surface. Apart from that it is also possible to increase the amount of exposed active centers by coating titania on appropriate support. There are different methods that can be used for coating titania on support, however, it is well known that the sol-gel process is the more favorable method. In the present work, TiO_2 nanocrystalline powder was prepared from a titanium tetrachloride precursor via a sol-gel process and hydrazine method. The nano TiO_2 obtained from these two different methods was compared. Transmission electron microscopy (TEM) and scanning electron microscopy (SEM) show that the product has uniform spherical structure with average particle size 11.50, 11.37 and 11.68 nm.

Keywords: Nanocrystalline TiO_2, Sol-gel process, Hydrazine method, Structural properties

INTRODUCTION

The studies on semiconductor as a type of photocatalyst for environmental clean up (Kanki et al., 2005), have been a hot topic since it was discovered in the 1970s. In the past 20 years, scientists have studied extensively and in depth on the modification of semiconductors such as TiO_2, SnO_2, WO_3, Fe_2O_3, ZnO, and CdSe (Tuprakay et al., 2005) in order to improve the activity and catalyst efficiency of these photocatalyst for the degradation of all kinds of organic substances in water and air under certain source of light. Although a wide range of catalyst has been tested, TiO_2 seems to be the most widely used catalyst because of its high catalytic efficiency (Baolong et al., 2003), conservative nature, low cost, low toxicity, corrosion resistant (Moonsiri et al., 2004) and high stability to light illumination. All of these advantages make TiO_2 a fine and attractive choice

of photocatalyst in the research area of waste water treatment (Baolong et al., 2003). TiO_2 is a polymorphic compound that has three polymorphous phases: anatase, rutile and brookite (Yang et al., 2002). The brookite phase is stable only at very low temperature and hence not so useful practically. Rutile is the one that is obtained after high temperature calcination and its fundamental properties like the electrical, optical and thermal properties are well studied. In contrast, the properties of the anatase form are not so well understood. The reason could be that the anatase phase is only stable at comparatively lower temperature. Nevertheless, it has gained significance after nanostructured materials and their synthesis method started to play a major role in materials science (Madhusudan Reddy et al., 2003). Recent studies showed that the photocatalytic activity of TiO_2 is greatly influenced by its grain size. The decrease of grain size implies the increase of surface area and high redox potential, which leads to high photocatalytic activity (Mao et al., 2005). Therefore, a lot of attentions have been focused on the preparation of nanocrystalline TiO_2, the unique properties of nanoparticles and their relations to photocatalytic properties. A part from that , it has been found that the physical and chemical properties of nanocrystalline TiO_2 are strongly related to its preparation methods (Wu et al., 2004).
In this study, nano crystalline TiO_2 was prepared from a titanium tetrachloride precursor via a sol-gel process and hydrazine method. The synthesized catalysts were characterized by transmission electron microscopy (TEM) and scanning electron microscopy (SEM) for their structural properties.

MATERIALS AND METHODS

Chemicals. All chemicals used in this study are with high purity and were supplied by Merck. The chemicals used are: titanium tetrachloride ($TiCl_4$), ammonia solution (NH_4OH), nitric acid (HNO_3), hydrochloric acid (HCl), haydrazine hydrate (H_6N_2O) and tetraethylorthosilicate (TEOS). The water used in all preparations was deionized.

Synthesis of nanocrystalline TiO_2. Nanocrystalline TiO_2 was prepared by sol-gel process and hydrazine method with $TiCl_4$ as the precursor. The flow chart for the synthesis of nanocrystalline TiO_2 using sol-gel process is given in Fig. 1. Detailed procedure for the preparation of the nanocrystalline TiO_2 is discussed as follow: 10 % NH_4OH was added drop by drop into the $TiCl_4$ solution and the white precipitate was obtained at pH=7. The precipitate was washed with deionized water, and then a certain amount of deionized water was added to form a suspension. HNO_3 was then added with vigorous stirring for 24 h at 70 °C. The sol was dried and calcined at 400 °C to obtain nanocrystalline TiO_2 powder (catalyst 1). In addition, a sample prepared by dropwise appropriate amount of TEOS as support to achieve supported nanocrystalline TiO_2/SiO_2 powder (catalyst 2). The flow chart for the synthesis of nanocrystalline TiO_2 by hydrazine method is given in Fig. 2. It was prepared by dropwise addition of $TiCl_4$ in hydrochloric acid solution with vigorous stirring. Subsequently, H_6N_2O was added dropwise till the pH reached 8. The solution was stirred for further 4 h. The precipitate was filtered and dried at 80 °C overnight in air. The powder was dissolved in ethanol and subjected to ultra-sonication for 30 min to separate out the agglomerates formed. The powder was filtered and thereafter calcined at 400 °C to get the nanocrystalline TiO_2 powder (catalyst 3).

Characterization method. The morphology of nanoparticles was investigated and the particles size was determined by means of both transmission electron microscopy (TEM) and scanning

electron microscopy (SEM). Transmission electron microscopy (TEM) images were taken on a Philips CM12 equipped with an analysis Docu Version 3.2 image analysis system. The samples for TEM were prepared by dispersing the final powders in water; the dispersion was then dropped on carbon film coated 400 mesh copper grids. Scanning electron microscopy images were taken on a Zeiss Supra Series with unique GEMINI column. The samples for SEM were prepared by dispersing the final powders on the carbon film.

RESULTS AND DISCUSSION

Fig. 3 (a), (b), and (c) show the TEM micrographs of catalysts 1, 2 and 3 respectively. The TEM micrograph data revealed that all the catalysts consist of uniform and spherical particles with an average nanoparticles size of 11.50, 11.37 and 11.68 nm for catalysts 1, 2 and 3 respectively. Comparing the TEM micrograph of catalyst 1 (Fig. 3 (a)) and catalyst 2 (Fig. 3 (b)), catalyst 2 was found to have small particle size and more aggregation as compared to catalyst 1. this difference could be due to the presence of support in catalyst 2. On the other hand, comparing catalyst 1 and 3, catalyst 1(Fig. 3 (a)) that was prepared by sol-gel process has smaller particle size than catalyst 3(Fig. 3 (c)) which was prepared by hydrazine method and also aggregation of particle in catalyst 1 is more than the catalyst 3.

Fig. 4 (a), (b), and (c) show the SEM results of catalysts 1, 2 and 3 respectively. Fig. 4 (a) shows that catalyst 1 does not have porous structure, however, when catalyst 1 was supported on SiO_2, the surface morphology of the catalyst totally changes. As shown in Fig. 4 (b), catalyst 2 was found to consist of fine aggregated particle on the surface and creating a porous structure. The aggregated particles were also found to have irregular shapes. Fig. 4 (c) shows that catalyst 3 consist of small irregular shape particle that all agglomeration together to form a porous structure. EDX analysis performed on the surface of catalysts 1, 2 and 3 is shown in Table 1. By comparing of EDX of catalysts 1 and 3, it is concluded that the amount of Ti in catalyst 3 is higher than catalyst 1 but the amount of O in catalyst 1 is higher than catalyst 3. By comparing of EDX of catalysts 1 and 2, it is observed that the amount of Ti and O in catalyst 2 is lower than catalyst 1 and there are Si and C elements on the surface of catalyst 2. The lower amount of Ti and O in catalyst 2 could be possibility due to the addition of SiO_2 as a support in the catalyst 2.

Table 1: EDX Elemental Composition of Samples

Element / Sample	Ti		O		Si		C	
	wt %	at.%	wt%	at.%	wt%	at.%	wt%	at.%
Catalyst 1	47.78	23.41	52.22	76.59	----------		----------	
Catalyst 2	30.75	14.73	44.34	63.59	23.68	19.34	01.22	02.34
Catalyst 3	53.96	28.14	46.04	71.86	----------		----------	

Madhusudan et al. (2003) also reported the average nanoparticles size for catalyst prepared by hydrazine method is 10-15 nm. It can be compared to the commercial one with particle size around 35-40 nm. The results for the catalyst 1 which is compared by sol-gel method without support can be compared with Dong-Seok Seo et al. (2001) who had successfully synthesized 20 nm TiO_2 powder by sol-gel method with precursor titanium tetrachloride.

CONCLUSIONS

In summary, nanocrystalline TiO_2 could be successfully prepared by sol-gel process and hydrazine method. Nanocrystalline TiO_2 supported on TEOS exhibits particle with the least average size however the amount of Ti and O because of the use TEOS is the least comparing to others. It would be important to improve a sol-gel process for supported nanocrystalline TiO_2.

ACKNOWLEDGEMENT

The authors would like to acknowledge the financial support provided by Ministry of Science, Technology and Innovation Malaysia (IRPA Grant No. 6012806, Short term Grant No. 6035220).

REFRENCES

[1] Baolong, Z., C. Baishun, S. Keyu, H. Shangjin, L. Xiaodong, D. Zongjie & Y. Kelian, Preparation and Characterization of Nanocrystal Grain TiO_2 Porous Microspheres, *Applied Catalysis B: Environmental*, Vol. 40, 2003, pp. 253-258.

[2] Dong-Seok, S., L. Jong-Kook, K. Hwan, Synthesis of TiO_2 nanocrystalline powder by aging at low temperature, *Journal of Crystal Growth*, Vol. 233, 2001, pp. 298-302.

[3] Kanki, T., S. Hamasaki, N. Sano, A. Toyoda & K. Hirano, Water Purification in a Fluidized Bed Photocatalytic Reactor Using TiO_2-coated Ceramic Particles, *Chemical Engineering Journal*, Vol. 108, 2005, pp. 155-160.

[4] Madhusudan Reddy, K., S. V. Manorama & A. Ramachandra Reddy, Bandgap Studies on Anatase Titanium Dioxide Nanoparticles, *Materials Chemistry and Physics*, Vol. 78, 2003, pp. 239-245.

[5] Mao, L., Q. Li, H. Dang & Z. Zhang, Synthesis of Nanocrystalline TiO_2 with High Photoactivity and Large Specific Surface Area by Sol-gel Method, *Materials Research Bulletin*, Vol. 40, 2005, pp. 201-208.

[6] Moonsiri, M., P. Rangsunvigit, S.Chavadej & E.Gulari, Effects of Pt and Ag on the Photocatalytic Degradation of 4-Chlorophenol and Its by-products, *Chemical Engineering Journal*, Vol. 97, 2004, pp. 241-248.

[7] Tuprakay, S. & W. Liengcharernsit, Lifetime and Regeneration of Immobilized Titania for Photocatalytic Removal of Aqueous Hexavalent Chromium, *Journal of Hazardous Materials*, Vol. 124, 2005, pp. 53-58.

[8] Wu, L., J. Yu, C. J. C., L. Zhang, X. Wang & W. Ho, Preparation of a Highly Active Nanocrystalline TiO2 Photocatalyst from Titanium Oxo Cluster Precursor, *Journal of Solid State Chemistry*, Vol. 177, 2004, pp. 2584-2590.

[9] Yang, S., Y. liu, Y. Gue, J. Zhao, H. Xu & Z. Wang, Preparation of Rutile titania nanocrystals by Liquid Method at Room Temperature, *Materials Chemistry and Physics,* Vol. 77, 2002, pp. 501-506.

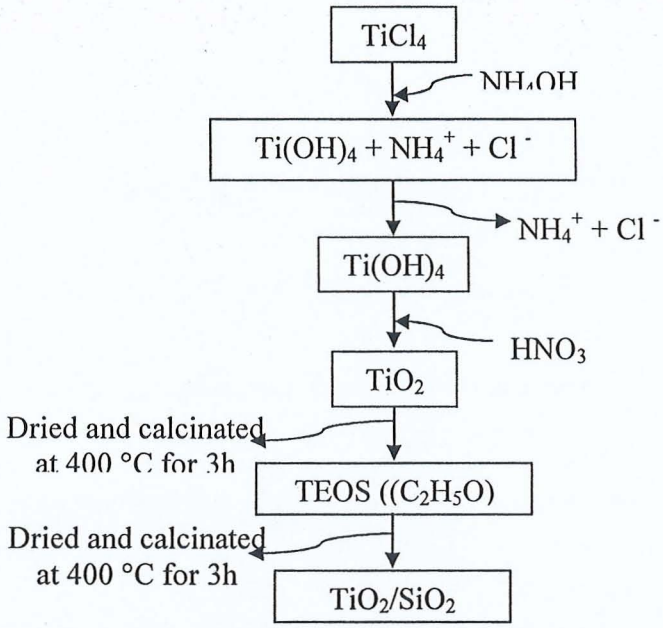


Figure 1: Synthesis of Nanocrystalline TiO_2 and TiO_2/SiO_2 by Sol-gel Process

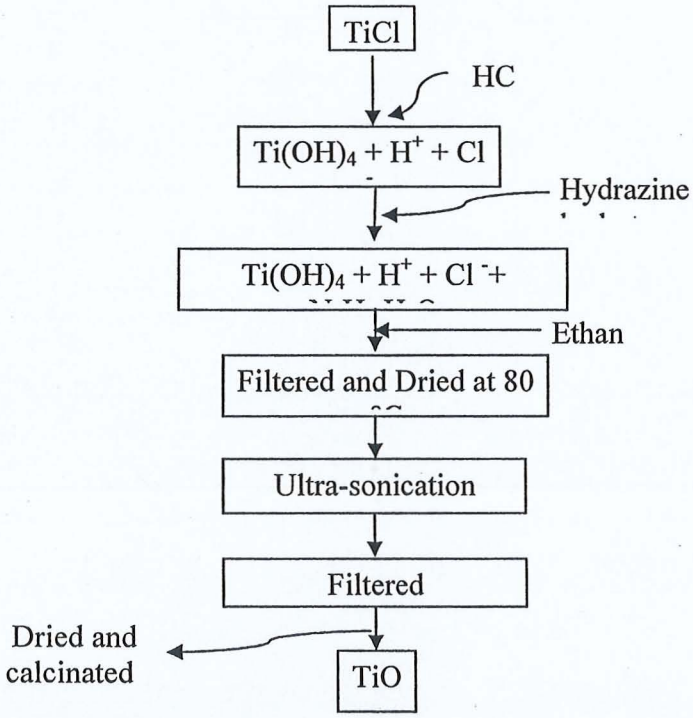
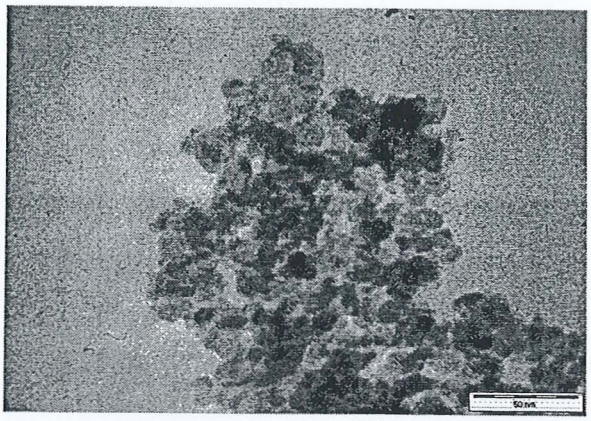
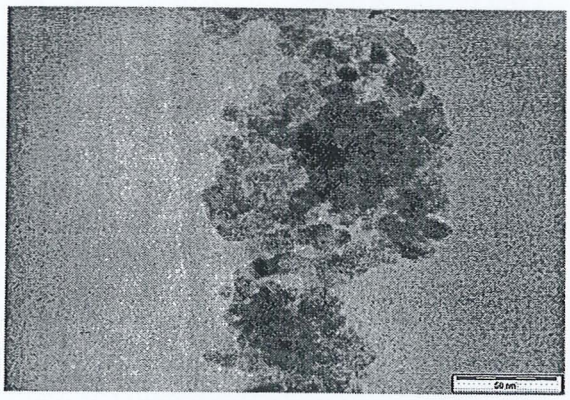


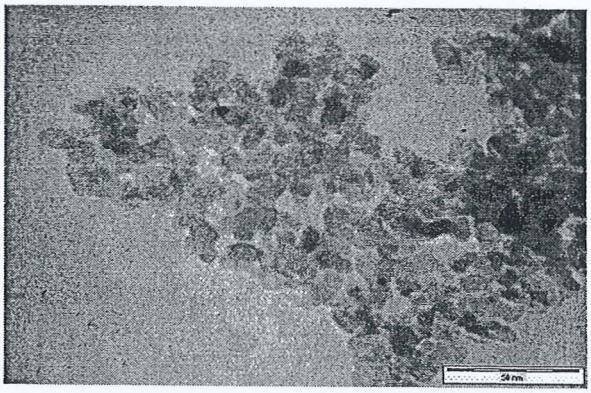
Figure 2: Synthesis of Nanocrystalline TiO_2 by Hydrazine Method



(a)

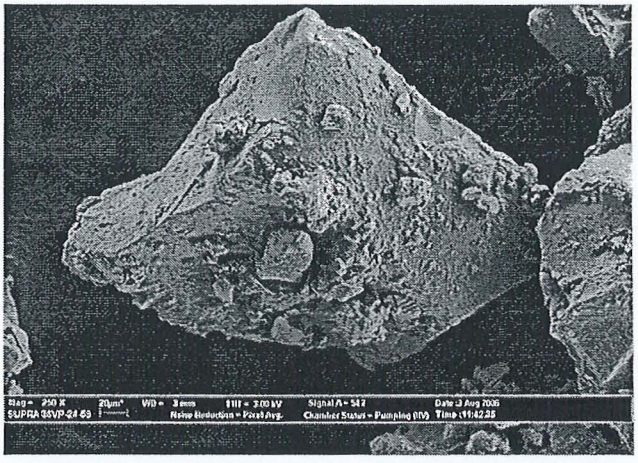


(b)

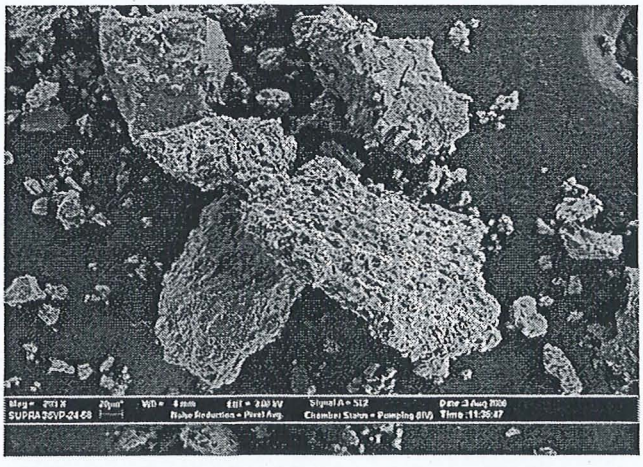


(c)

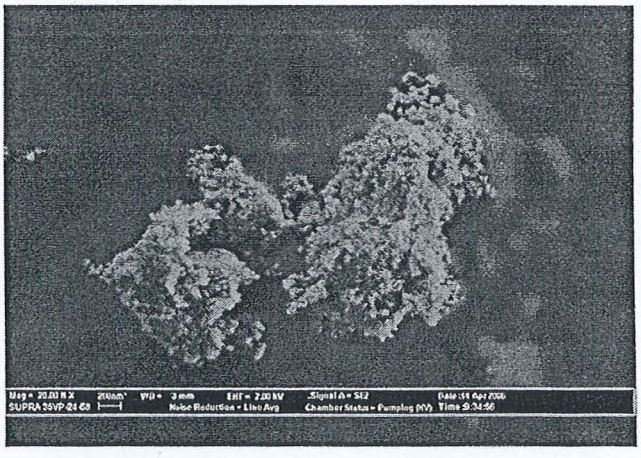
Figure 3: TEM Pictures of Nanocrystalline TiO_2 (a) by Sol-gel Process without Support (b) by Sol-gel Process supported on SiO_2 (c) by Hydrazine Method without Support



(a)



(b)



(c)

Figure 4: SEM Pictures of Nanocrystalline TiO_2 (a) by Sol-gel Process without Support (b) by Sol-gel Process supported on silica(c) by Hydrazine Method without Support

STUDIES OF PHOTOCATALYTIC DEGRADATION OF PHENOLS IN A FLUIDIZED BED REACTOR UTILIZING TiO_2 PHOTOCATALYST IMMOBILIZED ONTO INERT SUPPORTS

ZULFAKAR MOKHTAR, MOHAMAD ZAILANI ABU BAKAR, ABDUL RAHMAN MOHAMED*
School of Chemical Engineering, Engineering Campus, Universiti Sains Malaysia, Seri Ampangan, 14300 Nibong Tebal, Pulau Pinang, Malaysia.
*Corresponding author. Phone: +604-5996410, Fax: +604-5941013
chrahman@eng.usm.my

ABSTRACT

Photocatalysis offers a possible alternative in treating wastewater effluent containing phenols rather than conventional treatment techniques such as filtration and flocculation and carbon adsorption. These methods are considered troublesome as they merely transfer phenols from one phase to another, leaving the problem of disposal of phenols. In contrast, photocatalysis completely break down the phenols and end up as harmless CO_2 and water products. In the present study, photocatalytic degradation of phenols was carried out in a fluidized bed reactor. A modified sol-gel method incorporating Degussa P25 TiO_2 was used for the immobilization of TiO_2 onto quartz sand support. Comparison was made between the modified sol-gel method and the one which was not modified in terms of photocatalytic efficiency. Effect of initial phenol concentration was investigated.

Keywords: Photocatalysis; Phenol; Sol-gel; Fluidized bed reactor

INTRODUCTION

The presence of harmful organic compounds in water supplies and in the discharge of wastewater from chemical industries, power plants, landfills and agricultural sources is a topic of global concern. Conventional water treatment processes include filtration and flocculation, carbon adsorption, biological treatment, thermal and catalytic oxidation and chemical treatment using chlorine, potassium permanganate, ozone, hydrogen peroxide and high-energy ultraviolet light . All these water treatment processes, currently in use, have limitations of their own and none is cost-effective: (i) Phase transfer methods remove unwanted organic pollutants from wastewater, but they do not eliminate the pollutants entirely; (ii) Cost of biological treatment is low, however, some of the toxic compounds present are found to be lethal for microorganisms intended to degrade them, and there is a class of non-biodegradable organic products noted as bio-recalcitrant organic compounds; (iii) While chemical treatments based on aqueous phase hydroxyl radical chemistry are powerful to oxidize toxic organic compounds present in water, these processes either use high-energy ultraviolet light or strong chemical oxidants of hazardous and therefore, undesirable nature [1]. Moreover, several intermediates, which are more hazardous, are formed in these processes, and because of very low efficiencies, overall treatment cost becomes high if destruction of intermediates and complete mineralization are to be achieved, especially for treating dilute wastewater streams [2].

Phenol is primarily discharged in the effluent of the industries such as plastic, leather and paint industries, benzene refining plant and oil refineries. The presence of phenolic compound is potentially toxic to human, aquatic and microorganism life. Therefore, the water effluent should be treated to an acceptable level of phenolic amount that is less than 1 mg/L, enacted by the Department of Environment (DOE in Environmental Quality Act 1974 (Sewage and Industrial Effluent).

TiO_2 heterogeneous photocatalysis has been the subject of numerous investigations in recent years as it is an attractive technique for the complete destruction of undesirable contaminants in both liquid and gaseous phase by using artificial light or solar illumination [3]. Titania photocatalysis advantages of low operation temperature, low cost, significantly low energy consumption have led the relevant application to the stage of commercialization. However, most of commercially available TiO_2 suffers from its nanosized particle dimensions that require a difficult catalyst-recovery stage, which in turn significantly decreases the overall efficiency of the process [4]. Hence, much effort has been centered on developing supported titania catalysts that can offer high efficiency combined with better recovery properties.

Fluidized bed photocatalytic reactor systems have several advantages over conventional immobilized or slurry-type photocatalytic reactors. The unique reactor configuration provides both exposure of photocatalyst to UV light and good penetration of the light into the photocatalyst bed that allow more contact of photocatalyst and reactant fluid. Also, UV light can be more evenly distributed within the given catalyst bed [5].

This study is aimed to elucidate the effect of different sol-gel derived catalysts in the photocatalytic degradation of phenol in a fluidized bed reactor. A modified sol-gel method was incorporated with the addition of cheaply available TiO_2 Degussa P-25. Efforts have been made to compare the performance of the photocatalytic degradation of phenol between the conventional sol-gel derived catalyst and the modified sol-gel derived catalyst. Effect of initial concentration of phenol is also investigated.

MATERIALS AND METHODS

Materials and Chemicals. Quartz sand (Aldrich quartz white sand, Cat. No. 27473-9; r =2.4 g/cm^3; particle size: +50/-70 mesh) was used as the support material throughout the experiment. Quartz sand was washed with acetone (Fisher Scientific) prior to being used to remove organic matters. Phenol (Merck, 99.5%) was used as model pollutant. All solutions were prepared using deionized water from Milli-Q system and controlled by its resistivity (18 MΩ).

Commercial extra pure titanium isopropoxide (TTIP) (Aldrich), isopropanol (Fisher Scientific), diethanolamine (DEA) (Fisher Scientific) and nanophase TiO_2 Degussa P-25 powder (50 m^2/g; 15-30 % rutile + 85-70% anatase, mean diameter 50 nm) were used for the preparation of the sol.

Preparation of Sol-gel Solution. A 0.5 M solution of TTIP in isopropanol was prepared and subsequently a suitable amount of DEA was added to the solution. A molar ratio of DEA/TTIP = 4 was used. The solution was stirred at room temperature for 2 hours. Subsequently water was added drop by drop under vigorous stirring. A molar ratio of H_2O/TTIP = 2 was used. A clear sol was obtained. The sol was sealed and left for aging for at least one day before being used. It was observed that after storage for many months, the sol was remarkably unchanged. This sol was also stable at room temperature.

The modified sol-gel was prepared by addition of a calculated amount of TiO_2 Degussa P-25 to the sol solution. The powder was added slowly with vigorous stirring to

prevent the formation of agglomerates. A thick, white, viscous solution was obtained. This solution settled slowly over a period of two weeks. To prevent settling, the modified sol was stirred constantly while in storage between experiments.

TiO_2 Immobilization onto Support. An amount of 1g quartz sand : 1 ml of sol ratio was used for the immobilization process. The support and TiO_2 sol were mixed in a rotary evaporator by rotating it for 1 hour without applying heat. Subsequently, the mixture was evaporated until complete dryness under vacuum controlled condition. The coated support was further dried in the oven at 120 °C for 2 hours and then subjected to heat treatment in the furnace. The furnace temperature was increased at a ramp rate of 3 °C/min until it reached 100C and was held for 1 hour. Next, the temperature was increased at a ramp rate of 3 °C/min up to 600 °C and held for 1 hour. Finally, the furnace was cooled down to room temperature at a ramp rate of 3 °C/min. The support was weighted again to calculate the amount of TiO_2 film attached on it.

Experimental Set-Up. The experimental rig consisted of a quartz glass column as the main chamber for the photocatalytic reaction with an air distributor with mesh size of 200 micron to provide uniform fluidization of the photocatalyst. A UV lamp enclosure with four 20W UV lamps with wavelength of 254nm were used as UV source surrounding the quartz glass column. Air compressor was used to provide air for fluidization throughout the experiment. The experimental rig is depicted in Figure 1.

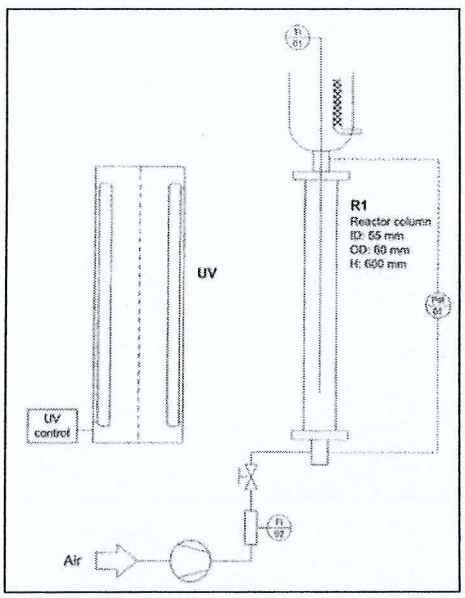


Figure 1: Fluidized bed reactor rig set-up

All reaction was carried out at atmospheric pressure and at temperature of 30 °C. The UV lamps were turned on after 30 minutes of dark reaction to ensure that adsorption equilibrium is achieved. Phenol concentration at this point was used as the initial value for further kinetic investigation of the degradation process. Samples were withdrawn every one hour. The analysis was done using High Performance Liquid Chromatography (HPLC) (Perkin Elmer).

RESULTS AND DISCUSSION

Effect of different catalyst. Figure 2 shows the comparison of photocatalytic degradation of phenol with two different sol-gel methods. Photocatalyst derived from the modified sol-gel

method (STQS) clearly performs better than the one derived from conventional sol-gel method (SQS). After 6 hours of reaction time, a 90.2% of phenol degradation was observed for the STQS photocatalyst compared to only 70% for the SQS photocatalyst. When the support is coated with P-25 powder enriched sol, the surface is covered with TiO_2 derived from the hydrolyzed TTIP and the P-25 powder. Compared with the conventional sol-gel method, the modified sol-gel method produced thicker film thickness per coating cycle. The increase in the amount of TiO_2 significantly enhance the activity [6,7].

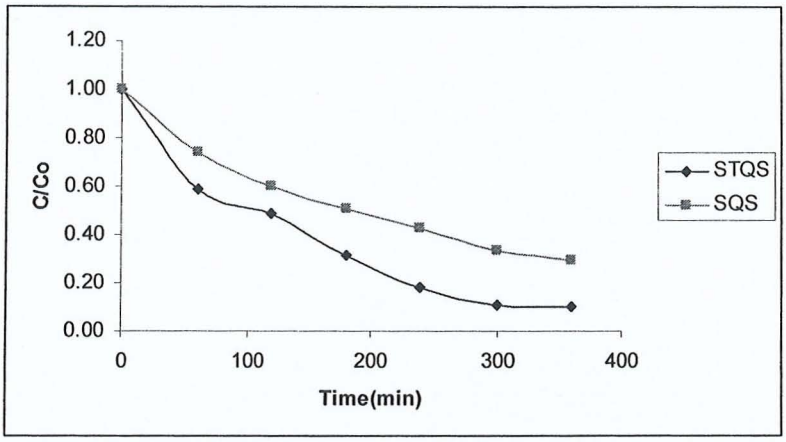


Figure 2 : Comparison of the photocatalytic activity of catalyst obtained from different sol–gel methods on quartz sand support; conventional sol-gel method (SQS) and modified sol-gel method (STQS). Conditions: T=30 °C, air flow rate=2L/min, phenol concentration=50 mg/L, catalyst loading=0.33 g/L

Effect of initial phenol concentration. The optimal phenol concentration was the first to be determined in process parameters study. At concentration further than this, the rate increment was little and in some cases observed rate was decreased [8]. Photodegradation of phenol at different initial phenol concentrations is presented in Figure 3. The half-life time, $t_{1/2}$ which is the global parameter to compare parameter in the process variable studies is used [9]. Half-life time of 44, 118, 181, 225, 310 and 384 minutes were observed at initial phenol concentrations of 25, 50, 75, 100, 150 and 200 mg/L respectively. The results were in agreement with Chen and Ray (1999) which indicated that the typical application of photocatalysis was in low pollutants range [10].

It was observed that as the initial concentration of phenol increased, the reaction rates decreased. This may be attributed to the fact that the all active sites on the photocatalyst are occupied at initial concentration. Thus, a further increase in pollutant concentration does not affect the actual photocatalyst surface concentration and therefore, this may result in the decrease of observed reaction rates at higher initial concentration [10]. The presence of intermediates formed during the process which was also adsorbed on the photocatalyst surface could hinder the process. This will reduce the amount of pollutant adsorbed on the photocatalyst surface [11].

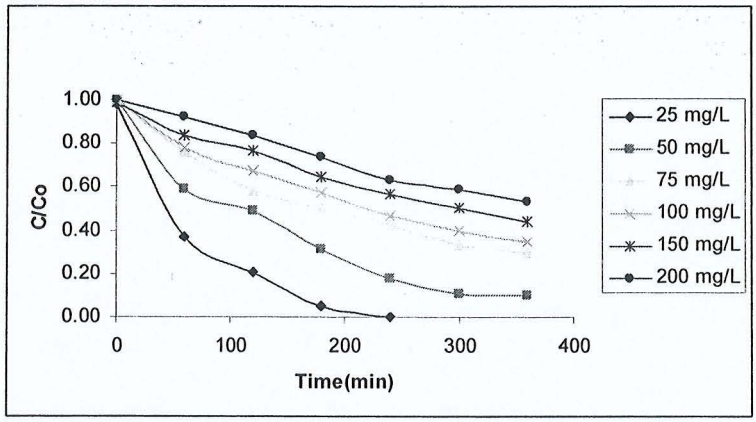


Figure 3: Photodegradation of phenol at different initial phenol concentration. Conditions: T=30 °C, air flow rate=2L/min, catalyst loading=0.33 g/L

Figure 4 indicates the linearized plot of ln C/Co versus time for degradation of phenol at different initial concentration. It should be noted that the slope of degradation of C/Co appeared in a good agreement with pseudo-first order kinetics. This is confirmed by the evidence of a straight line relationship of ln (C/Co) versus irradiation time.

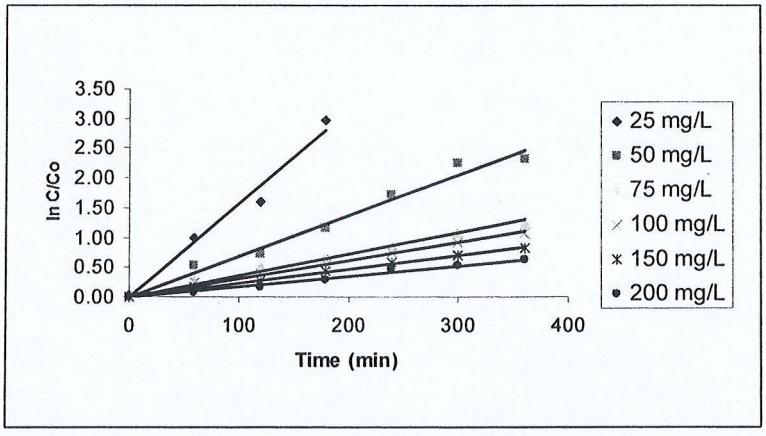


Figure 4 : Linearized plot of ln C/Co versus time for the degradation of phenol at different initial concentration

Generally, for photocatalytic process, Langmuir Hinshelwood model is used to represent the adsorption of reactants on the catalyst surface. The kinetic rate of phenol was expressed as follows:

$$R = \frac{kKC}{1+KC} \tag{1}$$

Where C is the concentration of phenol, k is the rate constant of the phenol and K is the equilibrium constant of adsorption. Eq. (1) can be transformed to the following equation:

$$\frac{1}{R} = \frac{1}{kKC} + \frac{1}{k} \tag{2}$$

A plot of reciprocal initial rate against the reciprocal of initial concentration gave a straight line as shown in Figure 5. Na *et al.* (2004) and Nam *et al.* (2002) investigated the reaction model for the photocatalytic degradation in a fluidized bed reactor and obtained linear dependency of reciprocal of initial rate against the reciprocal of initial concentration. Therefore, it could be concluded that the Langmuir adsorption model described the effect of initial concentration fairly well.

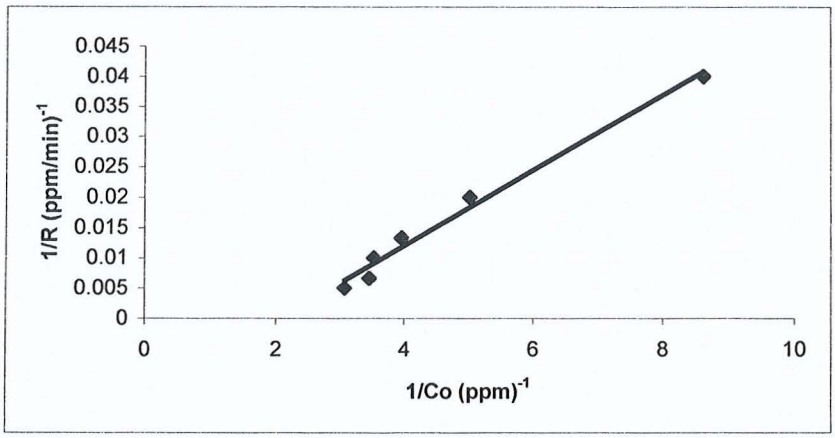


Figure 5: A plot of reciprocal of initial Photodegradation rate against reciprocal of the initial concentration of phenol (air flow rate=2L/min, catalyst loading=0.33 g/L)

CONCLUSIONS

The photocatalytic degradation characteristics of phenol have been determined in a fluidized bed reactor. The immobilized photocatalyst developed gave encouraging photocatalytic activity for decomposing organic compounds present in water and can be applied for water purification. Photocatalyst derived from the modified sol-gel method gave better performance compared to the conventional sol-gel method. It was observed that typical application of photocatalysis was in low pollutants range where photodegradation was higher with the decrease of initial concentration of pollutants.

ACKNOWLEDGEMENT

The funding and support from Ministry of Science, Technology and Innovation Malaysia (IRPA Grant No. 6012806) and Universiti Sains Malaysia (USM Short Term Grant) are gratefully acknowledged.

REFERENCES

[1] Roberts, D. and Malato, S., *The Science of the Total Environment*, 2002, 291, 85

[2] Ollis, D.F., Pelizzetti, E. and Serpone, N., *Photocatalysis: Fundamentals and applications*; Wiley: New York, 1989

[3] Toyoda, A., Zhang, L., Kanki, T. and Sano, N., Degradation of phenol in aqueous solution by TiO_2 photocatalyst coated rotating-drum reactor, *J. Chem. Eng. Jpn.*, 33, 2000, pp. 188-191

[4] Haque, F., Vaisman, E., Langford, C. H., and Kantzas, A., Preparation and performance of integrated photocatalyst adsorbent (IPCA) employed to degrade model organic compounds in synthetic wastewater, *Journal of Photochemistry and Photobiology A: Chemistry*, 169(1), 2005, pp. 21-27

[5] Lim, T. H. and Kim, S. D., Trichloroethylene (TCE) degradation by photocatalysis in annular flow and annulus fluidized bed photoreactors, *Chemosphere*, 54, 2004, pp. 305-311.

[6] Balasubramanian, G., Dionysiou, D. D., Suidan, M. T., Baudin, I. and Laine, J., Evaluating the activities of immobilized TiO_2 powder films for the photocatalytic degradation of organic contaminants in water, *Applied Cat. B: Env.*, 47, 2004, pp. 74-84.

[7] Balasubramanian, G., Dionysiou, D. D. and Suidan, M. T., Titania powder modified sol-gel process for photocatalytic applications, *Applied Cat. B: Env.*, 47, 2004, pp. 74-84.

[8] Pecchi, G., Reyes, P., Sanhueza, P. and Villasenor, J., Photocatalytic degradation of pentachlorophenol on TiO_2 sol-gel catalysts. *Chemosphere*, 43, 2001, pp. 141-146.

[9] Esplugas, S., Gimenez, J., Contreras, S., Pascual, E. and Rodriquez, M., Comparison of different advanced oxidation process for phenol degradation, *Water Res.* 36, 2002, pp. 1034-1042.

[10] Chen, D. W., Sivakumar, M. and Ray, A. K., Photocatalytic kinetics of phenol and its derivatives over UV irradiated TiO_2, *Appl. Catal. B.* 23, 1999, pp. 143-157.

[11] Grzechulska, J. and Morawski, A. W., Photocatalytic labyrinth flow reactor with immobilized P25 TiO_2 bed for removal of phenol from water, *Appl. Catal. B.* 46, 2003, pp. 415-419.

[12] Na, Y. S., Kim, D. H., Lee, C. H., Lee, S. W., Park, Y. S., Oh, Y. K., Park, S. H. and Song, S. K., Photocatalytic degradation of rhodamine B by fluidized bed reactor with hollow ceramic ball photocatalyst, *Koeran J. Chem. Eng.* 21(2), 2004, pp. 430-435.

[13] Nam, W., Kim, J. and Han, G., Photocatalytic oxidation of methyl orange in a three-phase fluidized bed reactor, *Chemosphere* 47, 2002, pp. 1019-1024.

Photocatalytic Degradation of Phenols and Chlorophenols: a Review

Zulfakar Mokhtar, A. R. Mohamed*, M. Z. Abu Bakar

Chemical Engineering School, Engineering Campus, Universiti Sains Malaysia, Seri Ampangan, 14300 Nibong Tebal, Pulau Pinang, Malaysia.
*Corresponding author. Phone: +604-5941012, Fax: +604-5941013
Email: chrahman@eng.usm.my

ABSTRACT

Photocatalysis as an environmental application is considered a novel approach with tremendous potential in the near future. In recent years, it has received considerable attention as an alternative for treating industrial waste water. Phenols and chlorophenols are groups of special interest due to their high toxicity which pose a threat to humans, aquatic and microorganism life. Therefore, efficient treatment of industrial waste water has become of immediate importance. An ideal waste water treatment process will completely mineralize all toxic species present in the waste stream without leaving behind any hazardous residues. This work attempts to evaluate the use of suitable catalysts, catalyst supports and reactor configurations highlighted by other researchers in the field of photocatalysis

Keywords: Photocatalysis, phenol, chlorophenol, titanium dioxide

1. INTRODUCTION

Nowadays, the emergence of highly industrialized environment with a multitude of potentially toxic agents poses a threat to the global community. The presence of harmful pollutants in the discharge of waste waters which often contaminate the water supplies is a topic of global concern. Since there is need for protecting human health and environment, especially in developing and industrial nations, continuous efforts are being made to develop method of treating hazardous waste by removing these impurities or by converting them into harmless forms.

Phenols and chlorophenols are common pollutants in industrial effluents which are toxic to humans and aquatic life. The industrial processes which discharge these potentially toxic compounds include petroleum refineries, tar refineries, leather and paint industries, plastic and steel industries, benzene refining plants and pesticide industries. Water effluent discharged from these industries should be treated to an acceptable level of phenolic amount that is less than 1 mg/l, enacted by Department of Environment (DOE) in Environmental Quality Act 1974 (Sewage and Industrial Effluent).

Photocatalysis offers a possible alternative to degrade these highly toxic compounds rather than using conventional water treatment technologies. Photocatalysis can be carried out in various media: gas phase, pure organic liquid or aqueous phases. The overall process can be decomposed into five independent steps: 1) Transfer of reactants in the fluid phase to the surface, 2) Adsorption of at least one of the reactants, 3) Reaction in the adsorbed phase, 4) Desorption of the product(s) and 5) Removal of the products from the interface region (Herrmann, 1999). When a semiconductor catalyst i.e. TiO_2 is illuminated with wavelength 400 nm or lower, an electron is promoted from the valence band to the conduction band of the semiconducting oxide to give an electron/hole pair. The valence band potential is positive enough to generate hydroxyl radicals at the surface and the conduction band potential is negative enough to reduce molecular O_2. The hydroxyl radical is a powerful oxidizing agent and attacks organic pollutants present at or near the surface of TiO_2 resulting complete oxidation to CO_2 (Byrne et al., 1998).

Table 1: Presentation of different methods to prepare supported TiO_2 film[a]

Precursor		Solvent	Stabilizing agent	Additives	Water (or HNO3)/Titania molar ratio
Nature	[Ti] Mol/l				
TTIP	0.44	Isopropanol		-	-
TTIP	0.43	Isopropanol	Acetic acid	-	-
TTIP	0.34	Isopropanol	Acetyl acetone	Water	1.1
TTIP	0.31	Butanol		Water	4
				HNO3 6N	0.1
TET	0.35	Ethanol	Acetic acid	Water	0.9

[a] Adapted from Guillard et al (2002)

3.1. QUARTZ SANDS

Studies with titanium dioxide immobilized on quartz sand were carried out by Pozzo et al. (1999) in a fluidized bed reactor. It was reported that the TiO_2 supported on quartz sand showed excellent mechanical stability of the coating for at least 12 hours of continuous operation in liquid solid fluidized beds. This was possible after treating the TiO_2 coated sand with fixation-calcining method at 673 K for 12 hours.

Haarstrick et al. (1996) also reported the use of quartz sand as support material. The photocatalytic degradation of 4-chlorophenol and p-toluenesulfonic acid was investigated. The coating of TiO_2 on quartz sand was stable between pH 3 and pH 7. Good stability of the TiO2 coating was also reported for a reaction time as long as 2h.

3.2. SILICA GELS

Silica gel was investigated as catalyst support by Lepore et al. (1996) in two distinct photochemical reactors with different geometry and irradiation arrangements using 2,4-dichlorophenol as a model compound. The first reactor was suited to powder samples with particle diameter of less than 1 mm while the second reactor was constructed for materials having diameters 2 – 8 mm. Two different sizes of silica gels were used namely Silica Gel 100 (70-230 mesh size) and Silica Gel 58 (3-13 mesh size). The work has shown that TiO_2 may be supported in porous silica (Silica Gel 100) as a phase which is either amorphous or of small enough particle size to give only wide lines in XRD powder patterns. In this form, it is a superior photocatalyst to TiO_2 crystals (P25) anchored on the surface of silica gel. It was also reported that if larger particle silica (Silica Gel 58) is used, hydrolytically formed TiO_2 can reach the particle interior. Activity for oxidation of 2,4-dichlorophenol is reduced, but photoactivity is demonstrated by generation of long-lived trapped electron color. The relative photoactivity of TiO_2 supported on a silica gel 100 is shown in Table 2.

Table 2: Relative photoactivity of TiO_2 supported on silica gel 100

Wt.% TiO2	Loading method	% 2,4-DCP[a] consumed
0.83	Sol-gel	9
1.5	Sol-gel	18
2.5	Sol-gel	29
2.8	Sol-gel	38

[a] Result of 2 h irradiation of 319.0 mM 2,4-dichlorophenol solution in reactor I

Matthews et al. (1992) studied the photocatalytic degradation of aqueous phenol solutions under natural sunlight using titanium dioxide immobilized on silica gels and freely suspended in the solution. Photodegradation rates were approximately three times faster with the free suspension than with the immobilized catalyst under the same conditions, and were dependent on the time of the year and the time of the day. The seasonal variation correlated roughly with seasonal solar irradiance tabulations for the UV component of the spectrum. For 10 ppm of phenol, the maximum rate of solar degradation resulted in a decrease in concentration to 10 ppb in less than 80 minutes with total mineralization in 110 minutes.

Gogate, P. R., Pandit, A. B., (2004). "A review of imperative technologies for wastewater treatment I: Oxidation technologies at ambient conditions" Advances in Environ. Research 8, 501-551

Guillard, C., Beaugiraud, B., Dutriez, C., Hermann, J. M., Jaffrezic, H., Jaffrezic-Renault, N., Lacroix, M., (2002). "Physicochemical properties and photocatalytic activities of TiO_2-films prepared by sol-gel methods" J. Applied Cat B: Environ. 39, 331-342

Haarstrick, A., Kut, O. M., and Heinzle, E., (1996). "TiO_2 assisted degradation of environmentally relevant organic compounds in wastewater using a novel fluidized bed reactor" J. Environ. Sci. Technol 30, 817-824

Herrmann, J. M. (1999). "Water treatment by heterogeneous photocatalysis" In *Environmental Catalysis* (Janssen, F. J. J. G., Santen, R. A., eds.), Imperial College Press, London

Hitchman, M. L. and Tian, F. (2002). "Studies of TiO_2 thin films prepared by chemical vapour deposition for photocatalytic and photoelectrocatalytic degradation of 4-chlorophenol" J. Electroanalytical Chem. 538-539, 165-172

Lepore, G. P., Persaud, L., Langford, C. H. (1996). "Supporting titanium dioxide photocatalysts on silica gel and hydrophobically modified silica gel" J. Photochem. and Photobiol. A: Chem 98, 103-111

Matthews, R. W., McEvoy, S. R., (1992). "Destruction of phenol in water with sun, sand and photocatalysis" Solar Energy 49(6), 507-513

Pera-Titus, M., Garcia-Molina, V., Banos, M. A., Gimenez, J., Esplugas, S., (2004). "Degradation of chlorophenols by means of advanced oxidation processes: A general review" Applied Cat. B: Environ. 47, 219-256

Piera, E., Tejedor-Tejedor, M. I., Zorn, M. E., and Anderson, M. A., (2003). "Relationship concerning the nature and concentration of Fe(III) species on the surface of TiO_2 particles and photocatalytic activity of the catalyst" J. Applied Cat B: Env 46, 671-685

Pozzo, R. L., Baltanas, M. A. and Cassano, A. E. (1997). "Supported titanium oxide as photocatalyst in water decontamination: State of the art" Cat. Today 39, 219-231

Pozzo, R. L., Baltanas, M. A. and Cassano, A. E. (1999). "Towards a precise assessment of the performance of supported photocatalysts for water detoxification processes" Cat. Today 54, 143-157

Pozzo, R. L., Giombi, J. L., Baltanas, M. A. and Cassano, A. E. (2000). "The performance in a fluidized bed reactor of photocatalysts immobilized onto inert supports" Cat. Today 62, 175-187

Ray, A. K. (1998). "A new photocatalytic reactor for destruction of toxic water pollutants by advanced oxidation process" Cat. Today 44(1-4), 357-368

Sobczynski, A., Duczmal, L., Zmudjinski, W. (2004). "Phenol destruction by photocatalysis on TiO_2: An attempt to solve the reaction mechanism" J. Molecular Cat. A: Chem. 213(2), 225-230

Yu, J., Yu, J. C., Cheng, B., and Zhao, X., (2003). "Photocatalytic activity and characterization of the sol-gel derived Pb-doped TiO_2 thin films" In *Sol-Gel Science and Technology: Volume 2* (Sakka, Sumio., eds.), Kluwer Academic Publishers, London